The University Of Sheffield.

An Investigation of Recombinant Systems in *Escherichia coli* Engineered for Increased Electroactivity

Simon Thomas Edward Hall

A thesis submitted in partial fulfilment of the requirements for the degree of Doctor of Philosophy

University of Sheffield
Department of Chemical and Biological Engineering

Declaration

This is a declaration that this thesis is the sole work of the author, and the all research presented a product of their work, unless otherwise accredited within the text. This work has not been submitted for any other degrees or qualifications.

“People think of education as
something they can finish.”

- Isaac Asimov

Acknowledgements

There are a great many people I wish to thank for their help and support over the long years that it took to get this thing written. Before I forget, I'd like to thank whoever I do end up forgetting to thank, particularly for their forbearance for this colossal oversight. But with that said I'd like to say a particular thanks to my Mum and Dad, without whom I quite literally would not be here. But who's support (or at least not incessant annoyance in the case of the latter – "So how's the thesis writing going" sound familiar?) helped me get to the point where I could submit this and not completely loathe what I'd produced. To my younger brother Tomas who managed to get a job before me, I promise not to bring up being a doctor too much if in return you don't mention that (this is, of course, assuming I pass my viva). Abuela, I'd like to thank you in writing for so much, but most especially for everything you've ever cooked for me. Ursula, I'd most like to thank you for keeping my Dad from being too much himself when I came to visit and needed a break from everything. And to all my family beyond, new and old, thank you for being there. From family to friends who are a lot like family, and I couldn't thank anyone before Liz Court. It has been a long and tumultuous ride from the beginning of undergrad to here, but I certainly couldn't have made it this last stretch with sanity (mostly) intact without your help. But the journey has been a crowded one, so I'd also like to give a shout out to the MBB massive (with no further exposition since I'm running out of page), including Danielle, Kate, Joe, JP, Bex, and Tom. Not forgetting all the friends made since; I won't embarrass myself by trying to name you all (especially given the size of the PhD office), but a particular warm thanks for tolerating me, to Sam, Lauren, Charlotte, Jack, Jo, Katie, Claire, Yash, Vi, and Andrew. More academically, thank are due to everyone in the MFC White Rose network, and Caroline Evans for her proteomics wizardry. But (last but not least) this section wouldn't be complete if recognition of the fellow survivors of G4b weren't given: Greg and Stephen, for all the support and advice you have given; Ben, for sometimes making me feel better simply because you seemed to be having a worse time; Juliano for occasionally not talking; Josie, and those with us briefly; and, of course, the man himself, Phil Wright; thank you. Thank you all.

Summary

Microbial fuel cell technology and other bioelectrochemical systems arose both out of a need to address important global issues, such as the availability of clean water and the need for renewable energy sources, and the opportunity afforded by bacteria capable of utilise extracellular, insoluble metals as electron acceptors as a part of their metabolism. Since then our understanding of extracellular electron transfer has increased dramatically, with electroactivity demonstrably engineered into *Escherichia coli*, and progress made in a range of synthetic biology applications. This thesis aimed to further explore the limitations and challenges faced when working with these heterologous extracellular electron transfer systems in the interest of progressing the field towards promising applications.

In order to overcome the variability between testing apparatus, a single chamber bioelectrochemical cell protocol was developed and presented with comparisons between the strains of various bodies of work. In the process of doing so a previously unobserved electrochemical effect specific to recombinant systems was discovered and investigated, revealing the mediator-like behaviour of the products of the chloramphenicol resistance mechanism. This work went on to present the development of a high throughput dye assay for the screening of electroactivity. This was subsequently used on genomic libraries of *Shewanella oneidensis* MR-1, a dissimilatory metal reducing bacteria, within *E. coli*, and a novel heterologous electroactive factor identified. Finally, the sensitivity of recombinant *E. coli* strains to variations in media within a bioelectrochemical cell was highlighted, prompting further investigation. A global proteomics-based approach was taken to characterising changes within *E. coli* expressing a heterologous extracellular electron transfer pathway within a bioelectrochemical cell. This recommended avenues for future developments of engineered, electroacive *E. coli* strains.

Abbreviations

aCm	-	Acetylated Chloramphenicol
BES	-	Bioelectrochemical System
BG5	-	Basic Green 5
CAT	-	Chloramphenicol Acetyltransferase
CE	-	Counter Electrode
Cm	-	Chloramphenicol
DET	-	Direct Electron Transfer
DMRB	-	Dissimilatory Metal Reducing Bacteria
EEA	-	Extracellular Electron Acceptors
EET	-	Extracellular Electron Transfer
FDR	-	False Discovery Rate
FMN	-	Flavin Mono-Nucleotide
HC	-	Half Cell
iTRAQ	-	Isobaric Tags for Relative and Absolute Quantification
LMP	-	Low Melting Point
MES	-	Microbial Electrosynthesis
MFC	-	Microbial Fuel Cell
MS	-	Mass Spectrometry
MTC	-	Multiple Test Corrections
nf	-	Nuclease free
OD	-	Optical Density
PCR	-	Polymerase Chain Reaction
PPP	-	Pentose Phosphate Pathway
RB5	-	Reactive Black 5
RR120	-	Reactive Red 120
SDS-PAGE	-	Sodium Dodecyl-Sulphate Polyacrylamide Gel Electrophoresis
SHE	-	Standard Hydrogen Electrode
TCA	-	Tricarboxylic Acid
WE	-	Working Electrode

Contents

Chapter 1 – Introduction

Biotechnology has been a useful resource for over a century, with some definitions placing its inception back thousands of years with the breeding of plant species to produce farmable crops. However, it is only recently, with the advent of genetic engineering, that it has grown to become a booming sector with great potential to tackle many of the challenges facing the world[1,2]. The scarcity of clean water in developing nations, organic and metallic environmental pollutants from various industries[3], and the rising acknowledgement of the need for more renewable energy sources among them[4].

Microbial fuel cell (MFC) technology and other bioelectrochemical systems (BESs) arose in order to address some of these challenges[5,6].

Extracellular electron transfer (EET) is an ability of dissimilatory metal reducing bacteria that allows them to utilise insoluble metals in their environment as end terminal electron acceptors in the absence of more energetically favourable alternatives such as oxygen[7]. These bacteria are often found in metal rich environments, within lake beds[8] or underground[8] and owing to their ability to reduce such metals are often resistant to levels that many other lifeforms would find toxic[9].

However, in an MFC this ability has been exploited as it allows them to reduce an anode instead, using it as an end terminal electron acceptor and ultimately generating current[10]. This has been coupled with wastewater treatment, using strains of these bacteria capable of feeding on the complex organic contaminant molecules, breaking them down while extracting energy, rather than expending it unlike traditional methods[11]. Other BESs have also been employed with a variety of designs and scales in a host of other industrial processes[3,12]. For example, microbial electrolysis cells (MECs) can be used to produce hydrogen, rather than electricity, taking advantage of its energy storage capabilities[12,13]. While microbial electrosynthesis (MES) operates using similar principles, but provides electrons to bacterial cells via a cathode to produce complex

organic molecules in a way that is far less energy intensive and may produce less chemical waste than alternative synthesis methods[14].

While MFCs and other BES technologies have great potential to help with the issues previously mentioned, and have advanced much since its inception, they still face their own challenges in order to become more feasible and cost effective for widespread adoption. The limited up-scaled application of MFCs in the literature can be viewed as the culmination of the technological challenges involved[12,15,16]. Given the need for electrodes that have high surface areas and catalyse the exchange of electrons readily in order to maximise efficiency[17], therefore being composed of expensive materials such as platinum, there is a financial investment involved in creating large scale MFCs for waste processing. This is compounded by the fact that many of the contaminants of complex waste streams can deteriorate these electrodes, shortening their lifespan and so driving up the cost for the technology[12,17], and can adversely affect other components of the equipment, such as membranes[3]. Add to that the need to maintain a stable culture of the microbial organisms that power the technology, which is complicated by contaminants in the waste streams they can feed on[3,12], and you see why the technology is not widespread.

Other BESs share some of these concerns, and more recent technologies (such as MES) have arisen from exploring design options and applying the principles of MFCs and EET to other applications[18]. Consequently, an increased understanding of EET can benefit all BES technologies. And applying engineering principles to the design of strains that can be modified to suit these different applications – strains possessing of extensive toolboxes of techniques and biological parts – could help realise these technologies and more. This synthetic biology approach desires host strains that are well studied and easily genetically manipulable[19]. However, the use of synthetic biology to overcome some of the limitations detailed above presents its own concomitant difficulties. For example, the handling and environmental contamination avoidance required for genetically modified microorganisms, as well as the challenges of heterologous expression[20,21]. However, for certain applications these may be outweighed by the potential benefits, or even addressed with further development.

While the bacterial component remains an essential part of the technology, the focus of much of the literature has fallen on the physical components. Though systems for EET have been identified and extensively researched in their native organisms, much still remains to be understood about the processes DMRBs use to achieve EET and how these interact with various BESs[22]. The limited genetic toolsets available for the more commonly used DMRBs have further hampered research into synthetic biology approaches. It was recognised, however, that the most well understood model organism, *Escherichia coli*, might be of use in this regard, and studies have been made of *E. coli* engineered with EET capabilities from the model DMRB *Shewanella oneidensis* MR-1[23,24]. This is a strong development from early attempts to make the *E. coli* electrogenic, which involved expensive and highly toxic chemical mediators to affect EET[25].

The design of MFCs and similar BES for testing electroactivity continues to rely on the same fundamental principles as at the technology's inception, however individual designs, equipment, and materials all vary from lab to lab[3,16,26–28]. The lack of standardisation of testing apparatus, and even methods, units, and data presentation in this interdisciplinary field, are a keen challenge facing development in the field (REF). It makes comparing results from different studies using the same strains incredibly difficult. And with the typically low throughput of such experimental procedures, this means that multifactorial investigation of small changes to experimental conditions that could impact metabolism are difficult. For example, media usage varies across published studies (REF REF), even within the same research group (REF REF) but provided reasoning behind these selections is limited. While less concerning for DMRB that have evolved regulatory apparatus to manage their EET, the same is not true for engineered *E. coli* strains, the regulatory responses of which may have unforeseen interactions with the heterologous EET pathway.

Heterologous expression of a complex pathway meant to interact with metabolic processes in *E. coli* strains to effect EET has presented its own challenges, and it is some of these that this thesis aims to address. The inferior electroactivity of existing strains, compared with natural DMRB, limit their usefulness directly for MFCs and other BESs.

Yet with the greater toolsets available for this model organism more may be achieved in the way of sensitive control and modification for specific applications. For example, the development of biosensors that tie the detection of specific molecules (biological circuits for many of which already exist) to current production, allowing a direct interface with devices[29–31]. Additionally, given the redundant nature of EET pathway components in DMRB, the use of *E. coli* may provide insights into electroactive proteins that wouldn't be possible when not studied in isolation, even given the concerns heterologous expression necessitates.

The EET pathway introduced into engineered *E. coli* strains is heterologous, and so does not have pre-evolved interactions with regulatory machinery to be fully utilised. Furthermore, an issue relevant to heterologous expression in general and therefore one to be aware of, there may be unanticipated interactions with other proteins within the cell leading to phenotypes that are likely to be detrimental[32]. Understanding how the *E. coli* metabolism links to the heterologous EET pathway to utilise an electrode as an end terminal electron acceptor, may be the key to future work to bridge the gap in electroactivity between such strains and DMRB. Such information could inform metabolic engineering that would allow *E. coli* strains to take full advantage of the EET pathway. Given that this is arguably the main disadvantage of engineered *E. coli* compared to DMRB it would open up its use in the applications previously discussed, allowing the extensive tools and libraries of genetic parts to be brought to bear on them.

These topics and more are outlined and explored in further detail in the proceeding chapter.

1.1. Chapter Structure and Aims

In this thesis we set out to establish a BES meant for investigation of electroactivity in *E. coli* strains at a throughput higher than easily achieved with MFCs, comparing several strains and investigating factors affecting electroactivity, and in so doing proceed to investigate a novel bioelectrochemical interaction, presented in Chapter 4.

In Chapter 5 a Fosmid library of *S. oneidensis* MR-1 in *E. coli* was created with the aim of identifying novel heterologous electroactive factors. A high throughput, azo-dye based approach to the screening is presented, along with the results of the screening process.

The focus of Chapter 6 lies on the investigation into metabolic and proteomic differences between engineered and control strains of *E. coli* that have adapted to conditions within our BES, as well as how their behaviour is affected by growth conditions beforehand, with an aim to inform future iterative improvement of an engineered electroactive *E. coli* strain.

Beyond these research chapters a review of the relevant literature is presented in Chapter 2, followed by the presentation of the materials and methods used in the proceeding work, in Chapter 3. Finally, the conclusions and possible directions for future work are discussed in Chapter 7. An appendix of relevant data follows this.

Chapter 2 – Literature Review

2.1. Introduction to Microbial Fuel Cell Technology

Issues with the worldwide reliance on fossil fuels have prompted much investigation into sources of renewable energy, with a myriad of technologies resulting [33]. Both for the sake of the global economy and to combat climate change resulting from our current energy consumption, technological advances must be made[34]. Microbial Fuel Cell (MFC) technology is one such technology, being developed to assist in cleanly reclaiming energy from waste water using bioelectrochemically active microbes[35]. The potential of the science on which it is built extends beyond this, however, as ongoing research into applications such as bioremediation[36] and microbial electrolysis[13] have arisen from it. Additionally, insights gained into electroactive organisms, which are able to transfer electrons to an acceptor outside of their cells, may benefit research into other areas of bioelectrochemical research, such as microbial electrosynthesis, wherein a current is used to stimulate a process of production[37], and biosensing[30] where bacterial environmental sensing is communicated in a technologically translatable fashion[38].

MFCs, much like other types of fuel cell, typically consist of two connected electrodes. They are distinguished by their use of a microbial catalyst, present on the anode, to produce a current[39]. In simple terms, organic matter is metabolised by the microbial community that has colonised the anode, with the anode being used as an electron acceptor[40]. Electrons donated to the anode flow through the circuit connecting the electrodes, resulting in an electrical current. Meanwhile, the protons released during microbial metabolism move to the cathode, where they meet the electrons and then typically react with oxygen to produce water, though other electron acceptors are possible, resulting in other products[15].

Figure 2.1. – Two Chambered Microbial Fuel Cell Diagram

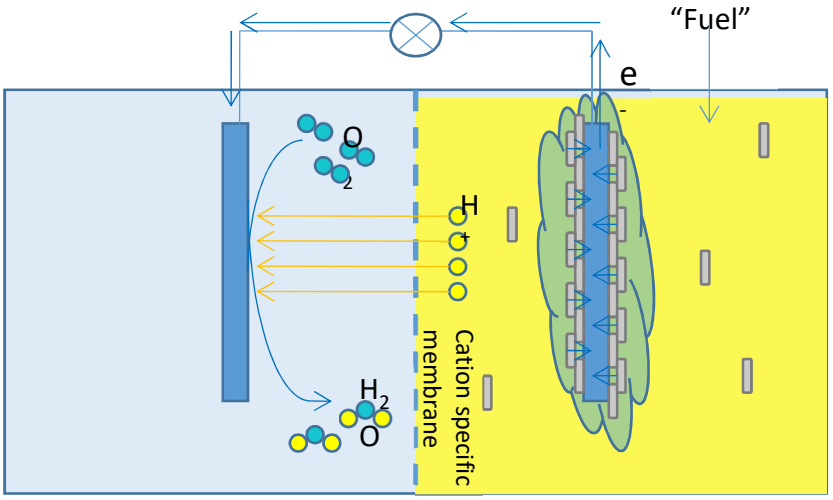

Fuel is added to the anaerobic anode chamber, and metabolised by the bacteria colonising the electrode, transferring electrons to it. Electrons react with oxygen and protons to form water at the aerobic cathode. With a load placed across these two electrodes power is generated.

A typical two chambered MFC[41] is depicted in Fig 2.1., with an aerobic cathode chamber separated from an anaerobic anode chamber by a proton permeable membrane (PPM), the two electrodes connected with a load placed across them, and microbial colonisation of the anode. Other designs exist, often tailored for specific applications such as scaling up[42]. The most common alternative involves an air cathode without a catholyte; the cathode is coated in a PPM (though it is absent in some designs) at its interface with the anolyte but is otherwise exposed to air, and therefore oxygen. Such designs often comprise a single chamber, with the cathode on the outside[43]. Consistent among these variations is, of course, a need for the microbiological component.

2.1.1. Current Microbial Fuel Cell Research

While the scaling up of MFCs to an industrial level is a challenge being worked on by many groups, with a small number of pilot studies having been conducted[11,44], there are many aspects of the fundamental MFC design that are still being researched to improve

performance[15]. Internal resistances and electron transfer resistances within an MFC design represent the most important limiting factors to power generation at theoretical maxima[45]. Given the engineering standpoint taken by many who work in the area, there is a great deal of research aimed at overcoming these limitations through the modification of materials, particularly the electrodes[46,47], and physical design of the technology[48]. However improving understanding and control of bioelectrochemical processes will help push the practical technology to a state of increased industrial viability, and will assist in the progression of other BES based technology[49]. For other applications this is more accepted, such as for bioremediation and nanoparticle production where studies often investigate the interaction between electroactive strains and specific metals or organic compounds[50,51].

Research into scaling up BES technologies to pilot scale are ongoing. Though pilot scales exist for wastewater treatment MFCs, these tend to focus on rich wastewater, such as that from breweries[12] or the dairy industry[52]. Nonetheless they seek to address the primary challenges in scaling up the technology, which all ultimately come to financial viability. Reducing the cost of materials, while maintaining a design that is effective and which maximises power output is essential[18].

2.1.2. Electrode Composition

The redesign of electrodes used in MFC technology is believed by many to be the largest problem in improving power generation and lowering costs enough to make it industrially feasible[49,53]. Electrodes must often be made of high-surface-area, conductive, catalytic materials such as platinum to ensure maximal efficiency[17] and for complex wastewater streams the deterioration of the electrodes can be fast[12,17]. While materials are a concern for reasons of cost, internal resistance, and robustness, the fact that the surface of the anode is colonised by the biological catalyst requires consideration. Cheap materials that provide a high surface area are used in a lot of biologically focussed MFC research; carbon electrodes, either felt, fibre, or graphite, are used primarily, though various metallic electrodes can also be found to be used[54] and an amount of platinum composing counter electrodes is desirable[55]. There is ongoing research into the potential use of nanoparticles, such as gold[56], or nanotubes in the

electrode design to improve their suitability to levels closer to more expensive options[47]. While these may provide a benefit to surface area, biofilm formation, and electrochemical interaction, the former still presents the issue of cost, of great importance when considering scaling up, and both have toxicity considerations, either for the bacteria[47,57] or for the environment given the wastewater treatment application of MFCs[58].

2.1.3. Microbial Fuel Cell Organisms

While research has been conducted using a range of organisms in MFCs, bacteria are most prominent, either in isolation or as consortia of different species; consortia often proving more effective than single strains[59]. In particular, the majority of research in the field focusses on species of the gram negative genera *Geobacter* and *Shewanella*, which often display extracellular metal reducing capabilities[60]. Specifically, within these genera there is a significant body of work on *Shewanella oneidensis* MR-1, *Geobacter metallireducens* and *Geobacter sulfurreducens* in particular[61,62], such that they are the best known electroactive organisms and may be reasonably called model organisms for MFC research[63]. Much of our current understanding of mechanisms employed by electroactive bacteria to transfer electrons to extracellular acceptors comes from their study. *Geobacter sp.* tend to be strictly anaerobic, while *Shewanella sp.* are typically facultative, non-fermentative anaerobes, making them easier to work with, though optimal electroactivity typically requires anaerobicity as oxygen is preferentially used as end-terminal electron acceptor[7].

These naturally electroactive bacteria are referred to as dissimilatory metal reducing bacteria, as the mechanisms that make them suitable for MFCs are naturally used by many of them to reduce extracellular metals[64]. A number of specific mechanisms have been identified that facilitate this process, which fall into three categories: direct electron transfer through membrane bound proteins, such as cytochromes; creation and secretion of electron shuttling mediators; and transfer through conductive pili-like structures known as nanowires[41].

2.2. Practical Considerations for Laboratory Scale Investigation of Bacterial Electroactivity

2.2.1. Measurements

Those working in the field of MFC research come from a variety of different backgrounds, and, while this can prove a boon for looking at problems from a range of viewpoints, it also results in a fair amount of variation in the way results are presented and equipment described[65]. It is important to bear the need for standardisation in mind, both for experimental design purposes and data presentation, and for the purposes of this study an understanding of the equipment and methods used to collect data from MFCs is crucial to doing so.

It is important to measure the potentials of the anode, particularly, and cathode, using a reference electrode; this measurement allows other equipment to maintain specific poised potentials at electrodes, which is important to facilitate electron transfer from microbial cells[66]. This poised potential makes the transfer of electrons to the electrode a more energetically favourable process. A potential of 0.2 V is typically used in work with *S. oneidensis* MR-1[27], but the ideal poised potential can vary with different organisms[66]; it may be necessary to test this with different engineered *E. coli* strains. While it is theoretically possible to predict potentials, variations in conditions within the cell and uncertain losses at interfaces necessitate measurement[65]. Combined with measurement of current and details of load (resistance placed across the circuit connecting the two electrodes in MFCs), chamber volume (including defined medium), and electrode surface area, data can be interpreted and presented in a way that allows conversion to a preferred format by those working from different perspectives; engineers typically give power and current readings with respect to volume, while those concerned with the electrochemistry prefer results to be given in the context of membrane or electrode surface area[65].

Other important ways of processing and presenting data include Coulombic efficiency for each electrode, and overall, which relates the number of electrons supplied by electron donors in a defined media to the current and/or reduction products created.

The substrate used in the defined media can affect this, so acetate is ideally used[67], though sodium lactate is used more widely due to early studies concluding that it was the optimal carbon source for maximising electroactivity[68]. Energetic efficiency is similar, relating energy input and output, while removal efficiency deals with the desired levels of degradation of specific compounds, being more useful for bioremediation or wastewater treatment studies[49].

2.2.2. Equipment and Throughput

Despite the extensive testing in this field, or perhaps because of it, there remains very little standardisation in terms of equipment[29]; there is no field-wide accepted commercially available standard. And this state of affairs only deteriorates when considering higher throughput. While 'multi-well' MFC designs have been published they are not commercially available nor are they used in studies beyond their initial publication[69]. Consequently, testing is limited, both by a need for comparative establishing experiments to verify that equipment behaves as expected, but also, typically, simply by the limited throughput possible with existing protocols. That being said, in spite of ranging methodologies, no baseline experiments are provided to facilitate cross comparison between setups, something we believe to be a gross oversight in the literature.

2.3. Bacterial Electrochemistry

Much early MFC research utilised exogenous mediators, such as methyl viologen, thionine, and neutral red[40], to communicate electrons from bacterial cells to electrodes, but doing so was prohibitively expensive and suffered from issues of toxicity that prevented commercialisation[70]. The use of bacteria capable of reducing extracellular solid metals such as Iron (Fe(III)), often referred to as dissimilatory metal reducing bacteria (DMRB), allowed development of MFCs that didn't require these mediators[71]. Though it has been shown since that the ability to reduce Fe(III) does not always correlate with the ability to generate current in an MFC, many bacteria identified as metal reducing have been shown to be capable of doing so[72]. Several specific mechanisms by which these bacteria transfer their electrons to extracellular sources have been discovered, but research is ongoing to identify more.

2.3.1. Endogenous Mediators

Endogenous mediators are low molecular weight electron shuttling molecules, naturally produced and secreted by many naturally exoelectrogenic strains, which facilitate electron transfer between cytochromes of the bacterial cell and an electrode or extracellular metal[73]. It has been demonstrated that they are able to facilitate this transfer even in strains not naturally exoelectrogenic, having implications for mixed culture MFCs, and being promising candidates for transformation into other organisms that might have issues with other mechanisms[49].

In contrast to *Geobacter sp.,* various *Shewanella sp.* have been confirmed to produce and secrete their own mediators to facilitate access to electron acceptors[74], including riboflavin and flavin mononucleotide[75], though it was earlier hypothesised that quinones acted in this capacity[49]. Figure 2.2. shows the skeletal formulae for these mediators. Noteworthy for their electrochemical role are the hydroxyl groups which will be reduced by the cell in order to transport electrons extracellularly[76]. These mediators have been shown to selectively interact with cytochromes in known direct electron transfer pathways, such as MtrC, increasing the efficiency of electron transfer[77]. Catalytic haem groups nearby FMN binding domains have been identified in a paralog of MtrC, for example[78]. Indeed it has been demonstrated that the ability of *S. oneidensis* MR-1 to utilise its mediators to respire extracellular electron acceptors is dependent on its expression of outer-membrane cytochromes[79,80].

Figure 2.2. Formulae of Riboflavin and Flavin Mononucleotide

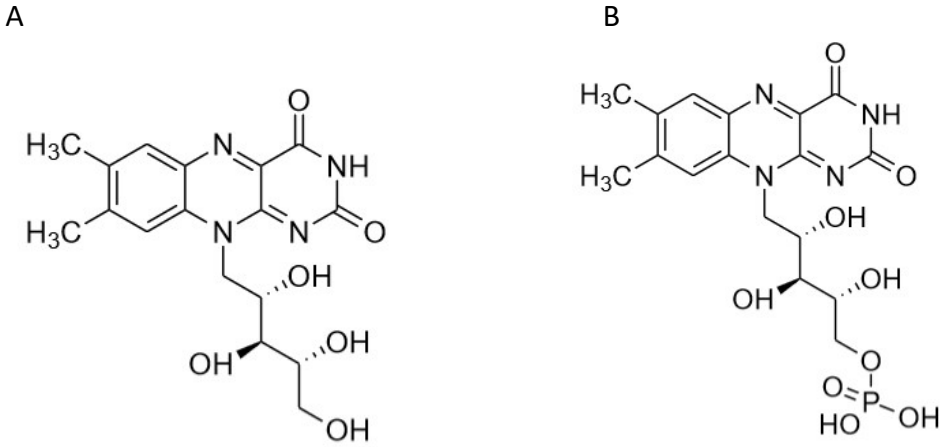

Structure of riboflavin (A) and FMN (B) created using ChemDraw. Of particular relevance to their role as electron mediators, they both possess many hydroxyl (OH) groups, which can be readily reduced, while maintaining sufficient electronegativity to be oxidised by insoluble iron (III) or an anode within an MFC.

It has been shown that *E. coli* can produce some polar species that can act as mediators under anaerobic conditions, despite not being considered an exoelectrogenic bacterium, which may provide an additional avenue for improving its exoelectrogenicity[49]. However these polar species are not as effective as the *Shewanella* mediators previously described. Unlike *Shewanella* sp., *Geobacter* sp. are not known to produce mediators[71].

2.3.2. Direct Electron Transfer

Direct electron transfer (DET) is achieved by electrochemically active proteins on the cell surface interacting directly with the extracellular electron acceptor[40]; though as previously discussed they can also reduce soluble mediators[77]. Understandably for this process to work, proximity is essential, which is why biofilm formation and characteristics may impact exoelectrogenicity; *S. oneidensis* was shown to bind iron surfaces under anaerobic conditions more strongly than it did aerobically, for example[71]. A great many c-type cytochromes have been identified in *S. oneidensis* and other

species, which are believed to be involved in DET, composing multiple pathways, though few have been characterised or studied in detail[81].

C-type cytochromes are a widely studied group of proteins, that utilise bound c-type haem to effect electron transfer within many important redox reactions[82]. They can bind a single or multiple haem cofactors through covalent thioester bonds[83], and are frequently membrane associated[82]. Structurally they are predominantly composed of alpha helices, with loops covering or providing access to the iron centre of their prosthetic haem groups[84], which in multihaem cytochromes are positioned to keep reaction centres within 15.5 Å of each other[85]. *S. oneidensis* MR-1 has 42 c-type cytochromes identified for it[81] with the recognised ability to reduce more than 10 end-terminal electron acceptors under anaerobic conditions[86,87].

The *omcAmtrCAB* operon comprises a particularly well studied pathway of DET, the process of which has been shown to be more effective at transferring electrons than that managed through the riboflavin mediator, with a standard rate constant two orders of magnitude higher[88]. OmcA, MtrC, and MtrA are all decahaem c-type cytochromes, with the former two exposed on the outside of the outer membrane and the latter being present on the inner side[89,90]; MtrB is a transmembrane porin that complexes with the cytochromes to transfer electrons across the membrane[89].

The current model of the pathway also involves CymA, which communicates electrons to the MtrCAB complex from the menaquinone pool in the inner membrane[91] via MtrA, which then passes them to MtrC; MtrC is then able to transfer them to extracellular acceptors directly, or indirectly, similar to OmcA[27]. Figure 2.3. illustrates this pathway transferring electrons from lactate, a commonly used substrate in defined media in MFC research. NapC, a substitute for CymA present in *E. coli* is also described[27,49]. Much like with OmcA there exist many homologous of these cytochromes within *S. oneidensis* MR-1, adding redundancy and adding specificity for additional terminal electron acceptors[82]. Orthologues exist plentifully in other species of the genus, typically well conserved[92].

Figure 2.3. – Extracellular Electron Transfer Pathway

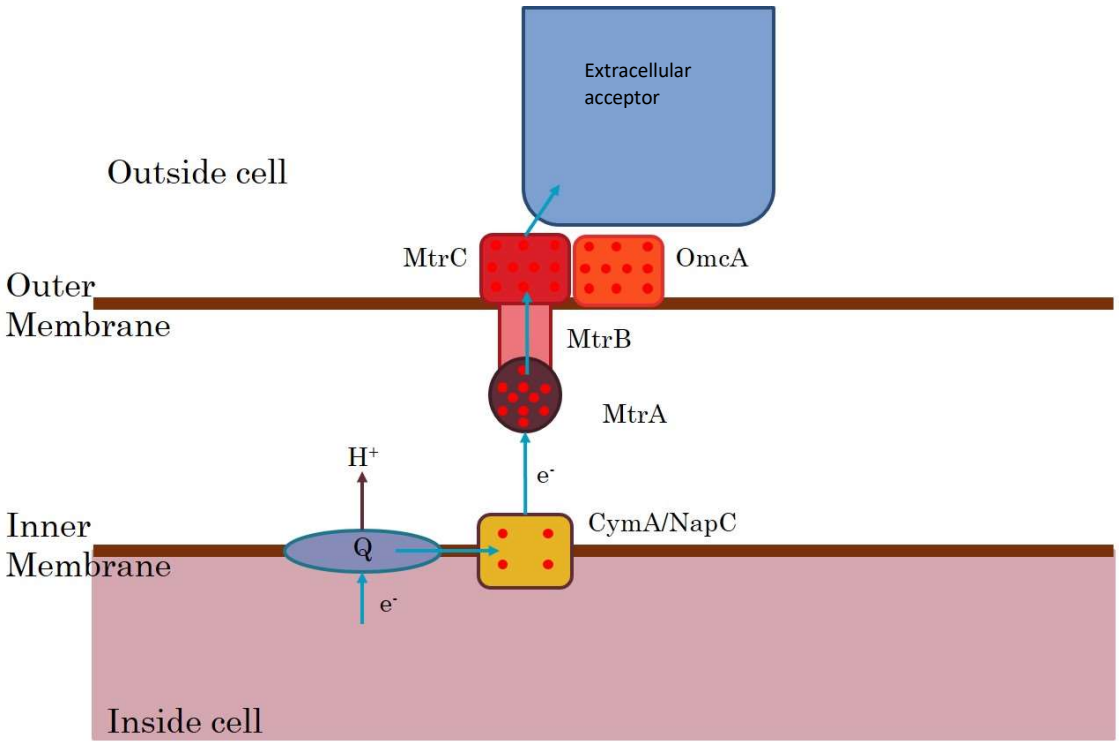

Lactate is metabolised to pyruvate, transferring electrons to the quinone pool via its specific dehydrogenase enzyme. From this pool in the inner membrane NapC in E. coli or CymA in S. oneidensis MR-1 transfers electrons to MtrA, part of the outer membrane MtrCAB complex. From MtrA they are passed to MtrC, thence to an extracellular acceptor either directly, through another outer membrane cytochrome such as OmcA, or an indirect mechanism.

Shewanella sp. are not alone in possessing cytochrome based DET pathways, as many have been identified in other bacteria, such as *Geobacter sulferreducens*, which has over 100 putative c-type cytochromes evident in its genome sequence[49], with a few involved in specific pathways having been characterised, similar to research in *S. oneidensis*[93].

2.3.3. Nanowires

The term “nanowires” covers multiple different structures, and these vary significantly, particularly between the *Shewanella and Geobacter* genera. Generally, nanowires are long, thin structures that extend from cell surfaces, linking cells to each other and the surface of any colonised extracellular acceptor, such as insoluble metal or an

electrode[94]. They are theorised to be involved in extracellular electron transfer by providing a conductive conduit for electrons from the cell to the surface of an electron acceptor[95]; other roles, such as in biofilm growth and structure, may also be performed by them[96]. It has been verified that they play an important role in electron transfer in MFCs culturing *Geobacter* sp., where they are required for extracellular electron transfer[97].

Geobacter nanowires are based on Type IV pili, helical peptide filaments that extent outside of their outer membranes to a multitude of purposes[92]. Those produced by *Geobacter*, though evidenced to have roles in biofilm formation[96] and cell aggregation[98], have been demonstrated to be conductive and play an essential role in the reduction of iron and other external electron acceptors[99]. Given their ordered structure, small size, and relative ease of production these structures are being investigated for biotechnological applications within and beyond BESs[98,99].

Morphologically distinct (from *Geobacter sp.*) nanowires have been identified in *Shewanella oneidensis* MR-1 that are found in thick bundles and have been confirmed to be conductive[100]. *Geobacter* nanowires typically extrude from one side of the cell towards the electron acceptor surface[100]. However it has been demonstrated that *Shewanella* nanowires likely consist of a number of c-type cytochromes set at intervals within a membranous structure, allowing electrons to hop along them[101]. Furthermore, the importance of outer membrane cytochromes in order to maintain conductivity has been shown[102]. These structures, in contrast to *Geobacter sp.,* are thought to be an extension of the outer membrane, rather than pili-like structures, formed through fusion of outer membrane vesicles[103]. Work is still needed to fully understand how they might be exploited in BES applications and the mechanisms involved, however[49,101].

2.4. *E. coli* for Electroactivity Research

E. coli, the gram negative, facultative anaerobic bacteria, has long been among the most highly studied organisms within science[104]. This has led to a wealth of tools and techniques for genetically manipulating it and achieving a level of control and understanding not possible in other bacteria. However, while it is well studied from a pure scientific standpoint, the principles of synthetic biology, which are so minded towards application and modularity, have only come to the fore to make use of this resource relatively recently[21].

2.4.1. E. coli and Synthetic Biology

Synthetic Biology is a relatively young field, though growing exponentially, which applies the principles of engineering to molecular biological research in order to produce either completely synthetic organisms, or modify existing organisms and biological systems, all towards a useful purpose[19]. It employs concepts such as standardisation and interchangeability of abstracted "parts" and "devices", genetic components that make up genes and operons with products that perform specific functions, to facilitate rational design of useful biological system in much the same manner as circuit design in electrical engineering[105]. The field enables a more applications-based view of genetic engineering and aims to progress towards a point where organisms can be tailor-made for specific tasks easily using simple abstracted design without a need to manually modify or string together sequences[106]. With fully characterised parts and well-designed computational tools for the strain design process, a thorough understanding of each individual part should not be necessary, speeding up the process of biological engineering.

Many standards exist in the field, and these have changed over time as it has developed. BioBricks are an example of such a standard. A BioBrick part is a DNA sequence that has a function, such as a ribosome binding site, coding sequence, or promoter. The principle behind the standard is that parts can be strung together easily to form devices that operate to each achieve a specific effect. Originally developed by Tom Knight[107], it has since been improved and is used by teams competing in the iGEM competition, which contribute to the growing registry of parts available in the public domain. Specific prefix and suffix restriction sites are used around the sequences for individual parts for ease

of genetic manipulation and interchangeability[108]. Unfortunately, while thousands of parts are available, very few have been characterised[108], and the usefulness of characterisation can vary due to the differences in functionality when different host organisms are used[20]. As such, while the registry can be a valuable resource it is not quite at the level of electrical engineering. Characterisation remains a challenge in general in the field[109]. Particularly as even the best studied model organisms are only partially understood, though it is clear that additional chassis organisms to suit different purposes are required to advance the field[110].

A few other key challenges further separate synthetic biology from other engineering disciplines, requiring consideration. The complexity of biological systems, coupled with our own incomplete understanding of them, features prominently. Continuing from that point is that parts, when assembled, will not always function together as expected, taking a great amount of time to correct[111]. The biological chassis organisms used, such as *Saccharomyces cerevisiae*[112] or *E. coli,* can also have interacting proteins of their own, and have limits in the amount they can be made to reliably express on plasmid based systems, with greater insert sizes resulting in lower viability and cell growth[113].

As the complexity of these designed systems grows, the more components used, the amount of time required to create them and test their functionality also increases. This increase in required resources can limit the feasibility of many studies; the full potential cost in time of any device creation and testing in future work should be carefully considered in advance to prevent overly ambitious plans[20]. Computational predictions may assist in the process, saving time by highlighting potential issues with designs, but can be limited by our understanding of the biological systems being used, which for exoelectrogenic processes is incomplete. Work to automate characterisation, not only of parts but of interactions between parts is ongoing[111], but is greatly aided by advances in high-throughput equipment such as with liquid handling robots[104]. Additionally, directed evolution, in which a sub-optimal device is mutated and mutants screened and selected for based on the desired phenotype, may be used to overcome the need to manually tinker with the design of a device in order to fully optimise it[20,114,115].

While *Shewanella oneidensis* MR-1 may be the initial resource for genes involved in exoelectrogenicity, *E. coli* strains, as previously mentioned, have been extensively studied with arguably more resources for genetic modification and other biochemical techniques than any other organism, which reinforces their position as optimum chassis organisms, and evidence them to be easily genetically manipulable [109,116,117]. They are also capable of growing under the anaerobic conditions required in an MFC anode chamber and utilising a wide variety of carbon sources[118]. However it is important to remember that incompatibilities may arise when expressing any foreign proteins, though tools exist to counteract certain effects [21].

2.4.2. The Challenges of Heterologous Expression

As discussed, for a synthetic biology approach to succeed characterisation of the required parts is needed, and unintended interactions between different parts and devices must be minimised by ensuring predictability[20]. Both of these depend upon an understanding of the mechanism of the devices involved. In the case of electroactivity, this means both a wider and deeper understanding of the mechanisms of EET not just in their native organisms, but how these operate heterologously. Given the requirement for effective dependence on a foreign electron transport chain for terminal electron transport, due consideration needs to be given to the host metabolism; full advantage may not be taken because the regulatory machinery for host processes hasn't evolved to be able to interpret the new situation. Localisation issues may also occur if signal sequences are not compatible between species, though fortunately there is not a problematic phylogenetic distance between *S. oneidensis* MR-1 and *E. coli*[119]. This applies, too, to gene expression where a promoter is not manually installed before heterologous genes – of particular relevance in library studies, as *E. coli* transcription and translation systems can recognise *S. oneidensis* MR-1 promoters to affect the expression of their associated genes[120].

One factor often considered when attempting to optimally express heterologous genes is differences in codon bias between organisms[32]. During the process of translation, where an RNA sequence is read by a ribosome, tRNAs convey the relevant amino acids to the translation machinery by recognising codons through complementarity – three base pair sequences that the ribosome exposes[121]. There are 64 possible codons, given the four nucleotides used, and of these all but three correspond to amino acids, while the rest signify stop signals[32,121]. However, as there are only 20 amino acids employed universally to form proteins, there is codon redundancy for each. Codon bias refers to the relative balance or prevalence of these redundant codons within an organism's highly expressed coding sequences[32]. The available tRNA pool for a specific codon can be depleted by expression, which is more likely to occur when it is a little used codon by the organism in question. In order to maximise efficient expression, then, the codon bias

of a given heterologous sequence is often adjusted to match that of the chassis organism.

Other concerns for heterologous expression go beyond transcription and translation. Assuming a sufficiently conserved or synthetic promoter prompts transcription, and that codon bias and conserved ribosome binding sites permit translation, maturation and localisation remain. This is particularly a concern for the large, multi-haem, integral membrane cytochromes involved in the MtrCAB EET pathway, as haem production and correct addition to the polypeptide resulting from translation of their transcripts is required for them to function, as is transport to and insertion into the outer membrane where relevant[23,122]. While *E. coli* host strains typically have their own cytochrome maturation genes to assist with the first part of this, most published engineered strains employ additional cytochrome maturation genes (induced or constitutively expressed) to ensure correct maturation[26,122]. These studies have also demonstrated that signal sequences are sufficiently conserved to facilitate correct localisation of these proteins.

For heterologous proteins or pathways that are correctly transcribed, translated, matured and localised, full functionality can still not be guaranteed. Interactions with host processes not evolved to utilise, regulate, or operate in the presence of this new pathway are the principle challenge then faced[104]. Unintended and often detrimental reactions between proteins or metabolites can occur, or the overexpression of a heterologous enzyme can deplete metabolites in a way that would cause the host to alter its regulation in an undesirable way[104]. For *E. coli* strains engineered to be more electroactive, the host strain hasn't evolved to utilise the heterologous EET pathway, and with the link between it and the host metabolism, we cannot be sure where rate limiting steps lie, or what regulatory process are resulting from its activity. At least not without further study.

2.6. Conclusions

Much remains to be understood about bacterial EET, not only in naturally electroactive bacteria, but also in recombinant *E. coli* strains. Yet we feel that the lack of standardisation and comparability between testing setups and strains has hindered progress. Researchers in the field do not do it any service by not being detailed about the specifics of their equipment and testing methodologies, but there is only so much that can be done without standardised, commercially available equipment and materials. This may come in time, but while BES design continues to change at a rapid pace it may not be feasible for private companies to invest in providing such technologies to small scale researchers.

E. coli particularly may be a powerful tool for research into electroactivity, given the ability afforded to study factors in relative isolation. With the greater genetic control and biological understanding possessed for it, it may even be a superior candidate for certain bioelectrochemical applications than DMRB. A focus however needs to be placed on characterisation and iterative improvement of an electrogenic *E. coli* strain, to make synthetic biology applications feasible in the near future. Closing the gap between the performance of engineered *E. coli* strains and the naturally electroactive DMRB will be essential to facilitate its success going forwards. The *S. oneidensis* MR-1 derived MtrCAB pathway, however, is a solid foundation on which to build. There is no strong argument to start from the ground up and develop strains reliant on *Geobacter sp.* nanowires, for example. Other features may later be introduced to improve electroactivity, and identification of such would be useful in the long run, but it would be best to focus on understanding and addressing the factors limiting current strains and their derivatives before investing in such alternatives.

Chapter 3 – Materials and Methods

3.1. Bacterial Culturing

3.1.1. General Microbiology

Unless otherwise noted, all bacterial starter cultures were inoculated by the transfer, via sterile inoculating loop, of a colony from an LB agar (Fisher Scientific) plate containing relevant antibiotics, into a 50 ml Falcon tube containing 10 ml sterile LB broth (Fisher Scientific). These were then incubated at 37 ^{o}C or 30 ^{o}C as appropriate to the strain (*E. coli* the former, *S. oneidensis* MR-1 the latter), 150 rpm overnight before use.

100 ml LB agar were prepared according to manufacturer's recommended concentration in 200 ml conical flasks. These were stoppered with sponge bungs and topped with tin foil before autoclaving at 121 ^{o}C, 1.05 bar pressure, for 20 minutes. Solidified sterile agar was melted prior to use over 2 minutes in an 800 W microwave, then placed in a 55 ^{o}C water bath to cool. Antibiotics were added before pouring, always to a 1 in 1000 dilution, due to stock concentrations. Benches were sterilised with 70% denatured ethanol (Crystel SILVER – Tristel), and a Bunsen maintained on a blue flame for the duration of the pouring and subsequent sterile work. Molten agar was poured into vented Nunc petri dishes (Thermo Scientific) and left to cool, before briefly drying in a drying oven at 37 ^{o}C. Between 4 and 6 plates were poured from each 100 ml flask, and storage of spare plates was maintained at 4 ^{o}C up to one week before use.

LB agar plates were inoculated by sterile loop. A metal loop was sterilised in a blue Bunsen flame for no less than 10 s before cooling beside it. This was then used to either transfer a colony from another plate, or dipped into a liquid culture, and streaked across the plate. After resterilisation of the loop, the plate was further streaked crosswise. This was repeated twice more, in order to ensure single colonies on the plate. Plates were then incubated at 37 ^{o}C or 30 ^{o}C as appropriate to the strain (*E. coli* the former, *S. oneidensis* MR-1 the latter).

Larger broth cultures were inoculated from starter cultures with a 1 in 100 dilution unless otherwise described. The sterile media was prepared similarly to LB agar, sterilised in the same way. Either LB broth or 2xYT (Fisher Scientific) was used, though the former more frequently and thus by default if not otherwise noted. These cultures were incubated under the same conditions as their respective starter cultures.

Sterile liquid transfer was most commonly achieved by either 10 ml or 25 ml serological pipette (Stripette – Sigma) using a serological pipette bulb (Fisher Scientific), with sterile technique. Alternatively, smaller volumes transferred by pipette (StarLab).

Glycerol stocks were prepared by mixing 500 µl overnight culture with 500 µl sterile 50% glycerol in a sterile 1.5 ml microcentrifuge tube (Eppendorf), vortexing or inverting briefly, then storing at -80 ^{o}C.

3.1.1.1. Antibiotic Stocks

Chloramphenicol (Cm), Ampicillin (Amp), and Kanamycin (Kan), were prepared at stock concentrations of 20, 100, and 20 mg/ml respectively. Each was diluted 1 in 1000 for use. Cm was prepared in 100% ethanol, Ampicillin in 50% ethanol, and Kan in dH_2O. Kan was filter sterilised with a 0.22 µm filter. All were aliquoted into 1.5 ml microcentrifuge tubes and stored at -20 ^{o}C.

3.1.2. Chemically Competent Cell Preparation

Prepared and autoclaved in advance were 80+ 1.5 ml microcentrifuge tubes (Eppendorf), 100mM CaCl2.2H20 (1.47g in 100ml), 100mM MgCl2.6H2O (2.01g in 100ml), 50% glycerol, and 200 ml LB in a 500 ml conical flask, as well as an overnight culture of the relevant strain. The morning of the protocol, the overnight culture was diluted 1 in 100 into the 200 ml LB flask and incubated at 37 ^{o}C, 150 rpm. After 1.5 hours the OD_{600} was measured spectrophotometrically at intervals of 15 minutes against an LB broth blank, until an OD_{600} of between 0.5 and 0.8 was reached, favouring a reading closer to the former. After this point was reached the flask was placed on ice for 10 minutes, with gentle agitation.

The cells were transferred to 4 50 ml Falcon tubes and centrifuged at 4000 xg for 10 min, 4 ^{o}C. The supernatants were discarded and the pellets each gently resuspended in 20 ml 100 mM $MgCl_2$, by swirling. They were then centrifuged again under the same conditions, and supernatant discarded.

The first pellet was gently resuspended in 6 ml 100 mM CaCl2, by swirling, then the suspension transferred to the second tube and the process repeated until all four pellets were resuspended in the 6 ml volume. This was then placed on ice for 1.5 h to facilitate competency, after which time 1.8 ml sterile 50% glycerol was added, gently swirling, to homogeneity. Aliquots of 100-200 µl were transferred into sterile 1.5 ml microcentrifuge tubes that had been pre-chilled at -20 ^{o}C, and placed on ice. These were then stored at -80 ^{o}C.

3.2. Molecular Biology

3.2.1. DNA Extraction

In order to conduct polymerase chain reactions (PCRs), digests, or sequencing, the extraction of DNA necessary for the purpose was required. In the case of plasmids, the Qiagen Spin Miniprep kit was predominantly used according to the manufacturer's instructions, with elution in 30 µl of nuclease free (nf) water previously heated in a 50 ^{o}C water bath to maximise DNA concentration. Fosmids were initially extracted by the same method, but it was found that using the recommended cell volumes for Midiprep kits with the Qiagen Miniprep kit (note: not the Spin Miniprep kit) gave greater concentrations, and so was used instead subsequently. Genomic DNA was extracted with the Qiagen DNeasy blood and tissue kit, again according to manufacturer's instructions.

DNA extraction from gels was either achieved with a Qiagen Gel Extraction kit in the case of agarose gels, or with the GELase (epibio) enzyme preparation, each according to their respective manuals. Gel fragments were recovered by excising with a scalpel.

3.2.2. Agarose Gel Electrophoresis

Concentrations of DNA extractions were tested by running a 1 µl aliquot on a 1% agarose gel as follows. 1.2g of agarose (Fisher Scientific) were added to 120 ml 1xTAE (diluted from 10x UltraPure TAE buffer - Thermo Fisher Scientific) and dissolved by heating in a microwave. 10 µl of ethidium bromide solution (Fisher Scientific) the intercalating agent that allows visualisation of DNA through fluorescence under ultraviolet light (UV), was carefully added after the solution was no longer bubbling, and the gel solution poured into the prepared gel casting tray with the appropriate gel comb inserted. After approximately 20 minutes of setting the gel was ready for use. The autoclave tape used to seal the ends of the casting tray were removed and the tray placed in the gel tank in the correct orientation. The tank was then filled with 1x TAE up to the fill line, and the gel comb removed to permit filling of the wells.

Standard well volumes would accommodate up to 20 µl, however, where necessary larger wells were created by taping comb teeth together. 5 µl hyperladder 1 (Bioline, UK) was run in alongside samples as standard, typically in the first lane. Samples were prepared by adding 1 µl (or more as required) DNA to 2 µl 6x loading buffer, then made up to 12 µl with nf water.

Gels were run at 120 mA for 40 minutes, though an additional 20 minutes of run time was used in cases where greater separation was desired. For fosmid separation, 30 V overnight was originally used to test shearing. Size selection was achieved by running a 1% low melting point (LMP) agarose unstained by ethidium bromide (Thermo Fisher Scientific) gel for three days at 4 ^{o}C (in a controlled temperature room); the recommended protocol in the CopyControl manual proved insufficient.

Gels were imaged using a UVP GelDoc-It TS, following the completion of their runs and removal from their tanks. These images were then transferred to a computer via memory card.

3.2.2.1. DNA Concentration Quantification

Comparative analysis of band intensity between samples and ladder was predominantly used for quantification of DNA concentration, however this was supplemented by spectrophotometric quantification using the nanodrop.

2 µl of dH_2O was pipetted onto the nanodrop and used to blank the machine before being wiped away. A further 2 µl dH_2O was applied and measured to check the cleanliness of the equipment. This process was repeated until appropriate readings were consistently detected (twice in succession). Subsequently, 2 µl of sample were pipetted out, then measured. For multiple samples, a 2 µl dH_2O was step was conducted as previous between each sample measurement.

3.2.3. PCR

Polymerase chain reaction was used to amplify specific sections of DNA through the binding and extension of primers. It was also used to add restriction sites to the ends of an amplified sequence as required. Details of this are discussed further in the primer design section. While a standard protocol is presented herein, for many PCR reactions conducted changes in annealing temperature was required to suit the primers, and variations in temperature, time, and DNA concentration were made in order to produce the products desired.

For an individual PCR mixture, 35 µl of nf water are added alongside 10 µl HF buffer, 1 µl dNTPs, 1 µl 100 µM forward primer, 1 µl 100 µM reverse primer, 1 µl template DNA, and 1 µl Phusion Hot Start DNA polymerase. All components other than the nf water, primers, and DNA were provided in the Phusion Hot Start II High Fidelity DNA Polymerase kit (New England Biolabs, UK). For multiple PCRs a mastermix was created of the components common to them all to save on pipetting time and equalising pipetting error across all PCRs being conducted. These reaction volumes were all set up in 200 µl PCR tubes before insertion into a PCR thermocycler.

While the Phusion DNA polymerase method was used predominantly in this work, for the fosmid overlap individual gene constructs success was ultimately achieved with Q5 High-Fidelity 2x Master Mix (New England Biolabs, UK). 25 µl were used for a 50 µl reaction, while volumes of template DNA and primers remained the same. The remaining volume was adjusted to the final volume with nuclease free water.

The standard temperatures and times used in the PCR thermocycler are as follows: 95 ^oC for two minutes in the first stage; 95 ^oC for 30 s, followed by annealing temperature

(typically between 50-72 ^{o}C) for 15 s, then 72 ^{o}C for 15-30 s per kb of product for the second stage; the second stage is repeated 30 times before the third stage consisting of 72 ^{o}C for 10 minutes, then 4 ^{o}C until end.

3.2.3.1. Primer Design

Primers initially and primarily comprise a complementary sequence to the target strand desired. Care must be taken to select the correct strand for complementarity as extension occurs only in a 5' to 3' direction. The sequence chosen should be specific, and lack repetitive sequences or long strings of adenine or thymine. Often a non-complementary sequence is added on to the 5' end of the primer in order to add in a restriction site. This restriction site must be selected with all sequences in the various stages of cloning in mind, as it should be a unique cutter to avoid complications. A few base pairs extra should be added onto the 5' of the restriction site to facilitate restriction enzyme binding to the sequence. The length of the sequence, particularly the complementary region can be adjusted, with GC content in mind, in order to adjust the melting temperature of the primer. All primers were designed using snap gene, and New England Biolab's online restriction calculator to check for buffer compatibility.

3.2.4. Homologous Recombination

While other approaches were attempted to replace the Cm^R cassette in the pEC86 plasmid with an Amp^R cassette, homologous recombination was the one that ultimately succeeded. It is first worth noting that all tubes solutions and cuvettes described herein were pre-chilled.

A starter culture of *E. coli* bearing pKD46 was set up and incubated at 30 ^{o}C. When OD_{600} reached 0.1 λ-red expression was induced by the addition of 20 µl L-arabinose stock, and growth continued to until OD_{600} reached 0.4-0.6. 1 ml aliquots were then made into 2ml microcentrifuge tubes, which were chilled on ice for 10 minutes, before centrifugation at 4000 xg for 10 minutes at 4 ^{o}C. Following discard of the supernatant the cell pellet was gently resuspended in 1 ml ice-cold 10% glycerol (in dH_2O), then centrifuged again under the same conditions. This wash step was repeated with 0.5 ml ice-cold 10% glycerol, then 50 µl ice-cold 10% glycerol.

The PCR product of the Amp^R cassette with added homologous ends to either side of the Cm^R cassette in pEC86 was added to these cells to a concentration of 0.5 µg, and the mixture transferred to chilled electroporation cuvettes. It is worth noting that the DNA sample used was salt free, due to elution in nf water when purifying, as to do otherwise would result in arcing within the electroporation cuvette. The cuvette was also dried before insertion for the same reason. The cells were then electroporated at 200 Ω, 25 µFd, under volts 1.8 kV, with a time constant of 4 ms. 1 ml of room temperature LB broth was immediately added to the cuvette following this, and the contents then transferred to a 1.5 ml microcentrifuge tube at room temperature.

Following incubation of these cells for 1 h at 37 ^oC (removing the temperature sensitive pKD46), with gentle agitation, the cells were plated on LB agar + Amp plates and incubated for 24 h at 37 ^oC. Cells that were not electroporated, were plated out additionally as a control. Colonies on the recombined plate were subsequently subcultured, minipreped, and the plasmids sent off for sequencing to confirm correct homologous recombination before transformation into BL21(DE3) alongside other relevant plasmids for testing.

3.2.5. Heat Shock

Chemically competent cells prepared as previously described were further aliquoted into pre-chilled 1.5 ml microcentrifuge tubes to a volume of 50 µl. 10 µl of ligated DNA, or 20-40 ng of plasmid DNA was added, and the cells incubated on ice for 30 minutes. The cells were then heat shocked for 90 s at 42 ^oC then place on ice again for 2 minutes. 1 ml of LB broth was added, and the sample incubated at 37 ^oC for 90 minutes, 150 rpm. The cells were then centrifuged at 4000 xg in a benchtop microcentrifuge, and 850 µl of supernatant discarded. The remainder was used to resuspend the pellet. 100 µl of the resuspended culture was then plated out on LB agar plates containing the relevant antibiotic(s) to the plasmid(s) used, which were then incubated for 16 h at 37 ^oC. In the case of ligations, a ligation mixture excluding the desired insert was used as a control. If unsuccessful in producing colonies, and assuming no or few colonies on the control plate, the remaining culture volume left incubating at room temperature was plated similarly.

3.2.6. Digest and Ligation Reactions

The standard digest protocol followed for DNA digests used 2 µl of the appropriate 10x buffer to the enzymes required (often CutSmart), an amount of DNA depending on need and concentration, with the volume made up to 19 µl by nf water in a 1.5 ml microcentrifuge tube. While this concentration was adjusted to optimise some reactions, the majority of reactions used the maximum possible, given available samples. Finally, after mixing, 1 µl of enzyme was added. The mixture was then incubated at 37 ^{o}C for 1 h (though times could be extended depending on enzyme), and either analysed on an agarose gel, or 1 µl calf intestinal phosphatase added if plasmid DNA for ligation were being digested. If the latter, the reaction was incubated for a further hour.

For ligation, once the samples were run on an agarose gel they were extracted as previously described. Alternatively, a Qiagen PCR cleanup kit could be used to facilitate purification. The ligation reaction was then set up as follows with template and insert volumes adjusted depending on concentration, size, and the results of a ligation calculator; typically a 3:1 ratio of vector to insert was used initially, but others were used in the course of optimisation for certain constructs. X µl linear plasmid DNA, X µl insert, 2 µl ligase buffer, 1 µl ligase, difference to 20 µl made up with nf water.

3.2.7. Fosmid Library Creation

As previously described, a genomic DNA extraction was carried out using 1 ml of OD_{600} 1.0 overnight culture of *Shewanella oneidensis* MR-1. The Qiagen Blood and Tissue Kit was used according to the manufacturer's instructions, though with the 200 µl eluted DNA passed through the spin column an additional time to maximise yield. Concentration was assessed by running a 2 µl aliquot on a 1% analytical agarose gel containing ethidium bromide at 120 mA for 1 hour.

With the genomic DNA of a suitable concentration, the manufacturer's instructions for creating a Fosmid Library using the CopyControl Fosmid Library Production Kit (Epicentre) were carried out. No Pulsed Field Gel Electrophoresis (PFGE) apparatus was available, so the manufacturer's alternative for assessing DNA shearing in the extracted

genomic DNA was conducted. With genomic DNA of the right concentration and shearing, an end repair reaction was initiated, the products of which size selected using a 1% low melting point (LMP) agarose gel with no ethidium bromide, running in the large lanes created by taping comb teeth together. The melting and smearing of the gel resulted in a re-evaluation of the protocol. Subsequent gels were run at 30 V, at 4^{o}C, for 3 days.

The sides of the gel containing the edges of the genomic DNA band, control DNA bands, and GeneRuler HR, were stained with ethidium bromide and visualised to guide the excision of the genomic DNA band in the desired size range. This excised gel band was stored temporarily at -20^{o}C before the DNA was extracted using GELase (epibio) according to the manufacturer's instructions, and its resulting concentration checked by running an aliquot of 1 µl on a 1% analytical agarose gel. Once the appropriate concentration was obtained, the ligation, packaging into phage capsid, and phage titre steps were carried out in order. The provided EPI300 *E. coli* cells were transfected at a titre expected to produce >600 clones. After the manufacturer's protocol proved inefficient, clones were harvested from agar plates for storage at -80^{o}C using a sterile plastic inoculating loop, resuspended in LB, with separate aliquots measured out before the addition of the glycerol to an end concentration of 20%.

3.2.8. Sequencing

All verification by sequencing was conducted using the University of Sheffield's Core Genomics Facility in the Medical School. Data was analysed using FinchTV, with sequences subsequently compared using SnapGene.

3.3. Bioelectrochemistry

3.3.1. Half Cells

Half Cells (HCs) were prepared using 250 ml Duran or Schott bottles, autoclaved containing 225 ml of M4m media supplemented with 0.4% Sodium Lactate. Red Rod reference electrodes (Radiometer Analytical REF201) were cleaned beforehand according to manufacturer's instructions with an interior saturated KCl wash, a pepsin (Applichem) wash, and bleach wash (Renovo X). Platinum wire counter electrodes (IJ

Cambria Scientific Ltd, UK) were cleaned with ethanol during HC disassembly and prior to assembly. Carbon working electrodes (Wes) were prepared by cutting disks the size of the lids of the 250 ml bottles, out from carbon veil (PRF Composite), leaving an overlap between every pair of circles so they could be folded over to give a two layered disk. Four nichrome wires (Scientific Wire Company – Nickel Chrome wire 0.45 mm, 125 gr) were then threaded through from the centre to the edge in four separate directions, and then the wires twisted around each other to form a thick wire leading from the centre of the disk. These electrodes were autoclaved before use in a foil-topped 1 L beaker. Glass pipettes (SLS) were also autoclaved within foil to sterilise for HC assembly.

Overnight cultures of 10 ml LB broth supplemented with any relevant antibiotics and grown at appropriate temperature (30^{o}C for *Shewanella* spp., 37^{o}C for *E. coli*) were used to inoculate conical flasks containing 200 ml LB broth (or 100 ml 2xYT in 200 ml flasks) with any antibiotics. These were grown at 200 rpm at 30^{o}C until an OD_{600} greater than 0.6 was achieved. 10 µM IPTG was used to induce MFe strains, while all others received 0.5 mM.

The volume required to be pelleted and resuspended in 25 ml, which was to be added to the 225 ml containing Half Cell to reach a final OD_{600} of 0.04 (or later for *E. coli* strains, 0.4), was calculated and measured out. Cells were centrifuged at 5000 xg for 10 minutes at 4 ^{o}C. Resuspended cells were kept on ice until HC assembly was conducted. Antibiotics and other supplements were added to the HC bottles prior to the assembly step.

HCs were assembled with all electrodes and glass pipettes accommodated through holes in the lid. The resuspended cells were then added to the labelled HCs. While a silicone sealant was previously used in the old two-electrode HC system to seal the top while assembly was conducted within an anaerobic cabinet, the permeability of silicone to oxygen made this unnecessary, and was ultimately replaced with the constant sparging through glass pipette. PicoLog voltage recorders (Pico Technology) similarly previously were used to measure potential at the WE while HCs inoculated to a starting OD_{600} of 0.25 were incubated in a water bath at 25^{o}C for a period ≥1 week. This was adjusted first to use a portable PG581 potentiostat (BioLogic) measuring the current of a single HC at

30 ^{o}C under a poised potential of 0.2 V vs Ag/AgCl reference electrode and constant sparging with N_2, then to use an Arbin FCTS (Arbin Instruments) to test 12 HCs in parallel under the same conditions.

One litre of M4m media was made from 0.221 g K_2HPO_4, 0.099 g KH_2PO_4, 0.168 g $NaHCO_3$, 1.189 g $(NH_4)_2SO_4$, 7.7305 g NaCl, 1.192 g HEPES, 10 ml $CaCl_2$ stock (7.13 g $CaCl_2{\cdot}2H_2O$ in 1 L dH_2O, autoclaved), and 10 ml trace mineral solution. 0.4% w/w of Sodium Lactate was added to media before autoclaving. Trace mineral solution comprised of 2.26 g $Na_2EDTA{\cdot}2H_2O$, 24.89 g $MgSO_4{\cdot}7H_2O$, 0.029 g $MnSO_4{\cdot}4H_2O$, 0.058 g NaCl, 0.068 g $FeCl_2$, 0.065 g $CoCl_2$, 0.029 g $ZnSO_4{\cdot}7H_2O$, 0.005 g $CuSO_4{\cdot}5H_2O$, 0.35 g H_3BO_3, 0.08 g $NaMoO_4$, 0.119 g $NiCl_2{\cdot}6H_2O$, 0.028 g $Na_2SeO_4{\cdot}10H_2O$, in 1 L dH_2O, autoclaved.

Similarly one litre of M1 was composed of 15.12 g PIPES, 0.3 g NaOH, 1.5 g NH_4Cl, 0.1 g KCl, 0.59 g NaH2PO4•H2O, 5.84 g NaCl, with 0.4% w/w Sodium Lactate added prior to autoclave, made up to 1 L with dH_2O and adjusted to pH 7.4. Subsequent to autoclaving, 2.5 ml each of the vitamin, mineral and amino acid stocks were added to each HC bottle just before assembly.

100X M1 vitamin stock comprised the following made up to 1 L with dH_2O, and filter sterilised: 2 mg D-biotin (B7), 2 mg folic acid (B9), 10 mg pyridoxine HCl (B6), 5 mg thiamine HCl (B1), 5 mg nicotinic acid (B3), 5 mg D-pantothenic acid, 5 mg hemicalcium salt (B5), 0.1 mg cobalamin (B12), 5 mg p-aminobenzoic acid, and 5 mg a-lipoic acid. Stored at 4°C, protected from light.

100X M1 amino acid stock comprised the following made up to 1 L with dH_2O, and filter sterilised before storage at 4 ^{o}C: 2g L-glutamic acid, 2 g L-arginine, and 2 g D,L-serine. 100X M1 trace mineral stock, prepared and stored similarly included: 2017.4 mg $C_6H_9NO_6Na_3$ (Na-NTA), 3121.2 mg $MgSO_4{\cdot}7H_2O$, 500.3 mg $MnSO_4{\cdot}H_2O$, 1000 mg NaCl, 100 mg $FeSO_4{\cdot}7H_2O$, 100 mg $CaCl_2{\cdot}2H_2O$, 100 mg $CoCl_2{\cdot}6H_2O$, 129.5 mg $ZnCl_2$, 10 mg $CuSO_4{\cdot}5H_2O$, 10 mg $AlK(SO_4)_2{\cdot}12H_2O$, 1 mg H_3BO_3, 2.4 mg $Na_2MoO_4{\cdot}2H_2O$, 2.4 mg $NiCl_2{\cdot}6H_2O$, and 25.1 mg $Na_2WO_4{\cdot}2H_2O$.

The HC experimental data were exported into a Microsoft Excel compatible format and subsequently analysed using GraphPad Prism.

3.3.1.1. Sample Collection for Proteomics

Following cessation of potentiostatic control by the Arbin FCTS (Arbin Instruments) HCs from which biomass was to be harvested were disconnected (reference electrode disconnected last), and removed from the water bath. Disconnected HCs were then disassembled, using sterile technique, with the WE removed last. WE removal was conducted after agitation to dissociate adhered cells. A final OD_{600} measurement was taken spectrophotometrically with 1 ml of the cell suspension against a blank of the appropriate media. The remaining volume was transferred to labelled 50 ml Falcon tubes and centrifuged at 5000 xg for 10 minutes at 4 ^{o}C, then the supernatant discarded. Cell pellets were then briefly stored at -20 ^{o}C before protein extraction.

3.3.2. Dye Reduction Assay

Overnight cultures were grown up in LB at 37^{o}C for *E. coli* strains and 30^{o}C for *Shewanella* spp. with agitation at 150 rpm for preliminary testing, however subsequent testing saw inoculation of a starter plate containing only LB broth with colonies picked from agar plates. The starter plates were grown under similar conditions. 1 in 100 dilutions in LB were performed for preliminary testing, while 15 µl per well were transferred from starter plate to dye plate subsequently. Antibiotics at necessary concentrations were included as required. Plates were prepared by pouring the media to be transferred to the plate into a sterile petri dish in a laminar flow hood, then transferring it to the 96-well plate with a multichannel pipette. Stocks and dilutions of dyes are detailed in Table 3.1. below. Once dye plates were inoculated, a Tecan plate reader (GENios Tecan) was used to take a zero reading at the absorbances indicated in Table 3.1., before separate plates were incubated at 25^{o}C aerobically and anaerobically for 72 hours, except where otherwise described. Observations of colour changes were made and a final reading was taken in the Tecan. Where a range of dye concentrations were used, 1 in 100, 200, 400, 600, 800, and 1000 dilutions were performed from stocks.

Following protocol changes the dye free wells were removed, granting space for multiple dyes to be used on the same plate, or higher throughput analysis with a single dye. Control wells containing just dye in LB were still used. After incubation and a pre-centrifugation reading, plates were spun down at 4000 xg for 10 minutes, then supernatant transferred to a new plate to be read in the Tecan. Wavescans were carried out using the initial dilutions listed in Table 3.1. using the Ultrospec 2100 Pro spectrophotometer's wavescan function.

Table 3.1. – Dyes Used in Colourimetric Screens

Name	Stock Concentration	Dilution for Use (Initial)	Dilution for Use (Optimised)	Absorbance Filter Used
Reactive Black 5	1% w/v	1 in 1000	1 in 100	595 nm
Reactive Red 120	50 mg/ml	1 in 100	1 in 1000	530 nm
Basic Green 5	2.7 mM	1 in 100	N/A	660 nm

3.4. Protein Methods

3.4.1. Protein Extraction

Cell pellets were thawed on ice before being resuspended in 1 ml extraction buffer (6 M Urea, 150 mM NaCl, 100 mM TEAB, 1 mM EDTA, pH8.0). Suspensions were sonicated on ice in 8 rounds of 15 seconds on, 45 seconds off, with the tip cleaned between rounds, then centrifuged at 21,000 xg for 30 minutes at 4 ^{o}C. Supernatant was extracted and placed in LoBind (Eppendorf) tubes. An aliquot of each was transferred to a separate tube and stored at -20 ^{o}C for analysis, while the rest was stored at -80 ^{o}C.

3.4.2. SDS PAGE

Precast 4-12% Sodium dodecyl-sulphate polyacrylamide gel electrophoresis (SDS-PAGE) gels (NuPage, Invitrogen, UK) were prepared according to instruction, being placed into the gel dock following removal of all packaging. The gel tank was then filled with MOPS SDS buffer, with 500 µl SDS-PAGE antioxidant solution added to the centre of the gel enclosure. The gel comb was removed prior to sample loading. Samples were prepared with 5 µl 4x loading buffer, 2 µl reducing agent, with 13 µl remaining for protein sample, the rest diluted to with dH_2O. Non-urea containing samples were boiled at 95 ^{o}C for 10 min prior to loading. Gels were run for 1 h 20 min at 150 V. Following this they were Coomassie stained with InstantBlue

3.4.3. Bradford Protein Quantification

To determine protein concentrations in solution using the Bradford reagent, which causes a spectrophotometric change at 595 nm, a standard curve must first be produced using known concentrations of BSA. BSA concentrations of 0.25, 0.5, 1, and 1.4 mg/ml were aliquoted out into multiple wells of a flat bottomed 96-well (nunclon) plate, then 5 µl of each well transferred to a fresh plate. 250 µl of Bradford reagent allowed to warm to room temperature was added to each well of this plate. Following incubation at room temperature for at least 5 minutes the plates were measured spectrophotometrically at 595 nm using a microplate reader (Genios Tecan). Measurement was carried out within 60 minutes of reagent addition. This process was repeated for dilutions of protein samples, with absorptions compared against the standard curve. Averages of at least 5 replicates were used to determine protein concentration.

3.4.4. Trypsin Digestion and iTraq Labelling

LoBind microcentrifuge tubes (Eppendorf) were used throughout to prevent protein loss due to tube surface binding. A 1 in 6 dilution of each protein sample was made with TEAB in order to dilute urea and EDTA concentrations. Subsequently 60 µl of each diluted sample was aliquoted out, alongside buffer only and BSA controls, with 5 µl removed from each and stored for later analysis. Samples were reduced with 5.5 µl TCEP (50 mM), being incubated at 60 ^{o}C for 1 h, then alkylated with 2.8 µl MMTS (200 mM stock) and incubated at room temperature for 10 min. Following this, trypsin (resuspended in 5 µl 50 mM acetic acid, 35 µl TEAB, to 0.5 µg/µl) was added in a 1:20 ratio to protein (5.5 µl stock) and incubated at 37 ^{o}C overnight to digest. 6 µl aliquots were obtained from all samples to compare to initial analysis aliquots by SDS-PAGE.

Following verification of digestion, samples were dried down using a speed vac to reduce the sample volume to approximately 30 µl, then carefully arranged and labelled according to relative iTRAQ label reagents to be used. Reagents were removed from -20 ^{o}C storage prior to use and briefly pulse centrifuged to ensure contents were collected at the bottom. 100 µl of isopropanol were added to each tube, vortexed briefly, then spun once more before transfer to each respective protein sample. A vortex and spin was repeated following mixing, then samples were incubated at room temperature, in the dark, for 2 hours. Following this samples were mixed together in a single tube, mixed and centrifuged once more, then separated into two tubes for drying via speed vac. One tube proceeded to fractionation, while the other was stored at -80 ^{o}C.

3.4.5. HPLC Fractionation

Samples were resuspended in 20 µl HPLC buffer (3 % CAN 0.1% TFA), vortexed, pulsed in a microfuge, then sonicated for 3 min in water bath, before centrifugation at 17,000 xg for 3 min to remove particulates. This was repeated with a further 20 µl, before HPLC fractionation via hypercarb column. Fractions were collected at 2 minute intervals. Following drying samples were stored at -20 ^{o}C.

3.4.6. Mass Spectrometry

Sample preparation for MS proceeded as above, resuspending dried fractions with 20 µl and extracting 4 µl to a mass spec sample tube following the centrifugation step. BSA standards were run before and after two fractions (40-42 and 50-52 min) were run on the amazon LC-MS (Bruker, UK) to assess quality. BSA scores and sample data permitting, 6 tubes with 4 µl of each of three consecutive fractions from 22-58 min were combined in mass spec sample tubes pending analysis on the Q Exactive HF Orbitrap (Thermo Scientific, UK).

Chapter 4 – Chloramphenicol Increases Current Production by Bacteria in a Single Chamber Bioelectrochemical Cell

4.1. Introduction

As discussed in Chapter 2, microbial fuel cells (MFCs) have their limitations for laboratory based study of bacterial electroactivity, particularly with regards to throughput.[3,123,124] The half-cells (HCs) used by Pereira-Medrano *et al*.[125] present a higher throughput option, however sacrifice much of the electrochemical insight provided by MFCs.[26] Further compounding the issues of BES selection for investigation of electroactivity is the lack of standardisation of equipment in the field, a consequence of a focus on MFC design and electrode composition in MFC research[3,12], which necessitates a comparison between any experimental protocol and the literature to confidently validate any data it is used to produce.

In this chapter we initially set out to adapt the sedimentary HC protocol used by Pereira-Medrano *et al*.[125] for more thorough electrochemical analysis of engineered *Escherichia coli* strains. *E. coli* strains engineered with systems from model dissimilatory metal reducing bacteria (DMRB) have performed poorly relative to those organisms, though they might outperform their respective controls.[26,28,126] However, while this makes them unlikely candidates for industrial scale, bioenergy MFC applications, the increased understanding of *E. coli* as a model organism for synthetic biology, and the concomitant toolsets available, makes them stronger contenders for other applications[126], as discussed in Chapter 2. Applications in biosensing in particular may benefit from a greater control of electroactivity at the expense of flux, providing power density does not drop low enough to be reflected in decreased sensitivity.[29]

Our three electrode, single chamber setup, under potentiostatic control, matched expectations from the literature for *Shewanella* mutants.[127,128] However, further adaptations were needed to resolve differences between engineered and control strains of *E. coli.* While testing these adaptations, unexpected observations led us to investigate potential interactions between chloramphenicol (Cm) and bacteria within a single chamber bioelectrochemical system (BES). Thus it is worth noting that Cm is an uncharged, bacteriostatic antibiotic that binds with ribosomes to inhibit protein synthesis.[129,130] The most common gene conferring high-level resistance is for chloramphenicol acetyltransferase (CAT), which acetylates up to two hydroxyl groups of the Cm molecule, using acetyl Coenzyme A (acetyl CoA).[131] This reversible reaction[132] prevents subsequent binding to the ribosome.

4.2. Results and Discussion

4.2.1. Half Cell Development

After it became clear that the analysis of negative potentials observed using the sedimentary HC protocol[26,125] would be insufficient to effectively differentiate *E. coli* strains for performance in other BESs, the protocol was adapted to make use of an additional electrode and employ a poised potential, necessitating the use of a potentiostat. The single channel, portable potentiostat used in preliminary testing was incapable of facilitating the number of replicates that would be required for a reliable study, let alone maintaining the throughput of the original protocol that we were interested in attaining. Through collaboration with Prof Peter Hall and his research group, access to a multi-channel potentiostat was utilised to produce the subsequent HC data.

The HC setup described in Figure 4.1. underwent a series of minor modifications during preliminary testing (data not shown), to reach the setup detailed, notably including the use of a larger platinum counter electrode (CE). The media selected for use in the HCs was a more strictly defined minimal media adapted from the M4 media used by Goldbeck *et al*.[27], and detailed in Chapter 3 (M4m). Sodium DL- Lactate remained the sole carbon source at 0.4% w/w. Briefly, replicate HCs were inoculated to a defined OD_{600} as later described with aerobic, LB flask-grown cultures of relevant strains,

through centrifugation and resuspension (in M4m) of a calculated volume based on culture OD_{600}. HCs were subsequently assembled, then placed in a water bath at 30 °C, wherein they were sparged with N_2, connected to the potentiostat, and the chronoamperometry experiment begun. All data presented is representative of at least three replicates unless otherwise noted.

Figure 4.1. Half Cell Diagram

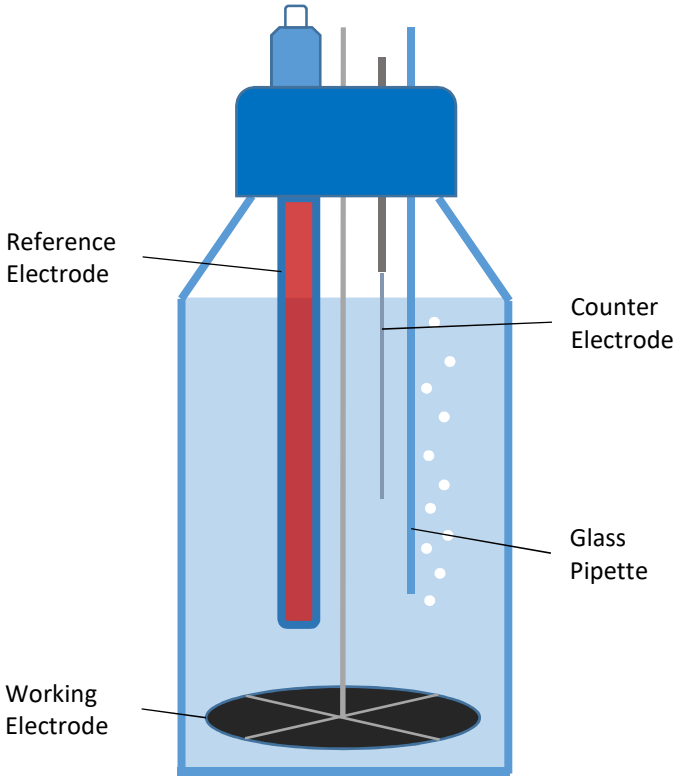

A diagram of the HC equipment used. Accommodated within the lid of the 250 ml bottle, from left to right, are a Red Rod Ag/AgCl reference electrode, a NiChrome wire and carbon veil working electrode, a platinum counter electrode, and a glass pipette sparging the media with nitrogen. Assembled HCs contain 250 ml of culture.

4.2.2. Comparison of *Shewanella* mutants

Validation of our HC protocol was conducted using *Shewanella oneidensis* MR-1 and four deletion mutants produced by Coursolle and Gralnick[128,133], and described in Table 4.1. These mutants had particular relevance as many of the deletions used were for

decahaem cytochromes involved in an identified, extracellular electron transfer (EET) pathway of *S. oneidensis,* which had been successfully transplanted into *E. coli*.[26,122,134] It was planned that such *E. coli* strains would be used in subsequent testing.

Table 4.1. *Shewanella oneidensis* Strains

Strain Designation	Gene Deletions	Source
MR-1	N/A – Wild Type	Prof. Gralnik
JG719	Δ*omcA*	[128]
JG731	Δ*mtrC*	[128]
JG1176 or "White"	Δ*mtrC* Δ*omcA* Δ*mtrF* Δ*mtrA* Δ*mtrD* Δ*dmsE* Δ*SO4360*/ Δ*cctA*	[133]

Table of Shewanella *strains used in this study. These were obtained from Prof. Gralnick and are all derived from* MR-1. *The white strain in particular has several deletions in recognised cytochromes involved in EET and their homologues.*

The results for the chronoamperometry experiments using HCs at a poised potential of 0.2 V vs Ag/AgCl (+0.197 V compared with SHE), and inoculating OD_{600} of 0.04, are shown in Figure 4.2B, alongside the results reported by Coursolle *et al*.[127] (reproduced with permission) in Figure 4.2A.

Figure 4.2B shows an initial rapid current increase of around 50 µA for the MR-1 and ΔomcA strains within the first few hours, both levelling off to a slower, steadier rate also observed for the other strains. The change in current over time appears more linear in Figure 4.2A. This difference, which is likely attributable to the methodological differences between the two experiments rather than biological differences, does not however obscure the general trends which can be drawn from the data, nor contest the conclusions that can be drawn therefrom. The ΔomcA strain is outperformed by the MR-

1 strain, and similarly outperforms the ΔmtrC strain, with the white strain producing the least of all. This reflects the importance of these cytochromes to EET to an electrode.[127,128]

There is a greater separation between the observed current for MR-1 and ΔomcA in Figure 4.2A, than in 4.2B, which we believe reflects biological adaptation by the ΔomcA strain within our HCs to compensate for its deletion.

Aside from equipment and electrode differences, the poised potential used by Coursolle *et al*.[127] of 0.242 V vs standard hydrogen electrode (SHE) – equivalent to 0.045 V vs Ag/AgCl – may be particularly accountable for the observed differences. As discussed in Chapter 2, there is no completely accepted optimum poised potential, however comparisons for MR-1 have shown greater current production occurs at more oxidising (positive) potentials, peaking at 0.2 V vs Ag/AgCl. Coulombic efficiency was comparatively seen to reach maximal values at 0 V vs Ag/AgCl.[126] Our selection of poised potential was made on the basis of this, and for ease of comparison to published BES data for *E. coli* strains.[27,28,126]

Figure 4.2 – *S. oneidensis* Mutant Comparison

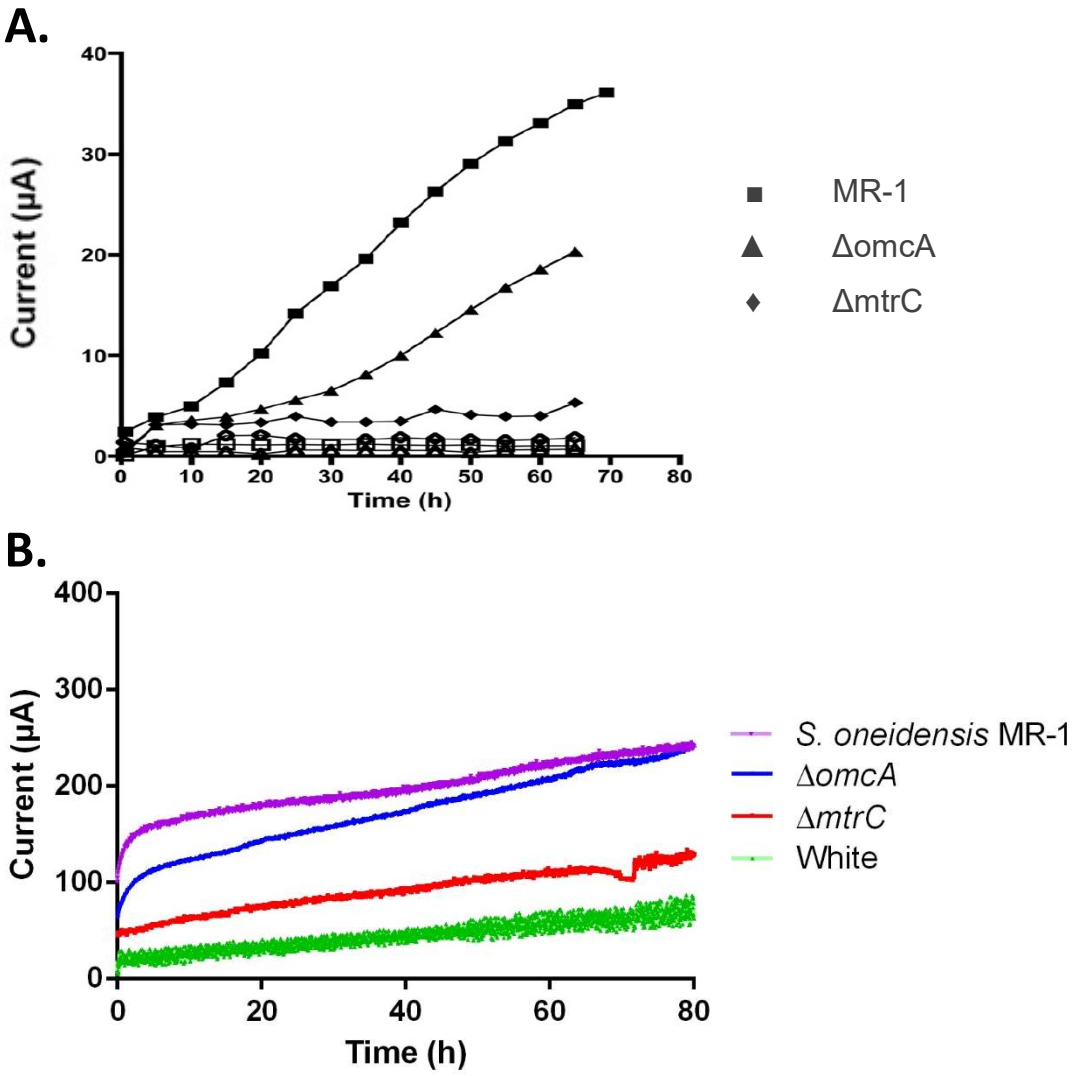

A comparison of published chronoamperometry data (A) and that produced by our HC setup (B) using the same strains. The unlabelled strains close to the x axis in (A) are not relevant to this study so not identified. Both graphs show a high performance for MR-1, followed by the ΔomcA strain, then the ΔmtrC (by a greater margin). The white strain also performs even more poorly, as expected. Error bars are not shown here to ensure clarity, but each line represents the average of three replicates.

4.2.2.2. S. oneidensis *Riboflavin Responsiveness*

As discussed in Chapter 2, riboflavin has been demonstrated to act as a mediator between the transmembrane EET pathway of MR-1 and extracellular electron acceptors (EEAs). Its supplementation into BESs can result in dramatic increases in current output.[73] 4 µM riboflavin was added to the HCs as described in Chapter 3 and Figure 4.3. clearly shows the effects of riboflavin addition to the HC setup for MR-1 to be consistent with expectation. A fourfold increase in maximal current after 4 hours was observed.

Figure 4.3 – Riboflavin Responsiveness of *S. oneidensis* MR-1

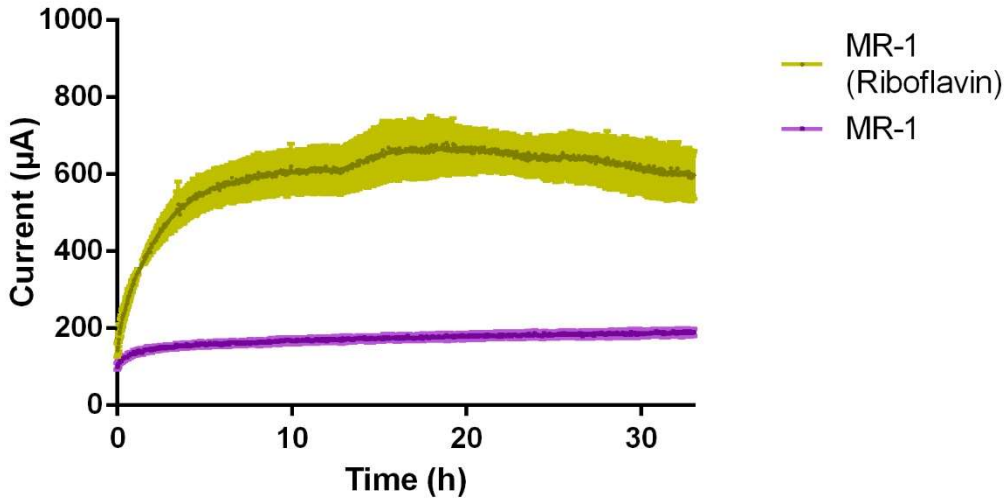

Chronoamperometry data showing the current produced by S. oneidensis MR-1 in the presence and absence of 4 µM riboflavin. The data for each line represents the average of three replicates with error bars highlighting the standard error of the mean. The presence of riboflavin clearly has a multiplicative effect on current output.

4.2.3. Methodological Adaptations for *Escherichia coli*

In order to achieve confidence in our experimental setup for the comparison of engineered *E. coli* strains we needed to observe differences between such strains and their relative controls that had been previously validated in other BESs. A full list of *E. coli* strains used in this chapter is presented in Table 4.2. The majority of plasmids were inserted into the expression strain BL21(DE3), save for those otherwise noted.

Table 4.2. – *E. coli* Strains

Base Strain	Plasmids	Additional Genes	Resistance	Source
C43(DE3)	-	-		Sigma
BL21(DE3)	-	-		Sigma
BL21(DE3)	pACYC Duet-1 + pRGK333	*ccmA-H*	Cm, Amp	Jaffe[26]
BL21(DE3)	pACYC CAB + pRGK333	*mtrCAB, ccmA-H*	Cm, Amp	Jaffe[26]
BL21(DE3)	pACYC CABO + pRGK333	*mtrCAB, omcA, ccmA-H*	Cm, Amp	Jaffe[26]
BL21(DE3)	pRSF Duet-1 + pRGK333	*ccmA-H*	Kan, Amp	Jaffe[26]
BL21(DE3)	pRSF CABO + pRGK333	*mtrCAB, omcA, ccmA-H*	Kan, Amp	Jaffe[26]
BL21(DE3)	pRSF Duet-1 + pEC86	*ccmA-H*	Kan, Cm	Jaffe[26]
BL21(DE3)	pRSF CABO + pEC86	*mtrCAB, omcA, ccmA-H*	Kan, Cm	Jaffe[26]
BL21(DE3)	pEC86	*ccmA-H*	Cm	Jaffe[26]
BL21(DE3)	pRSF Duet-1 + pEC86Amp	*ccmA-H*	Kan, Amp	This study
BL21(DE3)	pRSF CABO + pEC86Amp	*mtrCAB, omcA, ccmA-H*	Kan, Amp	This study
BL21(DE3)	pSB1A2 Cm^R	-	Cm, Amp	BioBrick[108]
BL21(DE3)	pACYC Duet-1	-	Cm	Novagen
BL21(DE3)	pBBR1MCS	-	Cm	Addgene

Initial comparison of *Escherichia coli* BL21(DE3) pACYC Duet-1/mtrCAB + pRGK333 (inducible *ccm* genes), as seen in Figure 4.4.A, using the same protocol as for MR-1 showed no significant difference between the two, and had in the region of a tenfold current reduction compared with *S. oneidensis*. Consequently, the inoculating OD_{600} was revised upward tenfold.

Figure 4.4.B presents these data, in which differences between the strains is observed. However, it is the control strain (pACYC Duet-1 pRGK333) which outperformed the engineered (pACYC CAB pRGK333). Furthermore, the two base strains tested (BL21(DE3) and C43(DE3)) behaved comparably to the strains in Figure 4.4.A, producing negligible current in the 0-5 µA range. Both observations were unexpected, and were further investigated in parallel.

While examples of use are present in the literature[26,135,136], the inducible pRGK333 plasmid is more commonly replaced by the constitutive pEC86 plasmid for the expression of additional cytochrome maturation (*ccm*) genes.[26,122,137,138] Optimising expression of the system is complicated by the co-induction of the *mtrCAB* genes with IPTG, which lie under a T7lac promoter. This promotor is known to be leaky (possessing non-zero basal expression) in many expression strains, including BL21(DE3), though this can be controlled with T7 lysozyme expression.[104,139] However expression of membrane proteins under its control can be better without induction due to its relative strength and ability to overwhelm localisation and other host processes when induced, yet better still when under a tuneable promoter.[27,140] Nevertheless the T7 RNA polymerase is effective at rapidly transcribing long sequences[32], which can be of use when trying to co-express multiple recombinant genes.

While the expression profile may have been suitable for detecting differences within an MFC, it may be the case that the HCs require a greater level of optimisation to be able to discern these differences. Alternatively, the decreased performance of this engineered strain relative to its control may be due to increased metabolic burden from the overexpression of the EET system, obscuring the EET activity, or other metabolic differences arising from varying conditions between the two setups.

The significant difference between the base strains and the plasmid containing strains must be accounted for in something contained on either the pACYC Duet-1 expression plasmid, the pRGK333 *ccm* plasmid, or both. It was hypothesised that there might be an unforeseen interaction between the host cytochromes and the working electrode (WE), subject to additional *ccm* gene expression. This, however seemed unlikely to have gone overlooked in previous studies. Alternatively, there may have been an interaction between the antibiotics, resistance mechanisms, or products, highlighted in our single chamber BES.

Figure 4.4. – Initial *E. coli* Strain Comparison

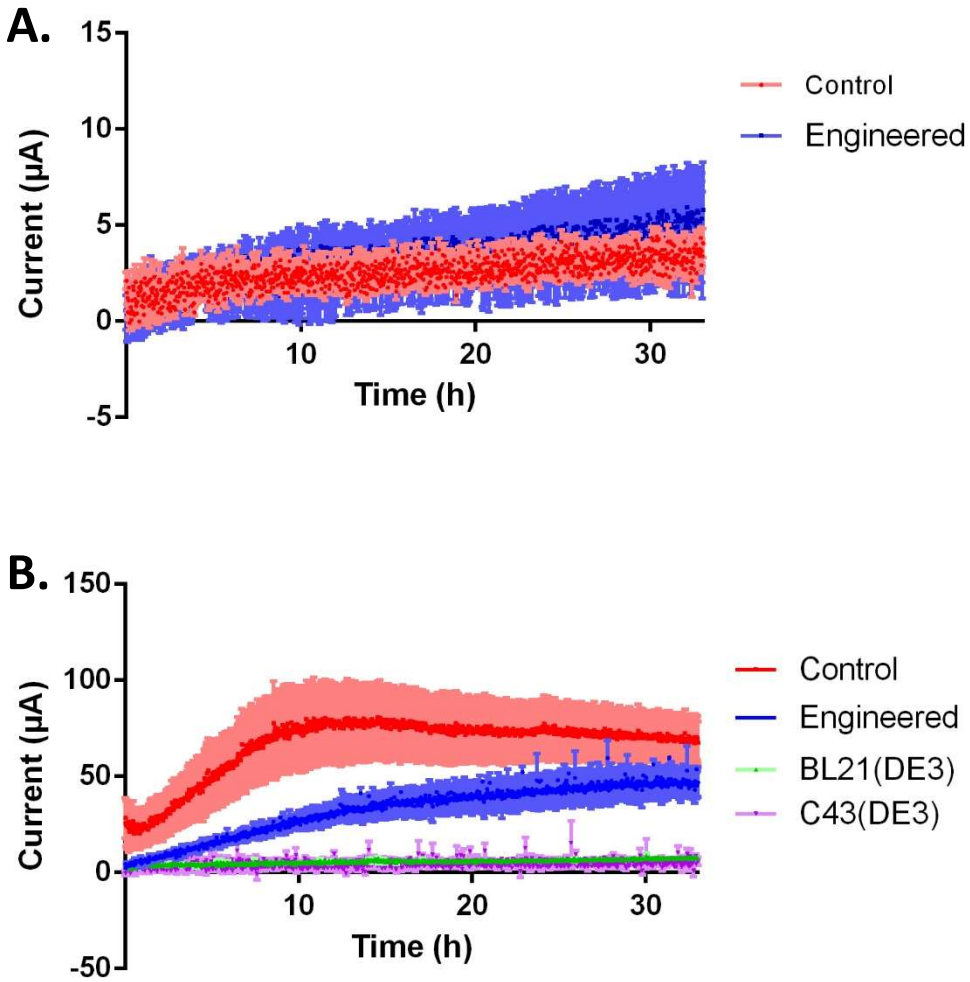

Engineered (pACYC mtrCAB + pRGK333) and control (pACYC Duet-1 + pRGK333) strains of E. coli are compared in HCs using a starting OD_{600} of 0.04 (A) as with previous S. oneidensis HCs, and 0.4 (B). The data for each line represents the average of three replicates with error bars highlighting the standard error of the mean. Increasing the inoculation OD tenfold appears to comparably increase the observed current, which importantly allows the different plasmid bearing strains to be differentiated. The base strains (BL21(DE3) and C43(DE3)) produce negligible current, far below that of the control, plasmid-bearing strain.

4.2.3.2. E. coli *Riboflavin Responsiveness*

Given the profound effect of riboflavin on MR-1, it was hoped that the addition of 4 µM riboflavin could improve electron transfer between the heterologous *mtr* pathway and the WE, overcoming potential limitations imposed by an increased metabolic burden of expression. These data are presented alongside those for the same strains from Figure 4.4.B in Figure 4.5. The general trends and current levels remain the same for both pACYC Duet-1 + pRGK333 and pACYC CAB + pRGK333 bearing strains.

However, since we cannot assume functionality of the mediator/EET pathway interaction heterologously, as discussed in Chapter 2, we could not conclude that the heterologous EET pathway itself was not working. Therefore, in order to further investigate both engineered/control strain performance and base strain discrepancy, additional plasmid systems were explored.

Figure 4.5. – Riboflavin Responsiveness of *E. coli* Strains

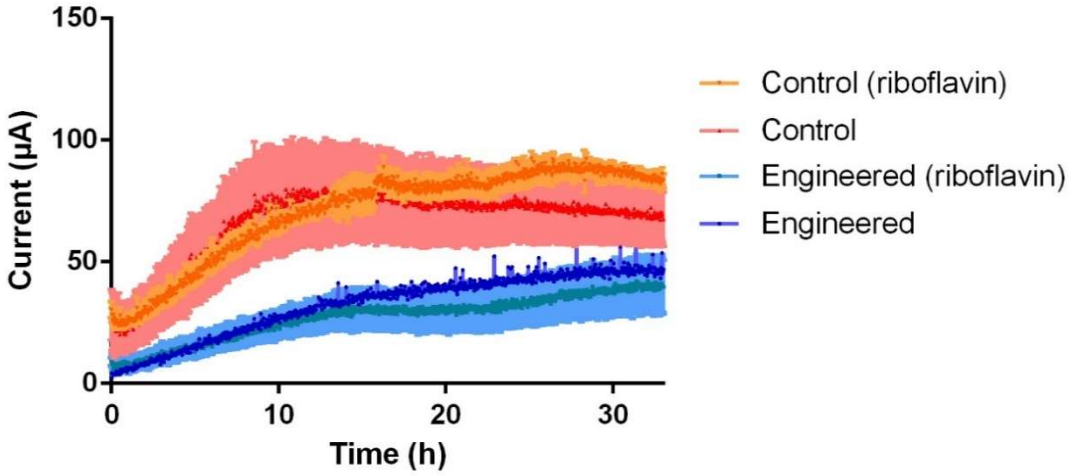

Engineered (blues – pACYC mtrCAB + pRGK333) and control strains (orange and red – pACYC Duet-1 + pRGK333) of E. coli are compared, with (light blue and orange) and without 4 µM riboflavin added to the starting HC media. Note that error bars for the engineered strain without riboflavin are excluded for the sake of clarity. The data for each line represents the average of three replicates with error bars highlighting the standard error of the mean. The data indicates not particular effect of riboflavin addition on current.

4.3. Effects of Plasmid Selection on Electroactivity in Half Cells

In order to isolate the causative factor for the differences seen between base and plasmid containing strains in HCs, substitute vectors were compared. The strain bearing pRSF CABO + pRGK333 performed well against controls in previous work [24], and the complementary pACYC version was available. Both Duet-1 vectors were originally produced by Novagen, the primary difference between them lying in the antibiotic resistance gene; Cm for pACYC Duet-1 and Kan for pRSF Duet-1.

Engineered and control strains were compared in HCs and the results presented in Figure 4.6. below. The pACYC CABO + pRGK333 strain performed similarly to its *omcA* lacking counterpart. Neither pRSF strain exceeded the 0-10 µA current range displayed by the base strains, however. This strongly pointed to the inclusion of Cm and its resistance gene being responsible for the dramatic increase in current output.

Figure 4.6. – pRSF/pACYC Vector Comparison

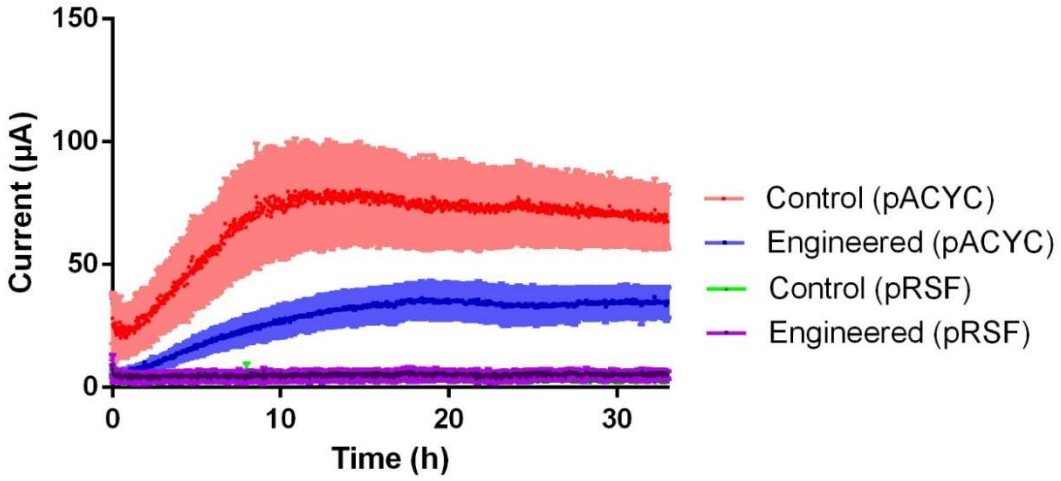

Chloramphenicol resistant strains are presented in red (control) and blue (engineered), while kanamycin resistant versions are presented in green and purple respectively, though overlap prevents these latter two from being easily visually distinguishable. The data for each line represents the average of three replicates with error bars highlighting the standard error of the mean. Both Cm^R strains demonstrate much higher electroactivity than the Kan^R counterparts, suggesting Cm^R or Cm is contributing to this phenotype

One advantage of the pRSF system over the pACYC, was its compatibility with the previously discussed pEC86 constitutive *ccm* plasmid. It was hoped that its use would improve heterologous cytochrome expression and maturation to produce higher current in HCs relative to a control plasmid bearing strain, and might otherwise support the role of Cm in increased EET. Additionally it would permit a comparison of induced against uninduced pRSF CABO, which might improve EET through a combination of expression and adjustment of metabolic burden. Figure 4.7. shows the results.

The addition of pEC86 clearly leads to the higher current levels predicted, due to its Cm resistance cassette, in all strains. The pEC86 only strain is representative of the pRSF Duet-1 + pEC86 strain for the purposes of controlling against the pRSF CABO + pEC86 bearing strain. Both the induced and uninduced HCs of which displayed increased current relative to the pEC86 control. Further controls are included for induced and uninduced pRSF CABO + pRGK333, which are not discernible from one another and remain comparable to BL21(DE3). However, as previously noted, due to the inducible nature of both plasmids, the lack of discernment may be due to a conflict between optimum expression for each of the plasmids to reach maximal matured and localised EET pathway. This could be explored further. Another potential factor to consider is the ampicillin resistance cassette used for pRGK333. Amp is weaker, degrades more readily, and so plasmid retention might be more likely affected.

A clear and significant difference between the induced and uninduced pRSF CABO + pEC86 strain was not observed overall, though current levels for the uninduced rose faster initially.

Figure 4.7. – pEC86 Strain Comparison

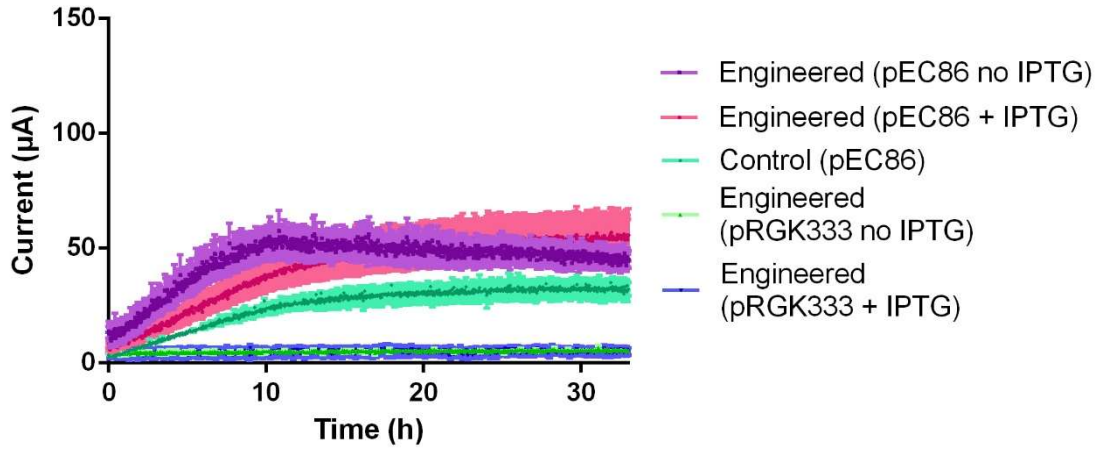

Engineered pRSF mtrCABomcA (purple and pink) and control pEC86 (turquoise) strains constitutively expressing additional cytochrome maturation genes on the pEC86 plasmid are presented. The pink and blue lines represent mtrCAB omcA expressing strains induced with 0.5 mM IPTG, with their uninduced equivalents represented by the purple and green respectively. The data for each line represents the average of three replicates with error bars highlighting the standard error of the mean. Induction with IPTG seems to have a minimal effect, however the use of pEC86 to express ccm *genes results in an engineered strain that can outperform its control.*

In an effort to see if the pRSF CABO pEC86 engineered strain and its control could be differentiated in the absence of the proposed "Cm effect", the Cm^R cassette of pEC86 was replaced with an Amp^R cassette from the BioBrick plasmid (pSB1A2). This was achieved through PCR of the original cassette, and plasmid excluding the Cm^R cassette, followed by digestion and ligation as described in Chapter 3. The construct was verified by sequencing.

Strains containing pEC86Amp and either pRSF Duet-1 or CABO were subsequently observed in HCs, both induced and uninduced for the latter. Figure 4.8. presents these data, which are clearly incomparable to those for the relative pEC86 strains. Current readings remained in the 0-15 μA range, and were not differentiable from one another. This suggests that within our HCs the Cm effect may be necessary for discerning the

differences between engineered and control strains. Furthermore, it rebuffs the argument that the *ccm* gene expression was responsible for the pEC86 current increase, and that something else accounted for the pACYC Duet-1 increase.

Figure 4.8. – pEC86Amp Strain Comparison

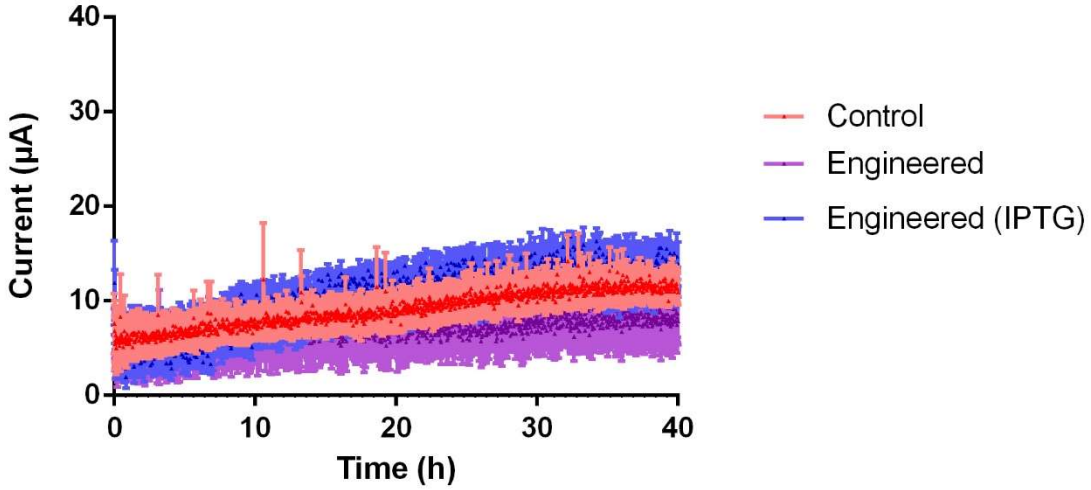

Control (pRSF Duet-1 + pEC86Amp) and Engineered (pRSF mtrCABomcA + pEC86Amp) strains are compared, the latter both induced and uninduced, in a chronoamperometry experiment within our HC setup. These strains produce current levels comparable to their host strains without plasmids; far lower than the versions that use Cm resistance to maintain pEC86. The control and engineered strains cannot be distinguished. The data for each line represents the average of three replicates with error bars highlighting the standard error of the mean.

4.4. Investigating the Basis of the 'Chloramphenicol Effect'

In order to investigate which component of the Cm^R pathway – that is whether the resistance protein, Cm itself, or the acetylated product – was accountable for the observed, increased HC current output, we aimed to test each component in isolation as much as practically possible. However, challenges were encountered in achieving this. Initially, a Cm concentration tolerable to BL21(DE3) was elucidated through the inoculation of starter cultures containing a range of Cm concentrations. A concentration of 200 ng/ml was found to be suitable (0.01x typical working concentration) and tested within HCs containing BL21(DE3), or BL21(DE3) containing the Cm^R BioBrick plasmid (maintained with an Amp^R cassette) as described in Table 4.2. previously. Any observed increased current would identify if Cm or CAT were responsible for the Cm effect. Figure 4.9. presents these data.

All strains behaved similarly, producing current in the 0-10 µA range. Some separation can be discerned between the strains after 30 h, with the BL21(DE3) with no Cm reaching marginally higher levels than its Cm containing counterpart, and noticeably more than the plasmid bearing strains. We attribute this to the comparative lack of stress, or metabolic burden placed upon the strain, respectively.

The absence of the Cm effect in the presence of the Cm^R cassette rules the CAT enzyme out as being independently responsible for the increase in current. Although, the low Cm concentrations used by necessity herein prevent us from concluding that Cm itself is not having an unforeseen interaction with bacterial constituents leading to increased EET. Conclusively demonstrating that acetylated chloramphenicol (aCm) was responsible could dismiss this concern, yet further investigation of this is limited by the reversible nature of the acetylation.[141] Alternatively, were it shown that the 'Cm effect' occurred within abiotic HCs containing the CAT reaction with constituents at comparable concentrations, then the responsibility of aCm for this effect could be asserted. However, this is hindered by the infeasible cost of sourcing aCm or conducting the CAT reaction abiotically at the concentrations necessary, within our HCs.

Figure 4.9. Current Effect of CAT and Low Concentration Chloramphenicol

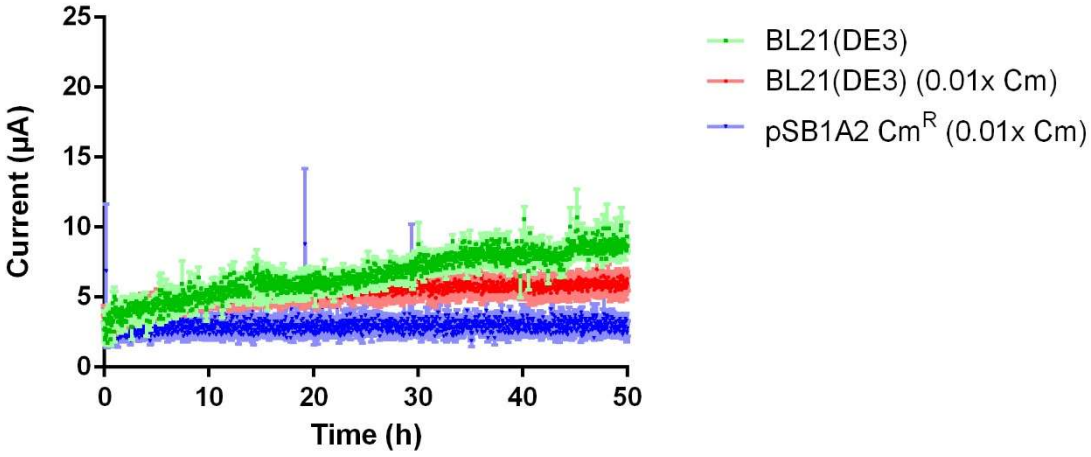

HCs containing E. coli BL21(DE3) (green and red) and BL21(DE3) bearing pSB1A2 CmR are represented. 0.2 µg/ml Cm, representative of 0.01x normal working concentration, was present for HCs represented by red and blue. The data for each line represents the average of three replicates with error bars highlighting the standard error of the mean. No electrochemical advantage is conferred by sub-inhibitory concentrations of Cm in BL21(DE3) or the Cm^R strain, which also rules out CAT as soley responsible for the Cm effect.

4.4.1. Chloramphenicol Effect in *Shewanella oneidensis* MR-1

In order to validate that the Cm^R accountable current increase was not restricted to *E. coli* strains, *S. oneidensis* MR-1 was compared against a pBBR1MCS (expression plasmid with Cm^R marker) containing strain. The results, shown in Figure 4.10, conclusively describe an increase comparable to that seen for *E. coli* strains. A 2-3 fold increase in maximal current is observed. This was conducted concurrently with the HC work presented in Fowler *et al.*[142]. A faster drop off in current is observed proceeding the maximal current peak than for other HC experiments. A gradual decrease in current was noted for other strains following peak current, however this behaviour is suggestive of some sort of depletion, perhaps of carbon source or mediator, due to the higher levels of current involved. It is worth noting that sub-lethal Cm concentrations can be used to

boost plasmid copy numbers but given the Cm^R cassette only run did not suggest it was causative, we did not expect that this would have much of an impact on current.

Figure 4.10. – The Chloramphenicol Effect in *S. oneidensis* MR-1

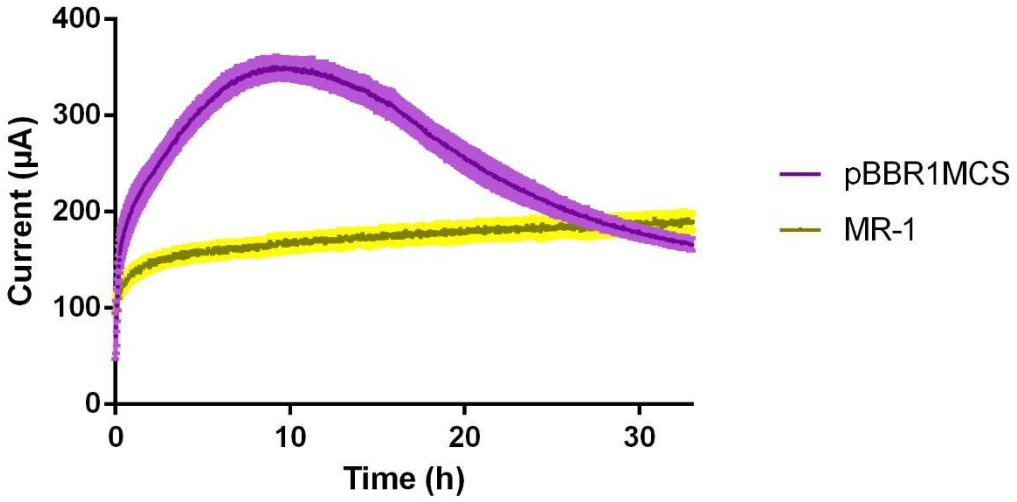

S. oneidensis *MR-1 and a strain with the pBBR1MCS expression plasmid added were tested in HCs. The latter has only an empty expression plasmid bearing a* Cm^R *cassette, with Cm added to the HC media. The data for each line represents the average of three replicates with error bars highlighting the standard error of the mean. It clearly demonstrates that the Cm effect is observable for other bacteria beyond* E. coli.

4.4.2. The Effect of Chloramphenicol Concentration on Current

Concurrently with the deduction of the upper limit for Cm tolerance for non-Cm resistant *E. coli*, that for resistant strains was also investigated. It was found that growth wasn't noticeably inhibited at up to 15 times typical working concentration aerobically. Consequently, a range of concentrations were tested within HCs to see if this would have an effect on current.

The pRSF CABO + pEC86 strain was initially selected for this comparison as it was felt that if a mediator based EET facilitation were occurring as part of the Cm effect, this might be more strongly observed with our engineered strain. Figure 4.11A presents these data, showing increasing maximal current levels with increasing Cm

concentrations. Figure 4.11B plots this relationship, indicating it to be linear within the range tested.

This observation is strongly supportive of a hypothesis for aCm (or another, unintended product of the CAT reaction in *E. coli*) acting as a mediator for the purposes of EET.

That an increase in current of our engineered relative to our control strains was previously observed could support a hypothesis for mediator interaction with the expressed mtrCABomcA pathway in *E. coli*. However, it is also possible that this improvement is due to direct electron transfer (DET) through the mtrCABomcA pathway, and that the mediator driven EET is separate, but facilitates sufficient end terminal electron acceptor access that the metabolic activity of the cell is improved, resulting in greater, observable electron flow through the artificial circuit.

The presence of ethanol in the media, used to solubilise Cm, is unlikely to account for the observed increases. The Amp stock solution used in this work contained 50% ethanol, and no comparative effect was observed for any Amp^R strains at intermediate values as we'd expect given the observed relationship between Cm concentration and current. Furthermore, Cm only HCs produced no current so an interaction between Cm and the electrodes can also be discounted.

Figure 4.11. – Cm Concentration Relationship with Current

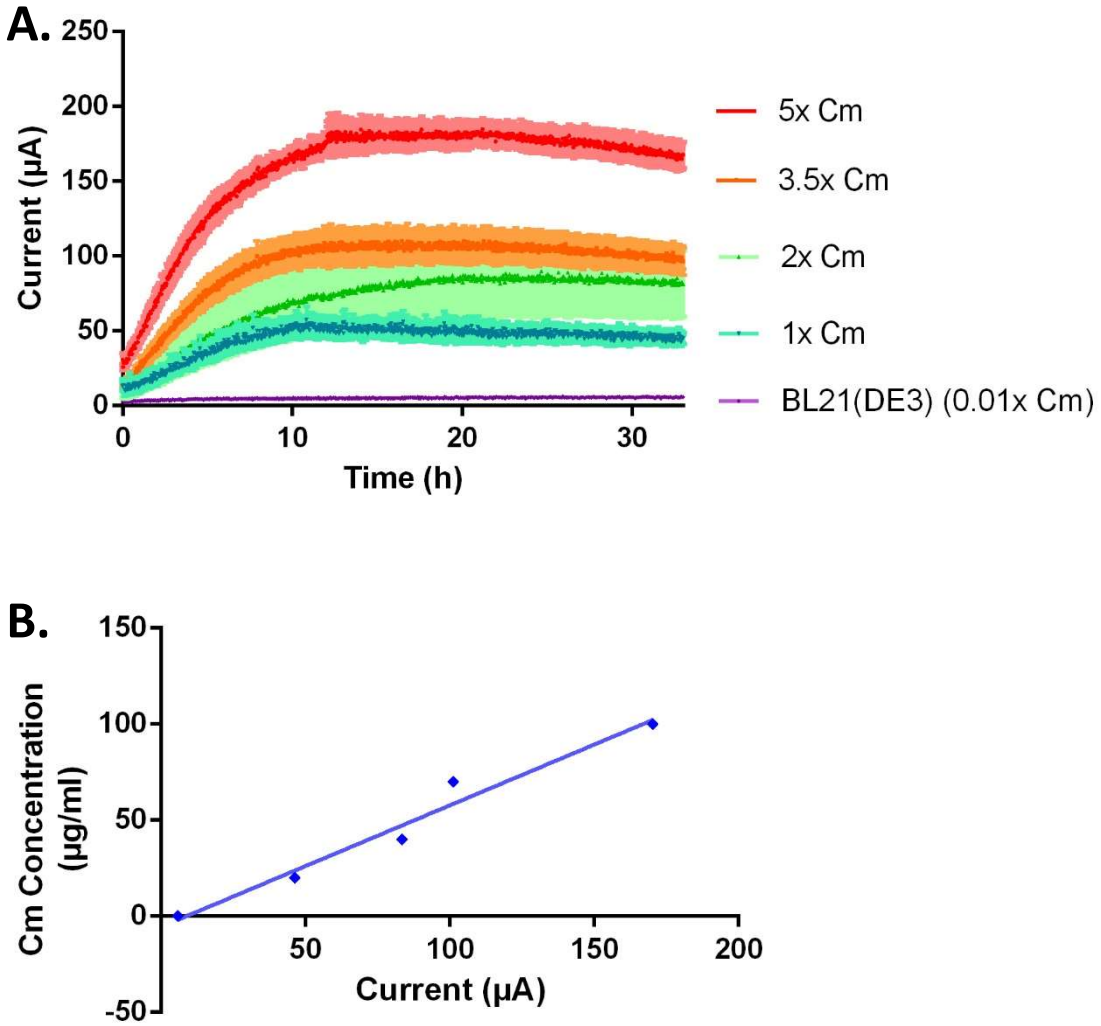

Current over time from HCs containing different Cm concentrations is shown (A) for the engineered pRSF mtrCABomcA + pEC86 strain, with a sub-inhibitory concentrationused with BL21(DE3) shown for baseline reference. The data for each line represents the average of three replicates with error bars highlighting the standard error of the mean. This shows an increasing current output when Cm concentration is increased. The average current after 30 h was taken for each concentration and plotted (B), along with a line charting linear regression, which suggests that this relationship may be linear.

4.4.3. Plasmid Selection and Chloramphenicol Concentration

In order to verify that the relationship between Cm concentration and current wasn't exclusive to the pRSF CABO + pEC86 bearing BL21(DE3) strain, and therefore dependent on its engineered EET circuit, BL21(DE3) bearing an empty expression plasmid with the Cm^R cassette was tested at a higher concentration. Concurrently, to investigate the potential effect of Cm resistant plasmid copy number on current in a Cm containing HC, pBBR1MCS was used. The pBBR1MCS plasmid has a medium copy number of 30-40[143,144], compared with pACYC Duet-1, which has a low 10-12 copies per cell.[145]

Figure 4.12. displays these data, clearly showing a comparable increase for the 5x Cm concentration HCs with the pBBR1MCS strain, to that seen previously for the pRSF CABO + pEC86 strain. This observation indicates that the relationship between Cm concentration and current persists in the absence of the mtrCABomcA pathway, or additional *ccm* gene expression. While higher error was noted for the pBBR1MCS strain compared with the pRSF CABO + pEC86 strain, it does not disrupt the trend observed. Such error may be accounted for by greater biological divergence between replicates or handling error during HC inoculation and setup, and occasionally occurs within HC runs regardless of strain.

There is minimal current difference between the pACYC Duet-1 strain and the pBBR1MCS strain at the 1x Cm concentration. Although there is a slight separation between 5-15 hours due to a faster initial current rise for the pACYC Duet-1 strain, beyond that they reach similar values. Consequently it can be concluded that plasmid copy number, and by extension CAT concentration, does not have a large impact on Cm effect dependent current levels at typical working concentrations.

Figure 4.12. – Plasmid Copy Number and High Cm Concentration Validation

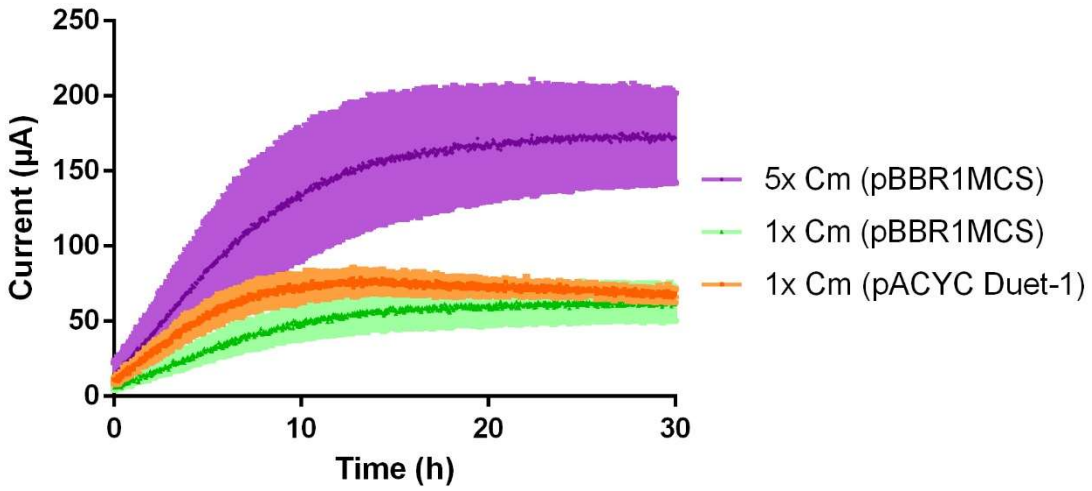

Chronoamperometry of BL21(DE3) bearing one of two Cm^R expression plasmids, each with a different copy number. A higher concentration of Cm is also used for pBBR1MCS, which responds similarly to data for previously tested plasmids. This demonstrates that copy number does not have a discernible effect on the electrochemical response to chloramphenicol, and that the effect is observable in strains only bearing empty expression plasmids. The data for each line represents the average of three replicates with error bars highlighting the standard error of the mean.

4.4.4. Chloramphenicol Depletion

As can be seen in many of the preceding figures, in Cm/CAT containing HCs current often rises rapidly within the first 10-15 hours, then begins to slowly decline. This becomes more apparent beyond 30 hours, for the remainder. It was hypothesised that this may be due to depletion of Cm, resulting in decreased mediator activity. An alternative hypothesis that this observation could be attributed to depletion of lactate within the media was also put forward.

In order to test these hypotheses, HCs containing pACYC Duet-1 bearing BL21(DE3) were setup and run concurrently. After 90 hours, after the current decrease had begun to stabilise, one of either Cm, sodium DL-lactate, or sterile dH_2O was added to HCs, with three replicates of each. Cm and lactate were added to equal concentrations to those

initially inserted into HCs during setup, while a comparable volume of sterile dH_2O was used.

As seen in Figure 4.13. the addition of lactate produces a minor increase of around 4 µA, but this represents only about 1/9th of the difference between the previous current value and the peak current. No change is observed for the water control. However, Cm addition produces an increase of 54 µA to current levels around 17 µA above those of the previous peak. The shape of this peak, and the subsequent downward trend, is similar to that of the initial peak observed in the same run.

The sharp peak followed by gentle downward trend in current suggests that it is not a breakdown product of Cm, or some interaction product thereof that is acting as a mediator, unless Cm degradation is unusually accelerated by the HC conditions. This conclusion is further supported by the peak currents occurring at similar times in Figure 4.11. as, assuming degradation rate was unaffected by Cm concentration, if the breakdown products were acting as mediators, then we would expect all conditions to behave the same, diverging one at a time as each reached maximal current.

Figure 4.13. – Investigation of Chloramphenicol Depletion

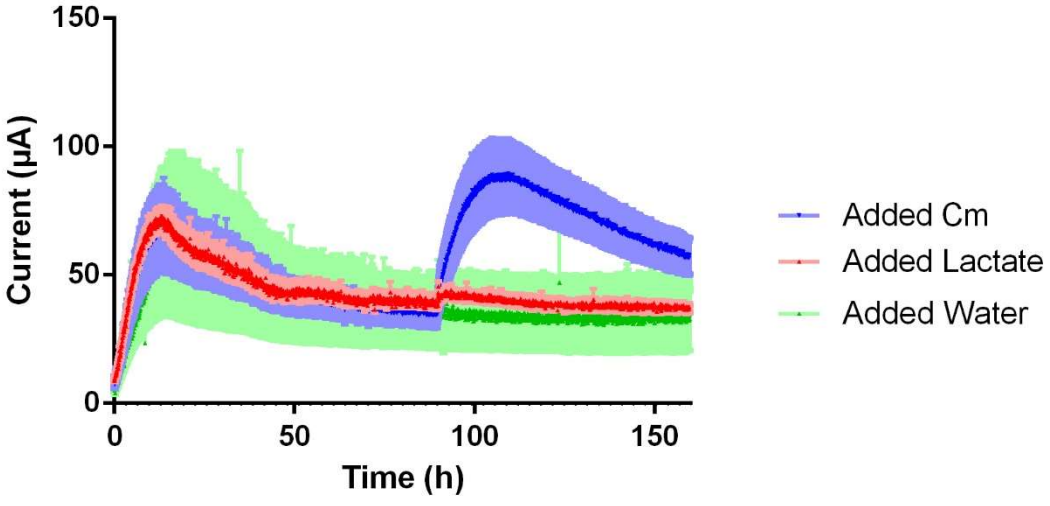

Chronoamperometry data for HCs containing BL21(DE3) bearing pACYC Duet-1. At t=90 h Cm (blue), sodium lactate (red), or sterile dH_2O (green) were added to the HCs. The data shows a rapidly rising current following Cm addition, in a similar pattern to initially

shown for all strains at the start of the experiment. A small increase is noted for lactate addition, but this does not affect the overall trend. The control continues without change. These data support the argument for Cm or aCm acting as mediator, rather than a breakdown product, and gradually being deplete or degraded rather than the decline being due to carbon source depletion. The data for each line represents the average of three replicates with error bars highlighting the standard error of the mean.

The specific degradation rates of Cm and aCm under the conditions within our HCs, if elucidated, could provide further insights into the nature of the mediator involved in the Cm effect. We contemplated three possible mechanisms for mediator activity summarised in Figure 4.14. below. While we accept that intermediate interactions with host processes between the CAT reaction and mediator driven WE reduction may be possible, in the interest of brevity the reiteration of this will be excluded from the descriptions that follow.

Mechanism A in Figure 4.14. proposes aCm reduces the WE, producing Cm, which can then be acetylated once more, regenerating the mediator. In mechanism B aCm reduces the WE then is regenerated by acting as an electron acceptor to the cell. In both of these, gradual degradation reduces the availability of the mediator, decreasing the current. Mechanism C proposes that aCm acts as a mediator, but is degraded in the process. We would expect this to result in a faster drop in current, however.

Looking at the chemical composition of chloramphenicol, as depicted in Figure 4.15., we can speculate further as to the specific mechanism. In order to operate as an effective mediator Cm would have to be able to oxidise cellular metabolites, be that quinone pool, cytoplasmic metabolites, or outer membrane cytochromes. It would therefore need to have a functional group that was strongly electron accepting, though we might accept an interaction with strongly reducing outer membrane cytochromes could permit a less strongly accepting functional group to fill this role. Coupled to this would be an ability for the resultant reduced group to be oxidised by the anode.

The chloramphenicol acetyl transferase acts on hydroxyl groups within Cm, starting with that identified in the figure. However, these acetyl groups do not fit the biochemical

profile outlined in the previous paragraph. Instead we propose that the nitro group highlighted in red is the most likely for the outlined electrochemical activity; nitro groups are strongly electron accepting[146]. The product of this nitro group reduction by the cell is likely an amine group (R-NH_2) but may be an intermediate, either of which would then interact with the electrode to be oxidised back or to a different form. While acetylation does not play a direct role in this proposed mechanism, it may have an unforeseen negative or positive impact on the rate of the reactions, leading to preference of one form or another, but this would require further investigation.

Figure 4.14. Abstracted Chloramphenicol Mediator Mechanisms

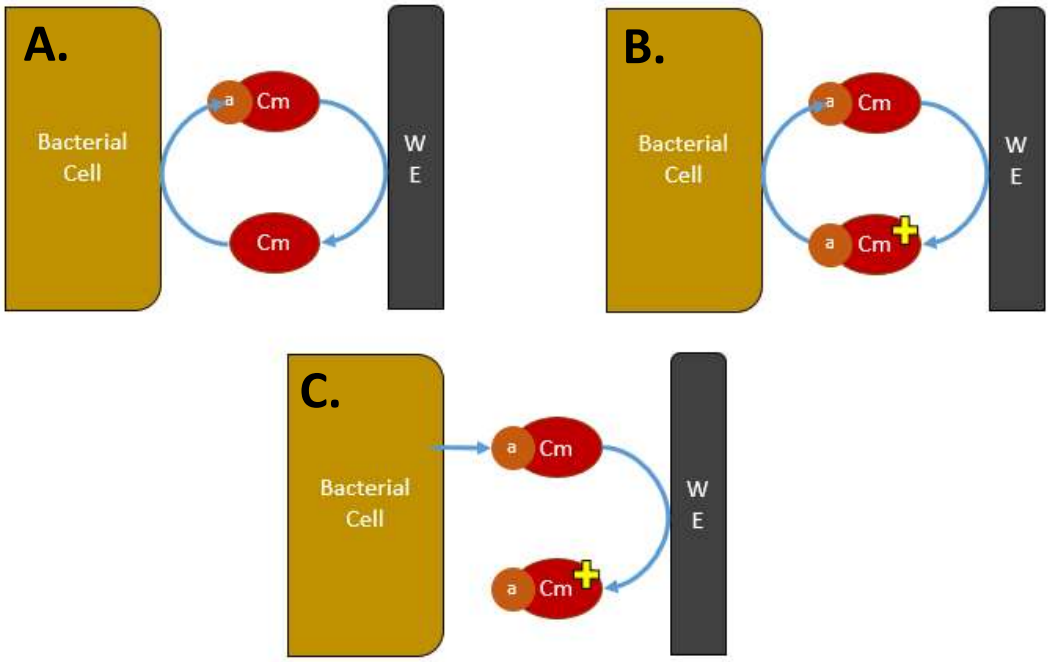

Suggested mechanism abstractions for the chloramphenicol mediated shuttling of electrons between cells and electrode are depicted. These portray a cyclic process of acetylation and deacetylation by the cell and WE respectively (A); a cyclic process whereby another active group of the acetylated Cm is reduced and oxidised by the bacterial cell and WE respectively (B); and a linear process whereby acetylated Cm is oxidised by the WE in a process that breaks it down or otherwise prevents its regeneration. Ultimately the mechanism most recommended by this study lies closest to (B), though the acetylation is not considered important to the process.

Figure 4.15. Chloramphenicol Skeletal Structure and Proposed Mediator Mechanism

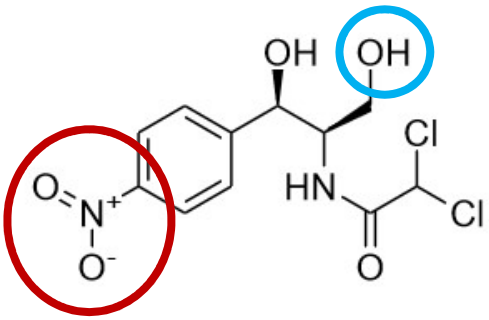

The skeletal formula for chloramphenicol is depicted, created using ChemDraw. Highlighted in blue is the hydroxyl group acetylated first during the CAT reaction, though it is possible for Cm to be multi-acetylated. Outlined in red is the nitro functional group we propose as responsible for the electron shuttling behaviour observed within our single chamber electrochemical testing apparatus.

High concentrations of Cm might have a desirable benefit for electroactivity, but the antibiotic effect and degradation rate under testing conditions raises concerns. Figure 4.15. identifies the hydroxyl group acetylated first by CAT, but this reaction requires acetyl-CoA. And maintaining high concentrations of Cm will deplete this energetic resource to some extent, which may have a wider metabolic impact. In order to maximise metabolic benefit of Cm or a derivative removing the antibiotic activity and increasing stability would be ideal. This could be achieved through the testing of available or synthesisable non-antibiotic derivatives, such as those presented by Corbett and Chipko[147]. Modification of different active groups as part of this would also allow for confirmation of those relevant to the mediator phenotype. Testing would follow two stages, first with synthesised or purchased derivatives tested for antibiotic activity at different concentrations or degradation rate if either has not been previously documented. Then with selected candidates tested at a range of concentrations within HCs as previously done for Cm.

4.5. Conclusions

In this chapter our single chamber half cell setup for bioelectrochemical testing was presented, with comparisons made to the literature to validate its efficacy for *S. oneidensis* strains. Following this validation, we attempted to differentiate engineered and control strains of *E. coli* expressing components of a recombinant, heterologous EET pathway, previously presented by Jaffe[26]. In doing so we highlighted the sensitivity of electroactive *E. coli* to methodological changes in BESs. While ultimately successful in replicating increased electroactivity in the engineered strain, in doing so the observation of a mediator-like current increase was observed for strains using Cm as a selection marker.

This 'Cm effect' was investigated further, and shown to occur independently of Cm^R plasmid choice, and being necessary for the resolution between engineered and control strains of *E. coli* expressing the *mtrCABomcA* pathway. The effect was not restricted to *E. coli*, occurring in *S. oneidensis* MR-1 bearing the pBBR1MCS plasmid, and was shown to be unaffected by plasmid copy number in the former, at the concentrations used.

The effect was not observed in CAT expressing strains in the absence of Cm, nor at sub-inhibitory concentrations for BL21(DE3). Furthermore, it was shown that current maxima increased with Cm concentration in a linear fashion. Though plotting this indicated that the sub-inhibitory concentrations of Cm for BL21(DE3) may have been insufficient to provide a discernible impact. However, it was observed that for Cm^R strains at working concentrations of Cm and above, after peak current was reached the current would begin to gradually decline. It was concluded that this was due to Cm degradation or depletion, and not lactate depletion, with lactate addition having a minimal effect on current. Ultimately, we propose a biochemical mechanism for the mediator-like EET.

Together, this work illuminated a previously unknown bioelectrochemical interaction that may be of great relevance to the field, particularly given the prevalent use of pEC86 for cytochrome maturation. Furthermore, given previous use of expensive and toxic mediators for *E. coli* strains within BES, were the mechanisms of this Cm effect mediator

activity fully understood, it might be harnessed in place of these in a range of applications. Experimental plans for exploring this were discussed.

Chapter 5 – Azo Dye Reduction Screening of a Genomic Library of *S. oneidensis* MR-1 in *E. coli*

5.1. Introduction

Given the limited research of heterologous expression of electroactive pathways and factors in *E. coli*, as discussed in Chapter 2, much potential appeared to remain within the *S. oneidensis* MR-1 genome. Discovery of such factors might even be made easier within *E. coli* due to redundancy in electroactive systems within dissimilatory metal reducing bacteria (DMRB) concealing their involvement through compensatory expression of others[134]. Consequently it was believed that a genomic library of *S. oneidensis* MR-1 within *E. coli* might lead to the discovery of novel electroactive factors.

In selecting a method for library creation, the potential issues surrounding the throughput of conventional bioelectrochemical analysis methods were considered. However, it was determined that a sacrifice in coverage would provide no benefit to the practical screening of the resultant library. The use of larger genomic fragments might also promote the identification of multigene factors that might otherwise go overlooked. In addition to strong promotors placed at the ends of any library fragments, the possibility existed for the recognition of heterologous promoters by the host transcriptional machinery, as previously discussed. Thus, the use of a Fosmid-based system was proposed; the CopyControl system by Epicentre was selected.

Fosmids are (usually) single copy number cloning vectors derived from the F' plasmid, and are capable of holding large inserts (up to ~40 kbp)[148]. They have previously been used to build genomic libraries, where large fragment sizes might have been advantageous[149,150]. Due to the large insert size, appropriate coverage can be achieved with a lower number of clones. Additionally, with the added potential for host interaction with heterologous promoters, and the clustered nature of the genes of

existing heterologous electroactive pathways in *E. coli,* it was felt that the possibility of identifying operons which contribute to electroactivity was improved [133].

Due to the challenges relating to throughput for bioelectrochemical systems (BESs), and practical considerations with iron reduction assaying[28,128] as discussed in Chapter 2, the ability to conduct a larger screen, such as would be required for a genomic library, was restricted. The use of mediators, such as riboflavin, to improve this process was considered, by initial experiments showed no sensitivity of *E. coli* to such (unsurprising given *S. oneidensis* MR-1's reliance on its outer membrane cytochromes to use it within BESs[79]). And we were not prepared to resort to toxic mediators. Given the bioremediation application of extracellular electron transfer (EET) to azo dye reduction (and so degradation) [3,151–153], it was conceived that this might be adapted into a higher throughput, colourimetric screen that would be adaptable to a 96-well plate.

One of the primary structural features of azo dyes is a strong, double bond between two nitrogen atoms linking their other groups[154]. It is this bond that makes them stable, unlike other dye types that more readily degrade autonomously. A few bacteria have been found to have azoreductases that can catalyse the reduction of this bond, where after further degradation can be more easily achieved[155,156]. However, it has been demonstrated that the reductive ability of DMRB EET pathway proteins can catalyse this degradation also[154]. Consequently, this makes such degradation a potential indicator of electroactivity. Figure 5.1. illustrates the key bond and the electroactivity mediated reduction of it.

This chapter presents the creation of genomic libraries of *S. oneidensis* MR-1 in *E. coli* strains including BL21(DE3) and C41(DE3) with the aim of screening these to identify novel candidate genes for increasing electroactivity. The development of a high throughput dye reduction assay for this purpose is subsequently presented, alongside the results of the screening.

Figure 5.1. Azo Dye Structure and Degradation

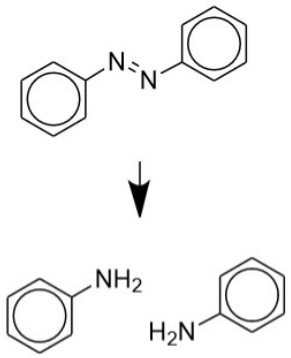

The key double bond that is present in azo dyes is illustrated, followed by the effect of electroactivity mediated reduction on it. This diagram created using ChemDraw.

5.2. Results and Discussion

5.2.1. Fosmid Library Creation

The "CopyControl™ HTP Fosmid Library Production Kit with pCC2FOS™ Vector" manufactured by Epicentre is designed to create a genomic library of ~40 kb fragments using a modified F' plasmid that can be induced to high copy number. The methodological workflow is diagrammatised in Figure 5.2., and briefly comprises: the extraction of genomic DNA from *S. oneidensis* MR-1 in our case, shearing and end repair of that DNA as necessary, size selection for fragments within the requisite size range, ligation of those fragments into the fosmid vector, followed by packaging the various clones into phage particles, analysis of the titre, then plating out the required number of clones for subsequent harvesting and storage.

Figure 5.2. – Fosmid Library Creation Workflow

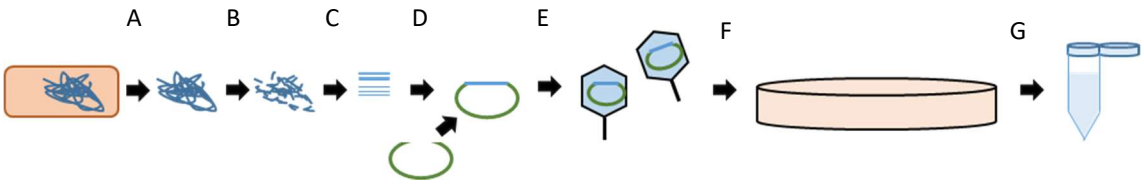

Comprising: genomic DNA extraction (A), shearing and end repair (B), size selection (C), ligation into Fosmid (D), packaging and testing titre (E), transforming and plating out (F), and harvesting and storage (G). The workflow for creating a genetic library using the CopyControl system is demonstrated.

A *S. oneidensis* MR-1 genomic DNA prep was initially required and carried out using the DNeasy Blood and Tissue Kit (Qiagen) according to the manufacturer's instructions. The concentration was checked by running a 1 µl aliquot on a 1% agarose gel, and found to be ~30 ng/µl, which was suitable for the proceeding step. The shearing of the genomic DNA was analysed by running a 4 µl aliquot on a 1% agarose gel at a low voltage (30 V) overnight, the result of which can be seen in Fig 5.2. below. This level of shearing, a product of the genomic extraction process, was sufficient for the purposes of Fosmid library production.

The next stage of the protocol required an end repair reaction followed by size selection of fragments around 40 kb in size. The manufacturer's recommended method suggested use of a pulsed field gel electrophoresis machine, useful for effectively separating high molecular weight DNA, however one was not available. Furthermore, the alternative method they presented, involving the use of low melting point (LMP) agarose and a low voltage over a long period of time, was found to require modification after initial attempts; it was found that the gel was partially melted during the course of the separation, and the recommended time was too short to effectively separate fragments of the required size.

Figure 5.3. – Shearing of Genomic DNA

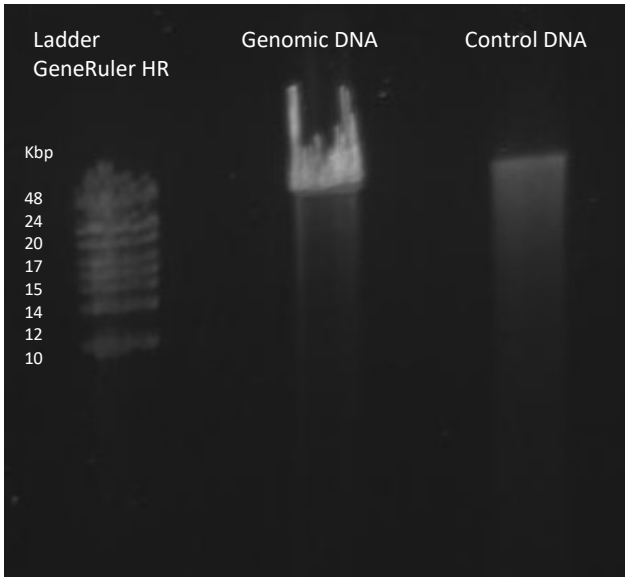

The genomic DNA shearing was tested as part of the CopyControl Fosmid Library creation workflow previously outlined. GeneRuler HR was used in addition to the Fosmid control DNA, and while the gel did not run evenly and the genomic DNA does show a lot of smearing, the pattern indicates a good concentration of fragments at the desired size - around 40 kb in size.

A LMP agarose gel was run in a 4 ^{o}C temperature controlled room, at 30 V, for three days. After this time the sides of the gel were cut off and stained with ethidium bromide according to the manufacturer's instructions, visualised, and markings made to indicate the region corresponding to the size of genomic fragments desired. The whole gel is not stained as ethidium bromide, an intercalating agent, would bind the genomic fragment DNA and likely disrupt subsequent steps according to the manufacturer's instructions. The gel band was subsequently excised and stored at -20 ^{o}C overnight prior to DNA extraction, ligation into the pCC2FOS vector, and packaging reaction.

The pCC2FOS vector contains a T7 promoter and a *lac* promoter flanking the fragment insert site. Given the absence of reference to induction of expression in the available documentation, contact with the manufacturers of the CopyControl Fosmid Library creation kit was sought. After speaking with the manufacturers, it became apparent that the Fosmid library, in the EPI300 T1^{R} *E. coli* host strain provided, was unsuitable for

expression of any inserted fragments. The strain did not contain the DE3 lysogen (T7 RNA polymerase controlled by a lacUV5 promoter), meaning transcription using the T7 promoter could not be induced. Given that we were interested in proteins expressed by heterologous promoters within the large fragments an argument that this did not matter was made. However, the T7 RNA polymerase can transcribe very long mRNA, which we felt would increase our coverage of fragment ends. If multiple library screen hits overlapped in their T7 adjacent regions it would also help us to narrow down the causative factor.

The two expression strains BL21(DE3) and C41(DE3) were selected as hosts for the library, consequently. The former due to its use in studying the top down engineered strains discussed in Chapters 4 and 6, and the latter due to the likelihood that novel electroactive factors that might be identified would be membrane proteins. Strain C41(DE3) was derived from BL21(DE3) and contains several mutations, including a reduction of the activity of its lacUV5 promoter, which causes it to be resistant to the toxic effects of the overexpression of certain membrane proteins [104,140]. Unlike the EPI300 $T1^R$ strain, however, these strains do not possess the machinery allowing for the induction of increased fosmid copy number. This would have an impact on fosmid extraction concentrations. It was decided that the benefits of the more commonly accepted and available expression strains outweighed those of the considered alternative (production and use of an EPI300 $T1^R$(DE3) strain).

The phage titre was then analysed, and it was calculated that 22 LB agar + Chloramphenicol (Cm) plates of *E. coli* transfected with undiluted phage would be required to provide the 600+ clones needed to ensure the desired level of coverage (99% probability that a given sequence is represented). This turned out to be an overestimate, as the phage titre was significantly higher with these plates. The library was stored using the manufacturer's recommended option, as a glycerol stock containing a mixture of all clones at -80^{o}C.

As with the alternative fragment separation protocol, the manufacturer's instructions for harvesting plates of cells were impractical, as they required a small volume of LB to

be transferred between each plate; in practice too much volume was lost when transferring the solution between plates. Consequently a sterile loop was used to collect cells from the plates and suspend them in LB within a 50 ml Falcon tube, before dilution with glycerol, aliquoting into 5 eppendorf tubes, and storage at -80^{o}C. The two host organisms were collected and stored separately.

5.2.4. Development of a Colourimetric Screen for Electroactivity

As previously discussed, DMRB have been used in the literature to reduce azo dyes, degrading and thus decolourising them [3,151–154,157]. We hypothesised that this could be harnessed to construct a high throughput screen capable of rapidly screening our genomic library for novel electroactive factors. As with the HC methodology and equipment presented in Chapter 4, following our initial protocol designs engineered and control strains of *E. coli* were used to test them.

While an agar plate based screen was initially considered it was believed a 96-well plate based assay would be more practical for higher throughput, and provide quantitative data, if feasible. Colourimetric experiments involving use of Reactive Black 5 (RB5), an azo dye, as electron acceptor by *Shewanella* spp. are documented in the literature [154,158], but in order to provide additional screening options for the Fosmid Library (and potentially constructed strains in the future) two others were identified for testing. Reactive Red 120 (RR120) and Basic Green 5 (BG5) have both been used to study bioremediation of waste water from the textile industry where they are used, and were readily available, with documented absorbance peaks and assay concentrations [159,160]. These concentrations were used in initial tests for both categories of assay.

5.2.4.1. 96-Well Plate Based Colourimetric Assay Method Refinement

As described in Chapter 3, overnight cultures of test strains were used to inoculate LB broth containing one of the three dyes being tested, which were then added to the wells of the 96-well plate. Following an initial absorbance reading at the appropriate relative absorbance peak, plates were incubated at 25°C, aerobically and anaerobically, for 48 hours before final readings were taken. Concentrations observed in the literature were used for each of the three dyes [159,160].

Initially, in addition to uninoculated control wells, wells containing LB broth inoculated with test strains but with no dye were used, as illustrated by Figure 5.4. for RR120. However, an issue with the concentration depicted became immediately apparent when the "zero" reading was taken for this plate; the absorbance of the RR120 at 500 mg L^{-1} was too high for the plate reader to measure. Consequently a series of dilutions were conducted to find a more suitable concentration. From the results it was gathered that a 50 mg L^{-1} final concentration would be ideal, as this was the highest concentration that returned a non-"overflow" result for every well.

Figure 5.4. – Initial Reactive Red 120 Plates

Aerobically (left) and anaerobically (right) incubated 96 well plates assaying the degradation of reactive red 120. Initial protocol used Shewanella baltica (another Shewanella species comparable to S. oneidensis MR-1), and E. coli strains bearing either pACYC Duet-1 + pRGK333 or pACYC mtrCABO + pRGK333. Decolourisation was clear for Shewanella baltica wells, but initial concentration of RR120 was too high for TECAN to read.

After incubation of the initial series of plates, absorbance readings were recorded and analysed. It was found that, while dye degradation could clearly be observed in the *S. baltica* containing wells for RR120 and RB5, the absorbance from cells present in the culture appeared to prevent any quantitative difference from being apparent. Attempts were made to compensate for bacterial growth in dye containing wells using absorbance readings from LB only wells but even after this, no significant difference was observable.

In order to eliminate the absorbance of the bacterial cells and get a clearer result of the dyes' degradation, the protocol was modified to include a plate centrifugation step proceeding growth. Following centrifugation, it was observed that the cell pellet was spread across the bottom of a number of wells, which would likely continue to affect absorbance readings, so the protocol was further revised to require transfer of supernatant to a sterile 96 well plate following centrifugation. This was carried out and the results analysed for absorbance differences correlating to degradation of dye. The only significant difference observable was for RR120.

It is worth noting that as a consequence of transferring the supernatant to a new plate bubbles were formed in many of the wells, which affected the readings in a number of them. Care was subsequently taken to avoid their formation. It was also noted at this stage that there may be a degree of error in the results accordable to uneven evaporation in the wells of the 96 well plates though this should be minimal given the temperature controlled conditions incubation is carried out under. Nevertheless, plates were subsequently sealed with parafilm and wrapped in damp tissue prior to incubation, in order to minimise evaporation.

To confirm the absorbance peak measurements were being taken at appropriate wavelengths, and so not responsible for the lack of quantitative difference, wavescans of each of the dyes were carried out using a spectrophotometer at the starting concentrations used on the last plates, as shown in Figure 5.5. below. RR120 produced a high, wide peak around 530 nm, as expected. Both RB5 and BG5 produced wide peaks at 595 and 660 nm respectively, each conforming to expectation also. However, the

peaks for RB5 were comparatively short, suggesting the need and scope to increase the concentration used.

Given this and the prior need for optimisation of RR120 concentration, it was believed that this process would be necessary for both RB5 and BG5. However, due to the relatively high concentration of BG5 being used, and concerns over the difficulty of producing a more concentrated stock solution, it was decided to discontinue development of 96 well plate screens employing it. RB5 concentration was subsequently optimised through testing of a range of dilutions; a 1 in 100 dilution of the 1% w/v stock, tenfold more concentrated than the previous working concentration, was found to be most suitable from those tested.

Figure 5.5. – Wavescans of Assay Dyes

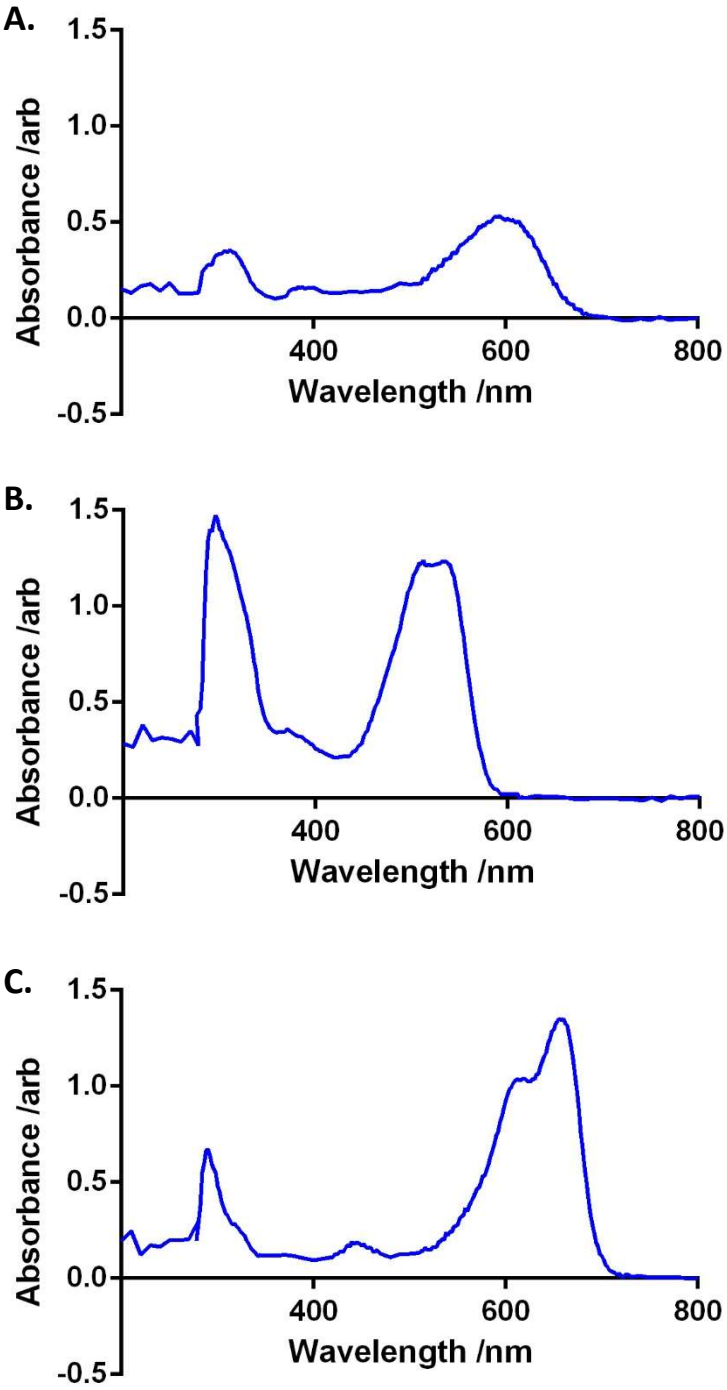

Wavescans of each of three azo dyes initially trialled for high-throughput degradation screening for electroactivity: reactive black 5 (A), reactive red 120 (B), and basic green 5 (C). Data points from the spectrophotometer were transcribed and graphs reproduced in GraphPad Prism. Reactive black 5 shows a clear need for a higher working concentration.

5.2.4.2. Comparison of E. coli *Strains with Colourimetric Screen*

In order to validate the screening protocol, strains previously used in HC experiments were tested. Initially this involved BL21(DE3) strains bearing pACYC Duet-1 or an mtr/omcA encoding equivalent, alongside the pRGK333 inducible *ccm* gene plasmid. Subsequent to the switch to pEC86 for *ccm* gene expression in HC experiments equivalent strains were also analysed.

Figure 5.6. – Normalised RB5 Reduction by *E. coli* Strains

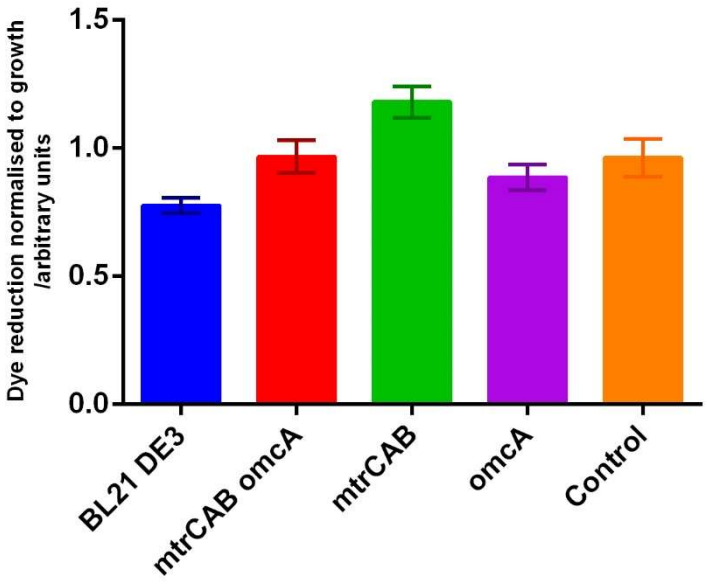

The host for all strains was BL21(DE3) with the relevant genes indicated being borne on the pACYC Duet-1 expression plasmid. The pRGK333 ccm gene plasmid was also present in all strains save for the BL21(DE3) only strain. The control listed above contained an empty pACYC Duet-1 plasmid. Displayed is the consolidated average data from three experiments each containing at least 7 replicates for each strain, with error bars representing the standard deviation. The mtrCAB strain significantly outperforms the others, including the control (unpaired t-test, $p<0.05$).

Figure 5.6. displays the data from the initial tests for RB5, which show an increased reduction in the mtrCAB strain over the plasmid free and control plasmid strains, as well

as omcA containing strains. This observation was made consistently, however the margin of difference is minimal making differences more prone to obfuscation through error, suggesting that the assay does not provide the same resolution of electroactivity as others. Additionally, while the engineered pACYC mtrCAB or mtrCABO +pRGK333 strains did not outperform their controls in the HC experiments discussed in Chapter 4, it was not unreasonable to expect variation in their ability to reduce soluble or insoluble electron acceptors under different conditions. Nevertheless, further strains were subsequently tested. Not included is the data for *S. oneidensis* MR-1 for reasons of clarity, as complete dye reduction was visually observed within the first hour proceeding inoculation.

In addition to the pRSF strains, the MFe444 (engineered) and MFe408 (control) strains published in Jensen et al. [28] were tested to provide a further comparison. In order to further validate the length of time required, three identical 96-well plates were set up using the same inoculating 96-well plate. These plates were incubated together anaerobically for one, two, and three days respectively. The resultant data are represented in Figure 5.7.A, 5.7.B, and 5.7.C for the respective plates.

While the overall trends do not appear to change across the varying incubation times, it is clear that the longest incubation results in the lowest error observed. This supports the decision to use a longer incubation time in the general protocol. Strain comparison highlights an unexpected difference between the engineered and control BL21(DE3) based strains and the comparable MFe strains in C43(DE3), with no clear distinction between the normalised RB5 reduction for the former, but a very clear one for the latter in the expected direction; the engineered strain reduced more dye per OD_{600} unit than the control.

The improved differentiation of the MFe strains may have been aided by their host strain. As can be seen for the non-plasmid bearing BL21(DE3) and C43(DE3) strains, the latter displays a higher level of normalised dye reduction. This may be due to variations in the cell membrane contributing either to improved uptake of the dye, or facilitating non-specific reduction, or in this instance a greater growth rate for BL21(DE3) under

these conditions skewing the result. Though, as will be later discussed in Chapter 6, we cannot conclusively assign this difference to strain choice or concomitant metabolic variation without additional cymA and mtrCAB constructs being produced, it is not necessary to do so to indicate that the dye assay is capable of highlighting some electroactive factors. While it may overlook some and be susceptible to error, any novel factors identified would be interesting, and its high throughput provides a significant advantage over other available methods.

Figure 5.7. – RB5 Reduction at Variable Time Points

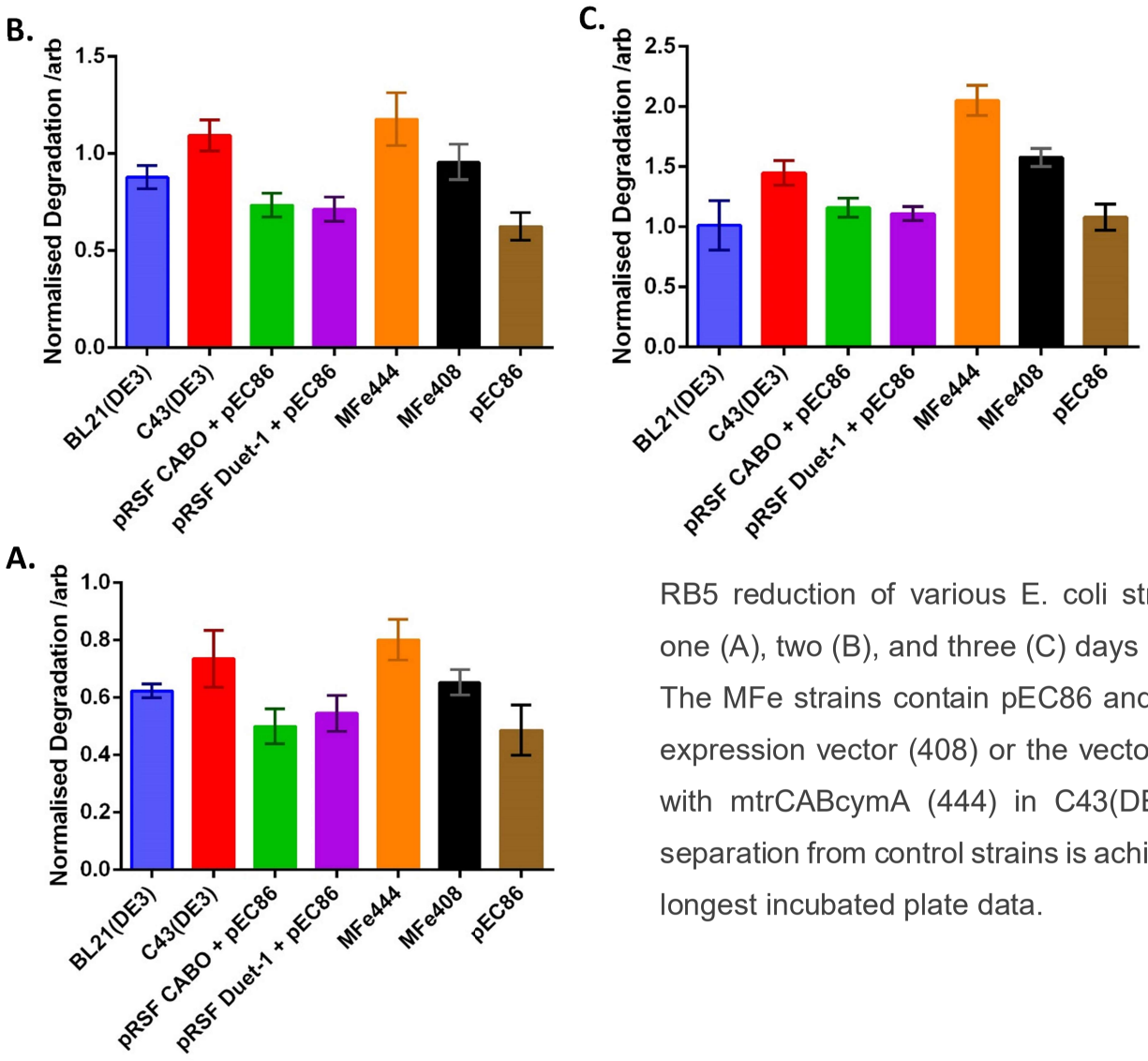

RB5 reduction of various E. coli strains, after one (A), two (B), and three (C) days incubation. The MFe strains contain pEC86 and pSB1ET2 expression vector (408) or the vector encoding with mtrCABcymA (444) in C43(DE3). Better separation from control strains is achieved in the longest incubated plate data.

5.2.3. Library Screening with Dye Reduction Assay

Libraries were screened using the 96-well plate based assay previously discussed. Briefly, a dye-free starter 96-well plate was inoculated with individual colonies from an agar plate cultured from the library glycerol stocks. The last column of each plate was used for four replicates each of cell free and BL21(DE3) controls, which would remain dye free in the dye assay. These starter plates were incubated aerobically at 37 ^{o}C overnight with 150 rpm shaking, before being used to inoculate the dye plates. Subsequently the wells were diluted in a 1:1 ratio with 50% glycerol and stored at -80 ^{o}C to facilitate access to specific clones identified during the screening process.

Following data collection, the dye reduction was calculated through the difference between the initial and final readings (post-centrifugation) and normalised to the average growth of the BL21(DE3) control wells. This decision was made due to concern over the likelihood for increased error when dealing with single replicates, and the confidence that the growth of BL21(DE3) could be used as a measure of general growth on the plate. While this may not be universally true, this formed the first stage of screening, with a second stage planned to address this issue. The results normalised (divided by growth – calculated by difference in OD between unspun and spun plates) in this fashion for the two dyes were combined and analysed. Approximately 1400 clones across the two (BL21(DE3) and C41(DE3)) libraries were screened. This data can be found in the appendix.

In the second stage of screening, four biological replicates of each clone were inoculated into designated columns of a 96-well plate. The cell free and BL21(DE3) controls were present as before. These starter plates were then used to inoculate RB5 dye plates, which were processed in the same fashion as with the various engineered and control *E. coli* strains tested in the previous section, being normalised to their own optical densities at the 595 nm measured. Approximately 60 of the best performing (most dye reduction observed) clones were tested in this fashion.

From the second stage of testing 8 clones were identified as being superior to the other strains tested and were taken forward for sequencing. As previously discussed the use

of a “Qiagen spin miniprep kit” for the extraction of the fosmid yielded very low concentration DNA, understandable given the fosmids’ sizes and single copy number. This hindered attempts to sequence the clones, however it was found that the use of midiprep volumes with the non-spin miniprep kits by qiagen resulted in improved yields. The locations of the ends of four of these clones on the *S. oneidensis* MR-1 genome are displayed in Figure 5.8. below.

Figure 5.8. – Screen Hit Fragment Ends on Genome Map

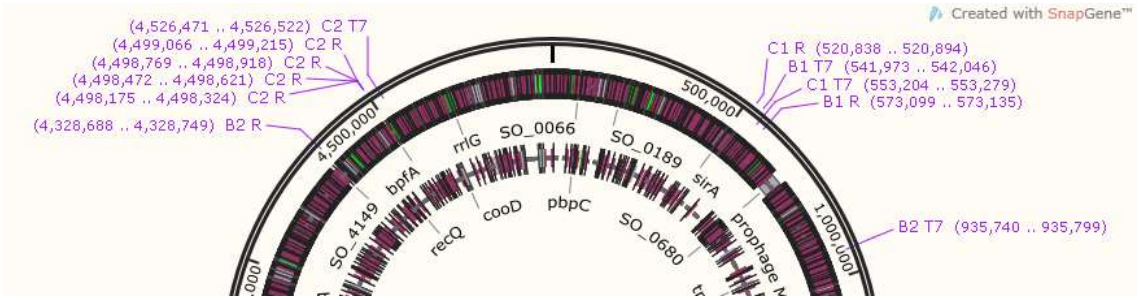

Four clones, two of each host strain as denoted by B (BL21(DE3)) or C (C41(DE3)) are represented on a S. oneidensis *MR-1 genome map produced in SnapGene. The number assignment here is arbitrary. The end of each primer relative to insertion in the fosmid is denoted by T7 (for the T7 promoter adjacent end) and R (for the reverse end). One clone’s end falls in a repeating region (C2 R), while another (B2) is clearly multiple concatenated fragments given the separation of the sequenced ends. Two clones (C1 and B1) overlap at their T7 ends – the region between B1 T7 and C1 T7.*

Several things can be drawn from this figure. Perhaps most obvious is the vastly distant end points identified for the B2 clone. As it can be safely ruled out that the clone contained a third of the *S. oneidensis* MR-1 genome, it is clear that some ligation of multiple <40 kb fragments prior to insertion into a fosmid occurred during the ligation step of the library creation protocol. We do not believe this presents a problem for our purposes, as overall coverage is unaffected. However, it does introduce additional challenges for the complete characterisation of such clones, as additional, tailored primers and a systematic approach would be required to identify the limits of each of the sub-fragments within the greater insert.

Secondly, as noted for the C2 clone, the sequence for one end (R) is compatible with multiple locations. This is simply due to the recurrence of this particular sequence multiple times within the *bpfA* gene, which encodes a 285.1 kDa protein involved in biofilm promotion.

Thirdly, and most interestingly, the fragments of the B1 and C1 clones overlap at their T7 ends. This overlapping region is just over 11 kbp in length, and detailed in Figure 5.9. below. We felt that for two different clones to have such an overlapping region made it worthy of further investigation; it suggested strongly that the determining factor for the increased dye reduction lay in the overlap. That the overlapping region occurred at the T7 ends of each of these fosmids further supported this conclusion, as genes within it were more likely to be expressed. Furthermore, the identification of this overlap occurred across the two base strains, indicating that the phenotypic activity of whatever causative element lay within it was strain independent.

Figure 5.9. – Fosmid Screen Hit Overlapping Region

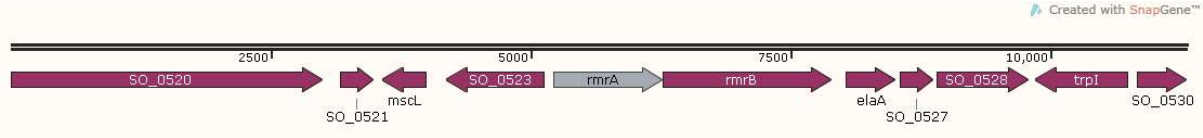

The overlapping region of two "hit" fosmids - comprises (in order from left to right) a heavy metal efflux pump permease component, a monooxygenase protein, a large conductance mechanosensitive ion channel protein, a LysR family transcriptional regulator, two multidrug efflux pump permease components, a GNAT family acetyltransferase, an antibiotic biosynthesis monooxygenase family protein, a radical SAM protein, a transcriptional activator of tryptophan biosynthesis, and a truncated RhtB family amino acid efflux protein. Only rmrAB appear part of the same regulatory element. This map was created using SnapGene.

5.2.4. Cloning of Overlap Region

Further investigation of this overlap region became the subsequent focus of work on the fosmid library. The reduced size relative to the expected fragment size (~11 kbp from ~40 kbp) helped to narrow down the causative loci significantly. It was initially planned to sub-clone the two halves separately into pRSF Duet-1 and pRSF *mtrCABomcA* for further bioelectrochemical testing. The primers would divide the overlap between the *SO_0523* and *rmrA* genes, such that *rmrA* and *rmrB* remained on the same fragment. It was thought that this approach would help to narrow down the causative factor (be that a single or multiple genes) further.

Attempts to sub-clone the two halves were persistently unsuccessful, and so a secondary approach of individually cloning each gene was pursued. Primers flanking each individual gene (including non-coding regions before each, to include potential regulatory elements) with compatible restriction sites to permit cloning of each individual gene or any number of continuous genes within the overlap (with the intention of also cloning *rmrA* and *rmrB* together) were designed for insertion into the second multiple cloning site (MCS) of the pRSF Duet-1. All primers were designed with a T_m between 54 and 58 ^oC to maximise cross compatibility.

PCR reactions were set up with the various primer pairs, with duplicate reactions of each set up so that both *S. oneidensis* MR-1 genomic DNA and fosmid DNA (C1 fosmid previously described) were separately used as template. Figure 5.10. shows the two gels on which the PCR products of expected size were observed for the individual genes, though further attempts to PCR the two halves of the overlap region remained unsuccessful.

Though *SO_0521* was not successfully replicated using the *S. oneidensis* MR-1 genomic DNA template (Figure 5.10.A and 5.10.C) it was successful with the fosmid template (Figure 5.10.B and 5.10.D). The reverse was true for the *rmrB* construct. For all other primer pairs it was possible to produce bands at the relative expected sizes. All of these bands were then subsequently gel extracted, and digested with AatII and FseI (New England Biolabs, UK) in CutSmart buffer at 37 ^oC for an hour, in addition to pRSF Duet-1

plasmid. The latter was subsequently treated with calf intestinal phosphatase (CIP) to prevent recircularisation. Following digestion, all samples were purified by agarose gel electrophoresis and gel extraction (Quiagen kit).

Figure 5.10. Agarose Gel Images of Overlap Gene PCR Products

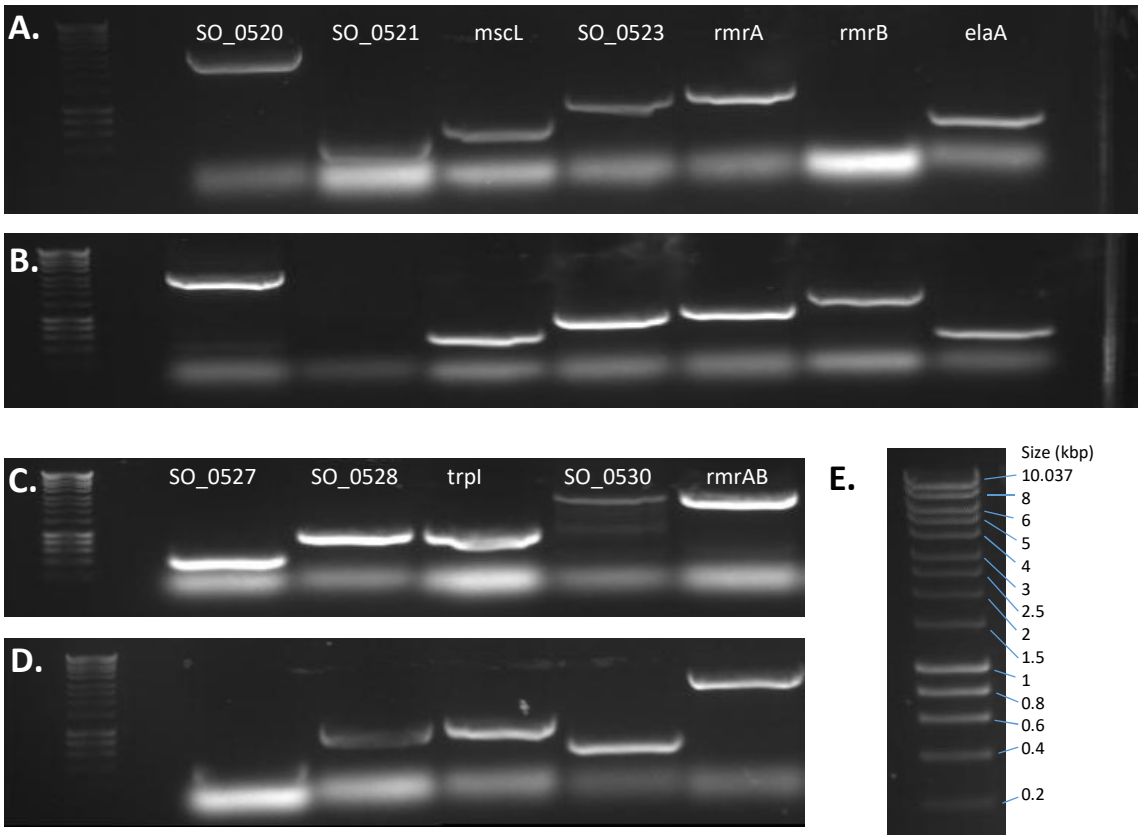

Images of PCR products of each of the reactions for cloning genes identified from the fosmid overlap sequence, using S. oneidensis *MR-1 genomic DNA (A and C) and C1 fosmid DNA as template (B and D). Ladder (Hyperladder 1kb, Bioline, UK) used is labelled (E) for reference. Images are grouped by target genes. Expected fragment sizes in base pairs were as follows: 3028, 423, 574, 1000, 1129, 1655, 532 (A and B), 386, 944, 946, 520, and 2756 (C and D).*

A 1:1 ratio of vector to insert for the ligation reactions ultimately produced colonies for all constructs, excepting *SO_0530*, following heat shock of DH5α chemically competent cells and plating onto LB agar plates containing kanamycin. Construction of pRSF SO_0530 was not pursued further; the truncated nature of the protein coded within the overlap fragment made it unlikely to be the contributing factor. Selected colonies were

grown up in overnight LB cultures and the plasmid DNA extracted using a miniprep kit (Quiagen). A nanodrop was used to quantify plasmid concentrations before samples were sent for verification by sequencing.

All individual gene constructs pursued, as well as the rmrAB construct, were successfully verified by sequencing, although several were inserted into the vector in the opposite orientation to that planned. This orientation was not initially expected to affect expression, however later caused concern over the confidence that could be expressed in derived data without validation of expression.

5.2.5. Overlap Gene Construct Comparison

In order to identify which of the genes from the overlap were responsible for the increased dye reduction phenotype, further 96-well plate dye reduction assays were planned. While it still remained possible that a combination of genes from the overlapping region of two of the 'hit' fosmids were accountable, excluding rmrAB which were to be tested, it was thought that a single gene would be more likely.

The RB5 dye reduction assay was used to investigate the overlap gene constructs. The protocol remained mostly as previously described. However, due to the loss of access to an anaerobic cabinet as used prior, the use of a sealable anaerobic jar was required. Once initial readings were taken and the plates sealed within the vessel, the jar was placed in a static incubator at 30 ^{o}C for the duration of its incubation.

The dye degradation after three days, normalised to growth, is presented in Figure 5.11.A and 5.11.B, with two replicate plates represented separately (A and B). While differences are marginal, it can be noted that the normalised degradation was consistently higher for three of the constructs across the two plates, than the others: constructs bearing *SO_0520*, *SO_0527*, and *rmrAB*. The significance of these differences was verified by unpaired T-tests ($p<0.1$). However, growth within these plates was poor, and while wells with a final bacterial OD_{595} less than 0.1 were excluded from the normalised degradation data presented, the poor growth casts further doubt on the strength of conclusions that can be drawn from this data; the statistical analysis can be misleading.

Figure 5.11. – Dye Reduction Assay of Overlap Constructs

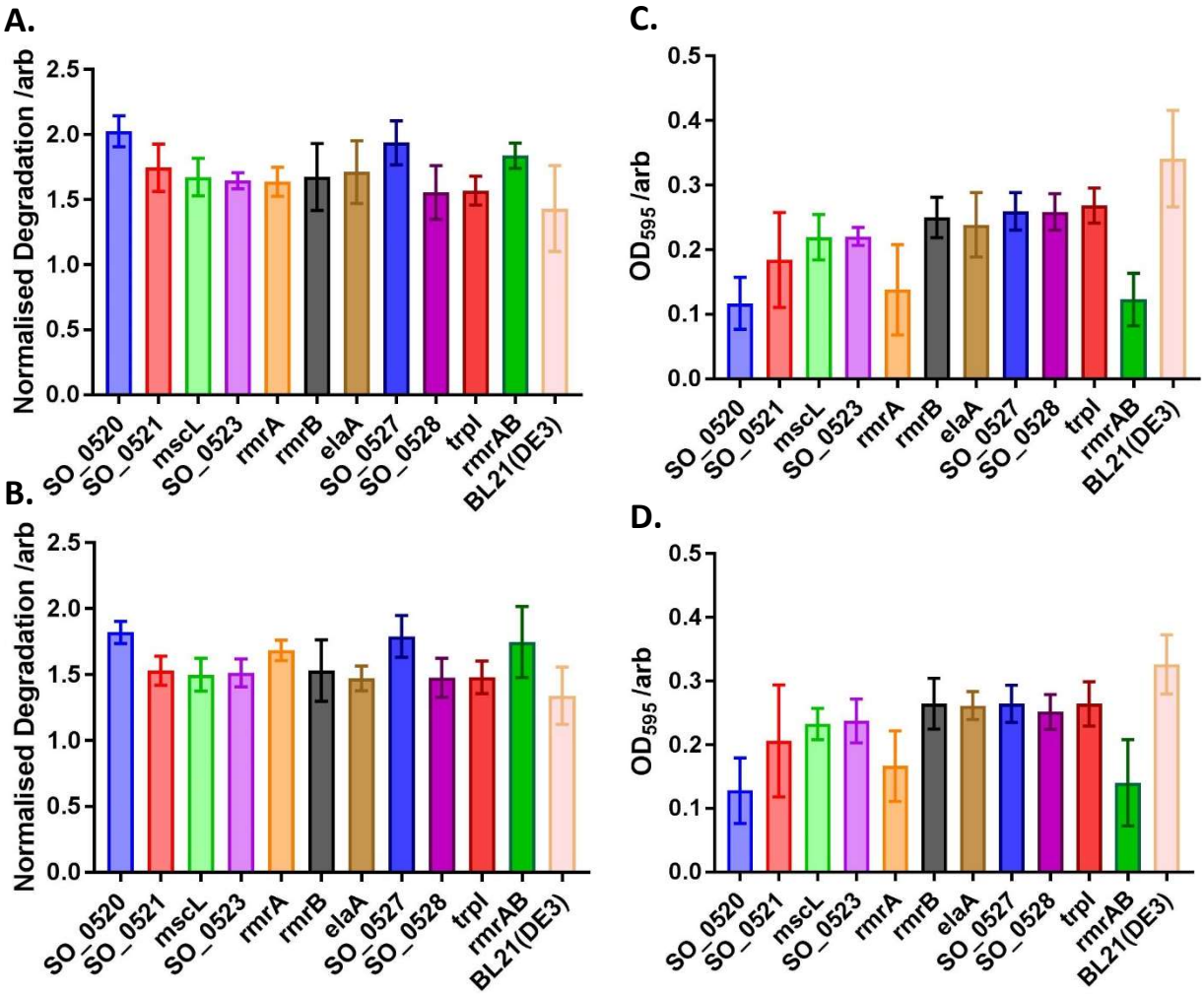

The reduction of RB5, normalised to growth, by various single and multigene constructs derived from the overlapping region of hit fosmids is presented for two replicate plates (A and B). The respective calculated OD_{595} corresponding to growth are presented alongside (C and D). Normalised degradation data excludes wells with a bacterial OD_{595} less than 0.1. Confidently differentiating clones is difficult.

Figure 5.11.C and 5.11.D show the calculated bacterial OD_{595} for A and B respectively. They clearly present an extremely low (mean of ~0.12) OD for two of the three potential strains of interest (*SO_0520* and *rmrAB* construct strains), significantly lower than the majority of the rest of the strains. This may have contributed to the higher normalised degradation observed; that the higher relative degradation was an artefact resulting from the exceptionally low growth of these strains. This conclusion reiterates the desirability of longer incubation times for resolving differences between strains, as

discussed in section 5.2.4.2., previously. However, it also emphasises how borderline the sensitivity of this technique may be; how much noise is present, and how difficult it can be to draw definitive conclusions.

In comparison, the *SO_0527* containing construct did grow comparably to the other strains yet was still observed to have a greater normalised degradation than them, however this identified "hit" should be taken in the context of the concerns discussed previously.

5.2.5.1. Discussion of Novel Reductive Factor SO_0527

UniProt Knowledgebase, pooling annotation from the J. Craig Venter Institute and Gene Ontology Consortium, describes the protein product of *SO_0527* as an antibiotic biosynthesis monooxygenase family protein. Monooxygenases incorporate hydroxyl groups into metabolites in reactions they catalyse with metal prosthetic groups, so it stands to reason that one might be electrochemically active; the enzyme might interact to reduce the azo dye bond directly, or else might modify it (or another metabolite) in a way that it becomes reactive, leading to the reduction of the bond. However, all ontology information is based on inference, either from electronic annotation or biological aspect of an ancestor. The "antibiotic biosynthesis" component of the descriptor is insufficiently explained to draw any links between this and the chloramphenicol resistance pathway mediator activity observed in our HCs as discussed in the previous chapter. However it would be something to bear in mind in any future work.

A *Vibrio fischeri* ES114 orthologue, VF_0710, was identified through EnsemblBacteria but no additional information was gained from this. And, indeed, an NCBI Blast search identified orthologues in other Shewanella spp., but again this ultimately did not prove enlightening as they were also uncharacterised with no additional auto-annotated information of use.

A general interrogation of the literature was found to be no more illuminating; unsurprising given the general quality of curation of the resources mentioned above. An attempt was subsequently made to identify SO_0527 detection in available datasets of

published "-omics" studies[142,150,161–163] in *S. oneidensis* MR-1. Though no such identification was discovered, we do not take this negative to be indicative of anything; even were detection of the specific protein guaranteed, the range of foci of the studies, as well as the possibility of the bioelectrochemical relevance being specific to *E. coli*, would provide ample reason for it not to appear in processed data.

Without further validation it is uncertain that SO_0527 did, in fact, have an impact on redox activity in *E. coli*. And even if we were confident in its electroactivity, as with soluble and insoluble metal reduction[127,128], this would not necessarily mean that activity would be reflected in an increase in electrode reduction. A knockout study using the original fosmid with each gene in the hit region sequentially knocked out could assist with the verification. Unfortunately, further validation of these findings and characterisation of this novel factor did not fall under the purview of this study, although this is further discussed in Conclusions and Future Work.

5.3. Conclusions

In this chapter we demonstrated the production of genomic libraries of *S. oneidensis* MR-1 in multiple *E. coli* host strains, commenting on potential pitfalls and methodological adjustments over the manufacturer's recommendations. The development and refinement of an azo dye reduction assay for the high throughput screening of this library for genes contributing to increased electroactivity was also presented, though it may be limited by its sensitivity. This assay was subsequently used to screen the *S. oneidensis* MR-1 genomic libraries in *E. coli*, identifying, among others, two clones with an overlapping region. Further investigation provisionally suggested the gene *SO_0527* as the causative, novel reductive factor. Further validation is required before engaging in investigation of the function of this protein.

Chapter 6 – Quantitative Proteomic Analysis of Engineered Electroactive *Escherichia coli* within a Bioelectrochemical System

6.1. Introduction

The continual, biologically-achieved electron transfer from bacteria to electrode within bioelectrochemical systems (BESs) relies on the energetic favourability of the process; it grants a metabolic benefit to the bacterial cell through the provision of an end terminal electron acceptor [10]. Dissimilatory metal reducing bacteria (DMRB) have adapted to be able to take advantage of extracellular electron acceptors, as discussed in the introductory chapters, utilising a network of sensor/regulators to adjust expression and activity of key pathways[164]. However, with heterologous extracellular electron transfer (EET) systems within *E. coli* it has not been shown that their metabolic processes have similar, interactive sensory/regulatory control to do this, nor would we expect otherwise[165]. *E. coli* is a facultative anaerobe, adapted to make use of a wide range of nutrients, within both the intestinal environment that it commonly occupies and beyond[166]. Its responses to anaerobic environments depend on numerous other factors, including: quinone pool redox state (ArcAB)[166], nutrient availability[167], acetate concentration[168], metal ion availability[169], temperature[170], and oxidative stress[171]. This complex regulatory web is not so easy to predict in how it will interact with the metabolic changes caused by engineered heterologous EET activity.

Other factors may still influence *E. coli* metabolic activity, both generally and specifically to the interaction with heterologous EET pathways, with consequent impacts on BES performance. For example, the maturation of recombinant EET pathway proteins following inoculation might be affected by limited availability of haem groups despite the additional cytochrome maturation genes, due to other metabolic pathways utilising necessary precursors, or an altered gene expression profile leading to more proteins

that require them being expressed and so depleting their levels[104,172]. This is something that Goldbeck et al. have investigated for Molecular Foundry strains, testing the levels of cytochromes in their strains throughout their experimental process[27], but still serves to illustrate the validity of such concerns.

The expression, maturation, and localisation of the EET pathway proteins are not the only factors that could affect EET. The activity of the heterologous pathway also relies on interaction with the host metabolic pathways to provide the electrons to transfer[126]. The exact nature of this interface is not fully understood and may even be greatly impacted by simple changes to carbon source or other environmental conditions. Indeed, the degree to which carbon source or media selection might impact the electroactivity of engineered, non-DMRB strains has not been well explored within the literature. In this chapter we set out to address this oversight, initially through comparisons within half cells (HCs), then through a global, quantitative proteomics approach to provide further insights into the regulation and metabolic activity of electroactive *E. coli* that might inform future strategies.

6.2. Results and Discussion

In order to explore the differences between our methodology and that used by TerAvest et al. [126], as well as decisions made as to host strain selection, the MFe444 (engineered with *mtrCABcymA* on an expression plasmid and pEC86 for *ccm* gene expression) and MFe408 (control with empty expression vector and pEC86 plasmids) strains were obtained. The host strain for these plasmids was *E. coli* C43(DE3), a strain usually used for overexpression of toxic membrane proteins.

We initially conducted a HC run, using the protocol previously devised, to allow a direct comparison between the strains used previously and these. As the published results for the TerAvest et al. strains[23,28,126] used different equipment, as well as other methodological differences, it was important to establish how different their activity was from the strains previously analysed. Thereafter, methodological changes to our own experiments could be made to discern the causative factors for any differences observed, either between the strains, or between the published results and ours for these strains.

The results are shown in Figure 6.1., where it is clearly observable that the control (MFe408) outperforms the engineered (MFe444) strain, in an inversion of the results seen for the strains previously tested within our HC setup (highlighted here as pEC86 and pRSF CABO + pEC86). Though this was reminiscent of the results obtained for comparable pRGK333, the inducible *ccm* plasmid, bearing strains. This could suggest a difference in functional expression of the Mtr proteins between the two engineered strains under these conditions. As the same *ccm* plasmid (pEC86) is used for all strains shown here, the cause for a possible change in functional expression could be due to differences between the expression plasmids used for the EET pathway genes, or the expression strain used. Yet given the minimal methodological differences for expressing the EET pathway genes in the TerAvest et al. study, and their clear result for a superior engineered strain, a metabolic difference seems more likely than drastic expression, maturation, or localisation changes.

Figure 6.1. – Initial Comparison of Engineered *E. coli* Strains

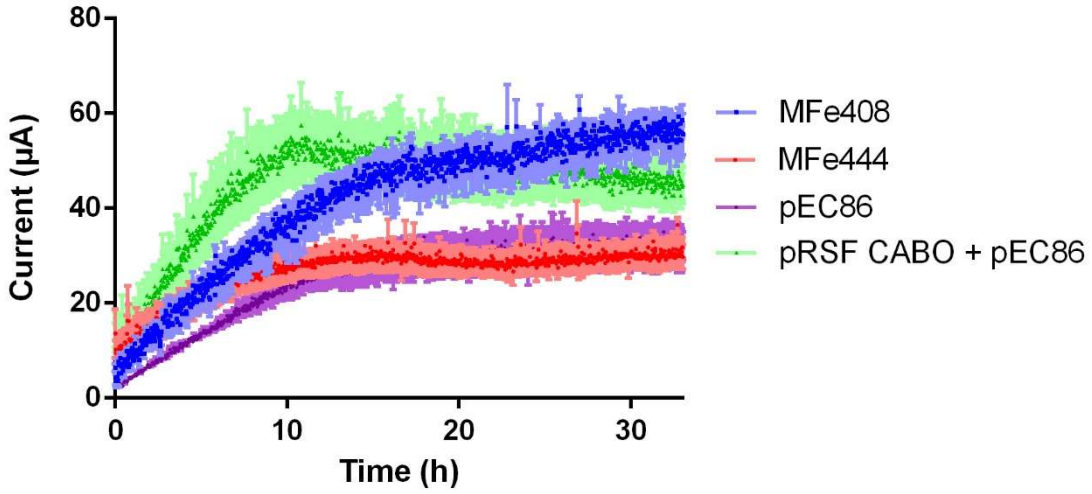

Chronoamperometry of engineered and control strains from different sources, and in different base strains, within HCs. C43(DE3) and BL21(DE3) for Blue/Red and Purple/Green respectively, the former colour of each pair being the control strain. In the M4m media used, unlike the BL21(DE3) strains, the engineered strain MFe444 is outperformed by its control; this contradicts expectations based on published activity in M1, a very similar media. The data for each line represents the average of three replicates with error bars highlighting the standard error of the mean.

With the clear improvement presented by TerAvest et al. [126] for their engineered strain using their methodology, this result was surprising. However, it leant evidence to the hypothesis that minor differences in media selection may be more important than so far presented in the literature; that electroactive *E. coli* EET was sensitive to minor metabolic shifts. Other differences naturally exist between the HC protocol used herein and that used for the work where these strains were originally presented, yet equipment differences would have been harder to explore, while a change of media and other methodology permitted a relatively quick and practical way to test this hypothesis.

6.2.1. Effects of Pre-Inoculation Growth Conditions on Electroactivity of Recombinant Strains

To rule out the differences in pre-inoculation growth and induction as responsible for the poor performance of the MFe444 engineered strain, the method outlined by TerAvest et al. was utilised. In the protocol used by TerAvest et al. the cultures grown for bioelectrochemical testing were grown in 2xYT, a richer media than the LB broth we used previously. Furthermore, in order to promote expression of the *mtr* multi-haem cytochromes, aminolevulinic acid, a haem precursor, was supplemented into the pre-HC cultures. In order to test the influence that these protocol modifications would have on the electroactivity of these strains, cultures were grown using these adjustments and tested within HCs.

The results, presented in Figure 6.2., show no change to the current production of the engineered strain with this method change. However, it also shows a drop in current for the control relative to the previous results, to levels matching those of the engineered strain. This may be an indication that the richer growth media before the minimal, anaerobic environment of the HC had an impact on metabolic processes in the control leading to a lower utilisation of the chloramphenicol mediated EET; or that it delayed the adaptation of the strain to its new environment. While it might be expected that this be borne out in lower readings for the engineered strain too, we suggest that the increased metabolic burden already depresses the metabolic activity obscuring this effect in the strain. The margin of impact may be relatively minimal.

Regardless, the over performance of this engineered strain relative to its control in a similar fashion to that observed in the literature [126] is not reproduced in M4m by the alteration of pre-HC growth conditions. Consequently, the investigation into the use of alternative minimal media was the next logical step.

Figure 6.2. – Effect of Pre-Inoculation Growth Conditions of Current in HCs

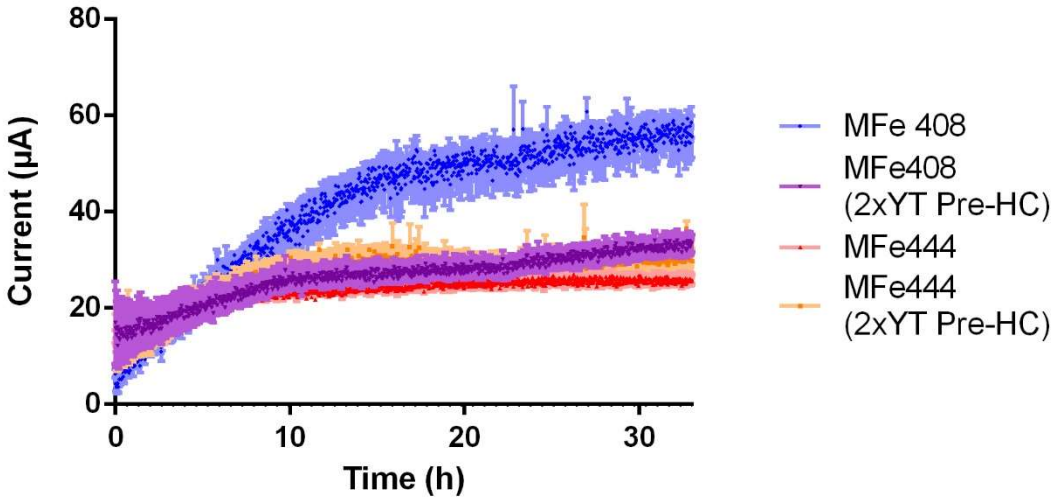

Chronoamperometry data for engineered (MFe444) and control (MFe408) strains, which varied in their growth conditions prior to inoculation into HCs. Using the richer media (indicated by 2xYT Pre-HC – orange and purple lines for engineered and control respectively) did not result in an increased performance of the engineered strain, though the control strain did perform more poorly. This suggests that the pre-inoculation growth conditions do not account for the differences in strain performance between our set-up and that published. The data for each line represents the average of three replicates with error bars highlighting the standard error of the mean.

6.2.2. Media Selection

In order to investigate the impact an alternative minimal media had on the electroactivity of engineered and control strains of *E. coli*, those used by TerAvest et al. [126] were compared in HCs containing M1 against the results for those containing M4m. This was followed with a similar comparison for the strains previously used in this work. While the full recipes for the media can be found in Chapter 3, the key differences that we noted were the addition of vitamin (B1,3,5,6,7,9,12, p-amino benzoic acid, and a-lipoic acid), and amino acids (glutamic acid, arginine, serine) to M1, and the use of HEPES rather than PIPES as buffering agent in M4m. It was thought that the inclusion of these

additional vitamins and amino acids might facilitate a higher metabolic utilisation of the EET pathway in engineered *E. coli* strains.

The results for the MFe408 control and MFe444 engineered strains are shown in Figure 6.3.A. These data show the engineered strain current increasing rapidly within the first 10 h, similar to the behaviour observed for the pRSF CABO + pEC86 engineered strain, before levelling off and gradually decreasing. The engineered strain clearly outperforms its control, but only once this M1 switch is made. It is worth noting that all MFe strains presented here were cultured in 2xYT as in the previous section, permitting a direct comparison with M4m containing HCs, the data for which are presented in Figure 6.3.A also.

Figure 6.3. – Half Cell Media Comparisons

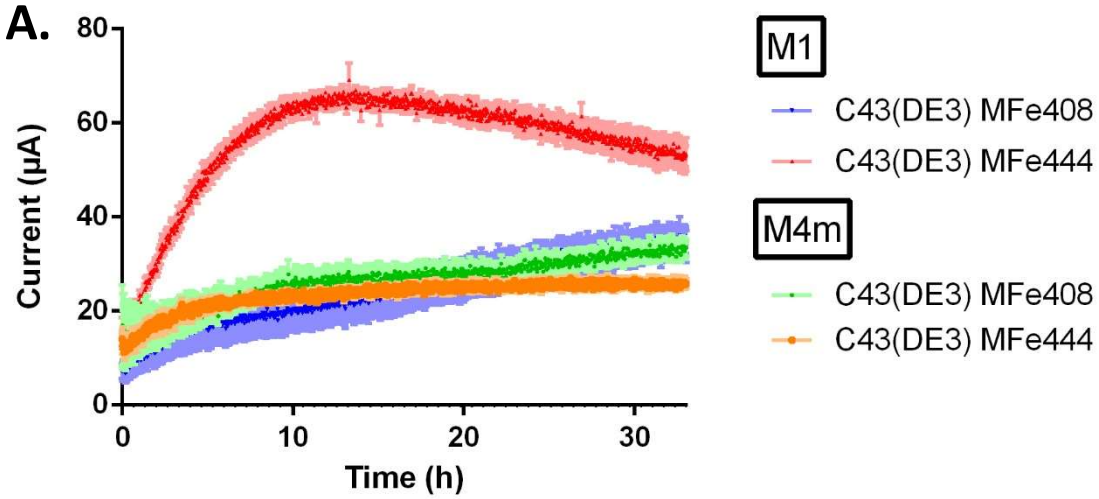

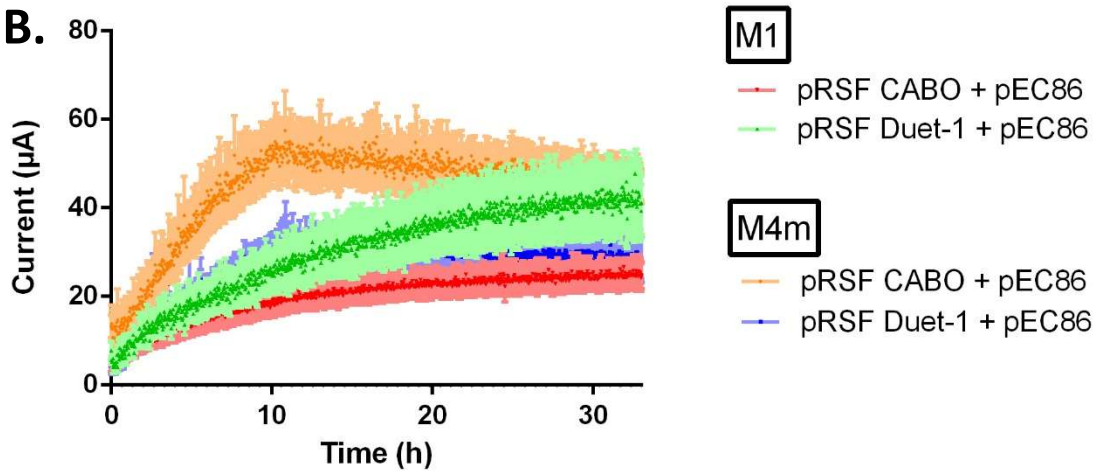

Media comparisons for engineered and control strains of electroactive E. coli used by TerAvest et al. (A) and previously in this work (B) in HCs under potentiostatic control are presented. The strains in (A) are not distinguishable in M4m, however in M1 the control strain clearly outperforms its control, following expectations from published results. The strains previously used in this thesis (B), show the inverse, however; the engineered strain clearly outperforms the control in M4m, but the reverse is true (though to a lesser extent) in M1. This suggests a strain dependent susceptibility to small changes in either metabolic activity or expression profiles caused by HC media that produces larger changes in EET. The data for each line represents the average of three replicates with error bars highlighting the standard error of the mean.

These results indicate a metabolic or biological change has occurred, likely as a consequence of an enrichment of the media with amino acids and vitamins, contributing to a greater effect of the recombinant EET pathway presence on electroactivity. This is unlikely to be accounted for by variations in biomass due to differences in growth following inoculation, as both media are still minimal and HCs anaerobic. Biomass is typically observed to decrease over the course of a HC run, an observation consistent with other BES testing [94,173]. Furthermore, clear differences are observed within a matter of hours beyond what we would expect possible for minor biomass fluctuations.

Figure 6.3.B presents the data for HCs containing M1 and the pRSF + pEC86 engineered (CABO - *mtrCABomcA*) and control (Duet-1) strains alongside those for M4m HCs. The

effect the media switch from M4m to M1 has on electroactivity of these strains interestingly appears to be the opposite of that seen for the MFe strains; in M1 the control outperforms, though only slightly, the engineered strain. This highlights and supports our concerns over the lack of clarity surrounding media selection and the impact it has on the metabolism, and by extension connectivity and utilisation of the heterologous electron transport pathway, of recombinant *E. coli* strains.

The changes in current observed for both sets of strains occurs rapidly, with engineered and respective control strains differentiating themselves within a matter of hours. While a short time frame does lend support to the argument that the activity of existing proteins that can influence EET pathway utilisation is being affected, it is also reasonable to suggest that expression shifts occur due to media differences, and that these might be causative. The trend for the engineered strain (in M1 for 6.3.A, and M4m for 6.3.B) is not entirely immediate, as a brief lag before trending upwards can be observed. This could be due to a delay in metabolic activity due to the media change and increase in temperature (as cultures are kept on ice just prior to inoculation) and the inoculated cells settling within the HC, on the working electrode (WE). Though it may also be explained as the time necessary to adjust the cells' expression of metabolically relevant proteins. Either way the differences between the two strains, and minor differences in the media used, show that heterologous EET pathway utilisation is quite sensitive to minor changes in media/metabolism.

While further analysis of proteomic differences became the focus of subsequent work, the differences between the strains compared here were considered for their potential influence on the data so far reported. The first key difference between the two pairs of strains investigated lies in the recombinant expression of either *omcA,* an additional outer membrane cytochrome similar in function to *mtrC*, or *cymA*, an inner membrane cytochrome also from *S. oneidensis* MR-1 that has reported, though contested, functional homology to the product of the native *E. coli napC* in interacting with heterologously expressed *mtr* pathway components and the quinone pool [134,174]. The former is present in the engineered strain presented by Jaffe [24] and tested previously in

this thesis, while the latter is present in the engineered MFe444 strain presented by TerAvest et al. [126].

The expression of *cymA* has been reported to improve flux through the mtr pathway in *E. coli* strains expressing it heterologously. Comparably, the addition of *omcA* is suggested to provide an alternative contact route between components of the mtr pathway and an extracellular electron acceptor (EEA). It may be the case that under more resource limiting conditions (M4m) electron flow between the quinone pool and the heterologous mtr pathway is not the limiting step, and so not noticeably assisted by *cymA*. Conversely, contact between EEA and mtr pathway under these conditions might be, thus the improvement seen in current production for the *omcA* containing strain. However, it is difficult to state this conclusively without further investigation.

The second key difference between these two strains lies in the host strain choice, BL21(DE3) and C43(DE3) for the Jaffe and TerAvest strains respectively, as previously mentioned. It might be the case that operation of the heterologous pathway in each of these base strains functions better in one media versus another. C43(DE3) is derived from BL21(DE3) and includes (among other mutations) a mutation in the LacUV5 promoter, leading to lower levels of T7 RNA polymerase in the cell[175].

In the context of the previous discussion suggesting that a change in expression profile is required by the cell in order to optimally utilise the heterologous EET pathway, this chassis strain difference could account for the observed difference between the strain pairs. C43(DE3) requires a richer minimal media to effect this change in expression while continuing to express the heterologous proteins. Meanwhile, in the richer media, BL21(DE3), with its greater T7 RNA polymerase levels, encounters issues with overexpression in the richer media. The latter half of this argument does not entirely hold up, considering the much richer media in which both strains are grown up prior to inoculation. Other metabolic differences might account for this, but it is difficult to speculate without further data.

It may be that host strain and media selection informed one another in previous studies. For example, for the constructs within the TerAvest strains if only M1 were used in BES

comparisons C43(DE3) would be observed to be the superior strain for electroactivity. We believe that it is the media impact on expression and metabolism, which varies between host strains, determining the electroactivity of engineered *E. coli* strains. This does not mark a refutation of the findings made in various publications, on the contrary given the sensitivity to metabolic fluctuation we suggest it is incredibly challenging to make the distinctions between strains that have previously been demonstrated. However, we believe that this presents both a need for greater metabolic control in future heterologous electroactivity studies, and highlights an opportunity for a further line of inquiry.

6.2.3. Consideration of Proteomic Investigative Pathways

For bioelectrochemical, synthetic biology applications, a robust strain that is resistant to minor metabolic variations influencing its electroactivity is desirable. Understanding and manipulating the metabolism of electroactive strains to better utilise the heterologous pathway might also help to close the gap between engineered *E. coli* strains and dissimilatory metal reducing bacteria (modified or otherwise). In order to inform potential metabolic engineering to this effect, as well as to generally investigate ways that existing strains might be improved, options for analysing the global proteome of electroactive *E. coli* strains were discussed. This work was conducted collaboratively with Dr Caroline Ajo-Franklin and Dr Moshe Baruch. Consequently, use of the MFe408 control and MFe444 strains for comparative purposes was decided upon.

Through this collaboration, the opportunity to additionally investigate an observed, interesting metabolic shift subsequent to carbon source addition (publication pending) was also afforded. In that study it had been observed that supplementation of glucose into a lactate containing BES following adaptation of the inoculating strains to initial conditions, resulted in an immediate increase in current. As increased fitness provided by the additional carbon source was ruled out as solely responsible for the increase in current, it was hypothesised that this observation was due to a spike in metabolic flux ultimately causing an increase in electron flow through the heterologous mtr pathway. It was determined that in addition to a control/engineered comparison following

adaptation to HCs, a comparison of the same strains subsequent to maximal, post-glucose supplementation current could provide valuable insights.

With four conditions to compare, an 8-plex iTRAQ (isobaric tags for relative and absolute quantification) was planned, with two replicates of each condition. In an iTRAQ experiment protein samples from different conditions are separately tryptically digested and labelled with specific isotopically weighted tags that covalently bind N-termini and amine groups[176]. Once labelled the samples are mixed and analysed via mass spectrometry. Using a predicted peptide database the resulting data is processed to provide quantitative comparisons of protein levels between the different samples[177–181].

6.2.4. Sample Collection for Quantitative Proteomics

Twelve M1 containing HCs were run concurrently to generate the samples for proteomic analysis, six of each strain (MFe408 and MFe444 – control and engineered respectively), with inocula grown as discussed in section 6.2.1., in keeping with the method used by TerAvest et al. [126]. All HCs were supplemented with 0.4% sodium DL-lactate, set at a poised potential of 0.2 V vs Ag/AgCl, and maintained anaerobically as previously described. Once current levels stably reached their maxima half of the HCs were harvested (three of each strain) while the remainder were supplemented with 0.2% glucose. These were monitored until they reached their new maxima and harvested together. Biomass harvesting is detailed in chapter 3, but briefly involved dissociating adhered cells from the working electrode before final OD_{600} measurement and centrifugation. Cell pellets were briefly stored at -20 ^{o}C before protein extraction. The protocol was designed to improve extraction of membrane proteins, without sacrificing proteins from other fractions, but recovering such proteins is widely known to be difficult.

Figure 6.4. displays the chronoamperometry data for the HC run. Due to the limitation to two replicates for each condition, one HC of each set was run for redundancy and was not used, and thus excluded from the data represented here. Current is observed to increase for the engineered strain, with some minor disruption, until 37 hours at which point the stability was sufficient that the A samples were harvested. Comparably the

control strain showed a slight increase in current between initial and sample A harvesting. A slight drop in current followed the addition of glucose in the engineered strain, though this subsequently rose until the point at which sample B was harvested.

While the immediate effect of glucose did not match that reported by our collaborators – a prompt, sharp rise in current to a new maximum – the gradual increase is still indicative of greater EET activity. It is possible that small amounts of oxygen were introduced during the glucose addition, leading to the initial drop. Although we did not feel this to be problematic for proteomic analysis, as we would expect any oxygen introduced would have been removed rapidly, and a current increase was still observed before harvesting of biomass. Alternatively, it may be that the act of injecting the glucose into the HCs disrupted the WE associated cells, reducing the number actively supplying electrons to the electrode until they settled or that number was built up again. A third option, that glucose repression of the EET pathway through *lac*UV5 repression, is unlikely given the immediacy of this effect; impact from changes to expression would not be so rapid. Following on from this, concerns over the repression of the T7 controlled EET pathway genes due to the presence of glucose following its addition were raised. The *lac*UV5 promoter was derived from the *lac* promoter to be less sensitive to repression by LacI in the presence of glucose[104]. And investigations into the additional mutations present in C43(DE3), including in *lacI* did not suggest a change in this, simply a decrease in leakiness of the *lac*UV5 promoter and lowered sensitivity to inducer for *lacI*[182].

Figure 6.4. Chronoamperogram of Samples Generated for Proteomic Analysis

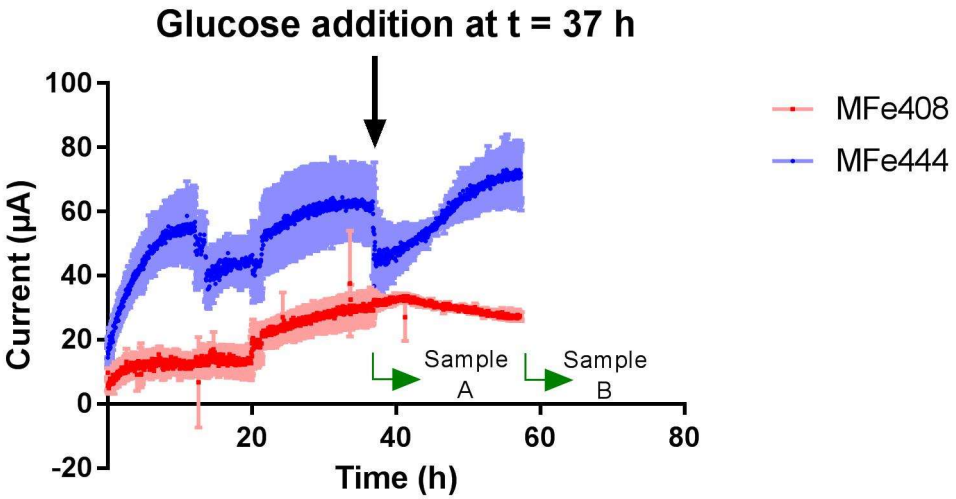

Combined HC data for the two strains inoculated into HCs and placed under potentiostatic control is shown, with indications for sample A and sample B harvesting (at 37 and 57 hours respectively, along with glucose addition). The control strain current, MFe408 (red), increases slightly from its starting value, but stays relatively constant from before glucose addition until the sample B extraction. The engineered strain current, MFe444 (blue), increases from initial values, with some disruption, until stabilising before sample A collection and glucose addition. Thereafter it suffers an immediate drop from which it steadily climbs until reaching a new maximum current before sample B collection. The data for each line represents the average of four replicates up until 37 h, then 2 replicates thereafter, with error bars highlighting the standard error of the mean.

Nevertheless, given the gradual current increase post-glucose addition, concerns were raised over the potential that it was due to a glucose driven biomass increase. This would not have invalidated the samples for further analysis, as an increase was not observed for the control strain, but it would necessarily inform interpretation of any resultant data. Figure 6.5. presents the harvested biomass data for the engineered MFe444 strain HCs, as determined by spectrophotometry at 600 nm. It shows the two samples to have been similar in biomass. No significant difference was detected between the two when compared with an unpaired t-test.

Figure 6.5. Comparison of MFe444 Biomass Harvested at Different Time Points

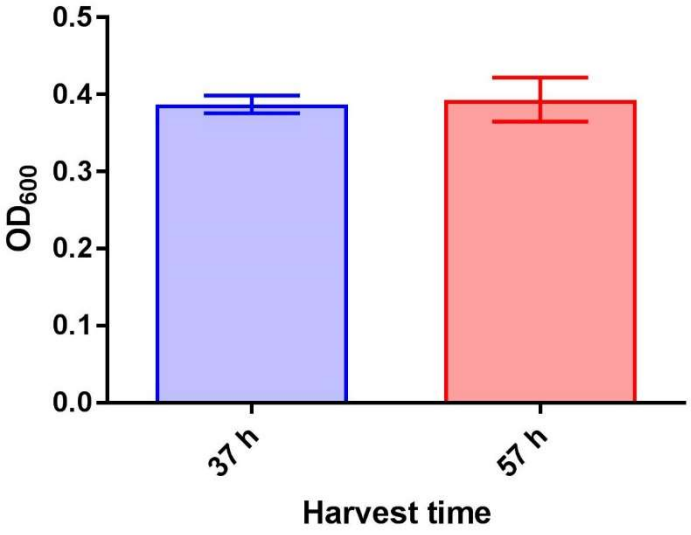

Comparison of harvested biomasses from the two time points/conditions MFe444 strains were extracted at, graphically represented for the MFe444 strain, as determined by spectrophotometry using M1 as a blank. Each column represents the data for three replicates with the error bars indicating the standard deviation. These two results were not significantly different (unpaired t-test, $p<0.01$), indicating that a hypothetical increase in biomass following glucose addition was not present, and so was not responsible for observed differences in current between the two sample points.

6.2.5. Sample Processing for iTRAQ

Protein extraction was achieved as described in chapter 3, with a 6 M urea, 1 mM EDTA containing, TEAB based buffer, and cell lysis achieved through sonication. Following extraction, samples were compared using sodium dodecyl-sulphate polyacrylamide gel electrophoresis (SDS_PAGE) as presented in Figure 6.6. below. The figure suggests a successful protein extraction, at a workable concentration, though quantification would be required for subsequent steps.

Figure 6.6. SDS-PAGE Gel of Extracted Protein Samples

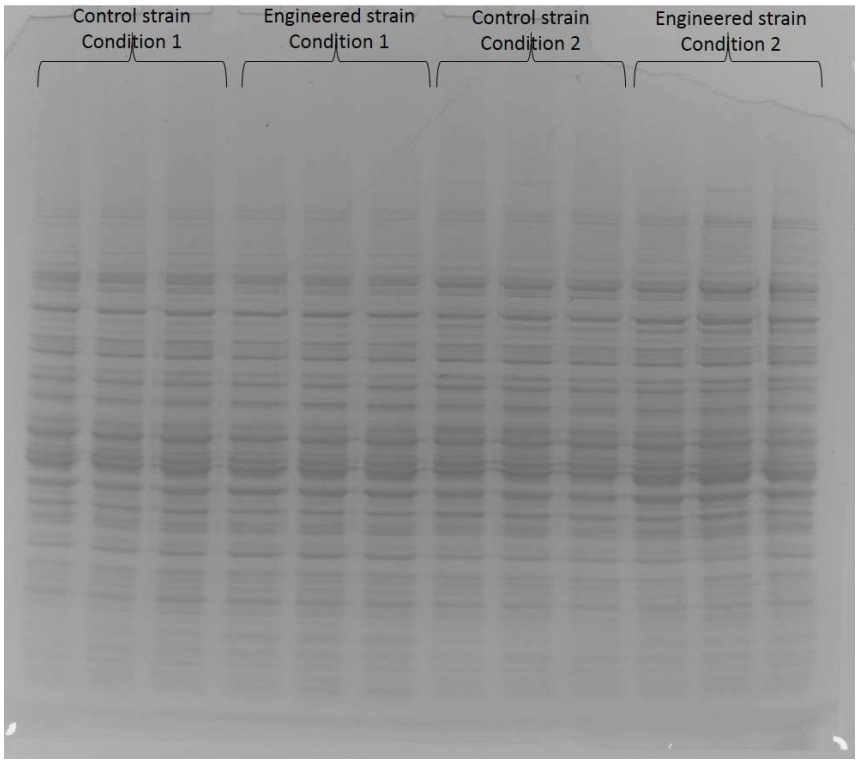

SDS-PAGE gel of all protein samples, including redundant replicates. Condition 1 relates to those HCs harvested at 37 h, while condition 2 relates to glucose supplemented HCs harvested at 57 h. Gel Coomassie stained with InstantBlue. The band distribution indicates a sufficiently broad range of proteins extracted to proceed, while intensities reassure that an acceptable concentration is present.

A Bradford assay was conducted as described in chapter 3, using a 96 well plate and microplate reader, indicating various protein concentrations in the 7.5-10 mg/ml range.

This was used to inform volumes used for the subsequent trypsin digest. Sample aliquots were diluted 1 in 6 in TEAB to dilute the urea and EDTA concentrations, then, alongside BSA and buffer only controls, reduced, alkylated, and tryptically digested in solution (1:20 ratio to protein, 37 ^{o}C, overnight).

An SDS-PAGE gel comparison of pre- and post-digestion aliquots (volumes adjusted for dilution) was used to verify digestion, with the resultant gel images shown in Figure 6.7. below. Alternate rows representing pre- and post-digestion aliquots for each of the digested samples make the successful digestion clear. The BSA control was successfully completely digested also, and no bands were detected in the buffer only negative control. Consequently, labelling of samples with iTRAQ reagents was proceeded with.

Figure 6.7. SDS-PAGE Gel Analysing Trypsin Digestion of Protein Samples

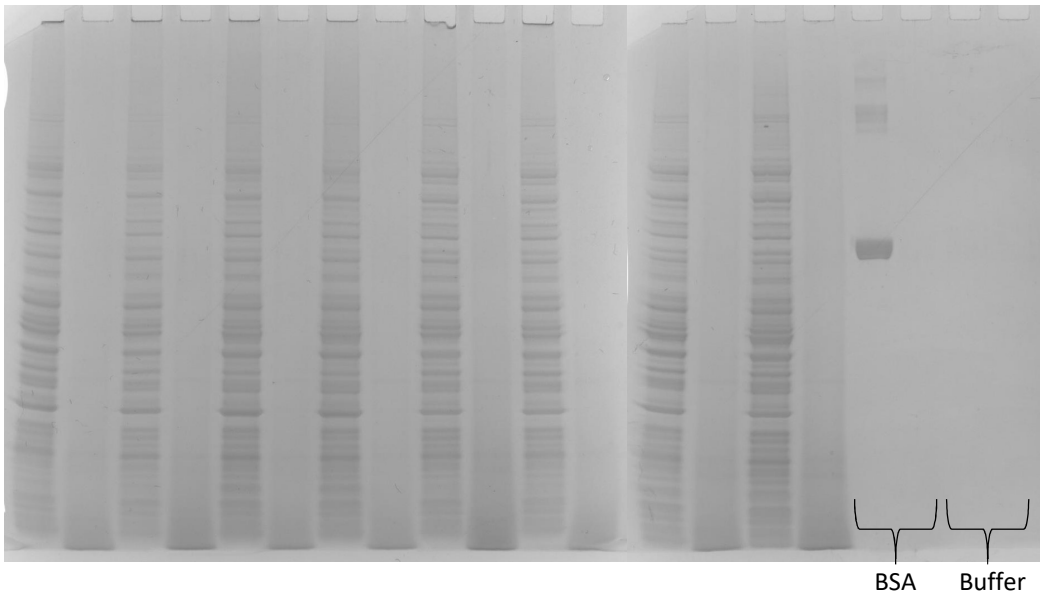

Alternately pre- and post- digestion aliquots of each protein run on an SDS-PAGE gel and Coomassie stained with InstantBlue. Sample pairs, left to right, are ordered: condition 1 control 1 and 2, then engineered 1 and 2; condition 2 control 1 and 2, then engineered 1 and 2. Digest controls are labelled. Correct digestion can be observed for all samples.

---

iTRAQ reagent labelled samples were mixed according to protocol and fractionated by HPLC with an Hypercarb column. Fractions were collected at two minute intervals. Two fractions (40-42 and 50-52 minutes) were subsequently checked for quality control

purposes via MS, before 18 fractions from 22 to 58 minutes were run on the QE HF Orbitrap.

6.2.6. iTRAQ Data Processing

The raw iTRAQ data was processed using MaxQuant, a freely available software package for quantitative proteomics analysis. MaxQuant identifies detected in spectra, with corrective measures to minimise false discovery rate (FDR), through reference to a provided protein database for the assessed organism[180,181]. Initially an NCBI protein database for C43(DE3), with the 14 additional protein sequences encoded on various plasmids used, was utilised in this process. However subsequent use of various bioinformatics tools was inhibited by the lack of recognition of the identifiers present in the database. While it was possible to individually convert some of these identifiers into comparable ones in UniProt reviewed strains, the process was lengthy and not easily automatable. Consequently the decision was made to reanalyse the raw iTRAQ data in MaxQuant against the UniProt reviewed database for *E. coli* strain K12[183], with the additional 14 proteins previously mentioned.

It was argued that, while some losses in protein identification numbers might occur, the strains were broadly similar. Furthermore the potential insights provided by ease of data interpretation using the K12 processed data outweighed expected protein identification losses. However, in order to investigate the effect of this database selection on protein identification figures, subsequently processed outputs from the two processes were compared. In total 1517 proteins were identified using the K12 database, compared with 1556 for the C43(DE3) database, a difference of 39. Of these 1278 and 1316 had two or more unique peptides identified for them, respectively, a difference of 38. These minimal losses were considered acceptable.

Relevant data columns were extracted from the MaxQuant evidence output file, and placed into an excel document following a format compatible with our in house proteomics pipeline. Protein quantification was achieved separately for each of the iTRAQ labels using uTRAQ v4.0 algorithms[177,184], with comparisons made to detect proteins with significant fold changes carried out using Signifiquant v4.0[177]. Comparisons between conditions were conducted relative to each of the replicates present, both with and without multiple test correction (MTC) applied, and at a significance level of 0.05 and 0.01 for the latter, with only 0.05 applied for the former.

These three stringency levels were selected to ensure a thorough overview of the proteins within each of the samples was achieved, while identifying those whose change was considered most indisputable. All identified proteins can be considered valid for evaluation in the context of the following discussions. Though greater confidence is assured by identification at a higher stringency level, the MTC may remove valid protein changes. And given the limitations of protein extraction, particularly with regards to membrane proteins and low abundance proteins[177], changes in these may only be observable at lower stringency values.

Only proteins with 2 or more unique peptides identified were included in the results. And each condition comparison is the compiled result of comparing changes with respect to one of each of the four replicates (two per condition) four times, once for each replicate, with only proteins presenting in three or more of the resultant lists being presented. All of these steps go further towards ensuring confidence in identified protein changes. Full protein lists are presented in the appendix, including a breakdown of UniProt IDs by frequency across the four protein lists for each comparison and stringency level.

6.2.6.1. Overview of Processed Data

To get an overview of identified proteins, a gene ontology breakdown (GO) for each comparison was generated using PANTHER (**P**rotein **AN**alysis **TH**rough **E**volutionary **R**elationships)[185]. This is a large curated database of protein families, and classifies them based on a variety of criteria, including molecular function and biological process.

For the Control vs Engineered strain comparison, more than a third to more than a half of the proteins identified are involved in metabolic processes, as can be seen in Figure 6.8. below. The next largest group represented is cellular processes, covering over a quarter of the proteins identified. Proteins involved in localisation, response to stimulus, biological regulation, and cellular component organisation or biogenesis make up the remainder. As can be seen, the three stringency levels (Figure 6.8.A. and D. being the highest, through to Figure 6.8.C. and F. as the lowest) produce similar results. Though for biological processes the highest (MTC $p<0.05$) shows fewer metabolic process proteins, with the other processes expanding proportionally. For molecular function, catalytic activity makes up the majority of proteins identified, with around a quarter being involved in binding. Antioxidant and transporter activity cover the rest for the highest stringency level, with signal transducer, structural molecule, translation regulator, nutrient reservoir, and receptor activity ontologies being recognised in the lower ones.

For the Control + Glucose vs Engineered + Glucose comparison protein changes previously identified for the initial comparison were disregarded, as well as controls for unrelated changes due to glucose addition as indicated by overlap with the control vs control + glucose comparison. Consequently, a smaller pool of protein changes remained, so only the ontology overview for the third stringency level (no MTC, 0.05) is presented in Figure 6.9. below. Figure 6.9.A. shows the biological processes breakdown, which much like the previous comparison is predominated by metabolic and cellular processes. Some cellular component organisation or biogenesis proteins also remain. Figure 6.9.B. shows the breakdown of molecular functions, which also broadly mirror those for the previous comparison at the medium stringency level.

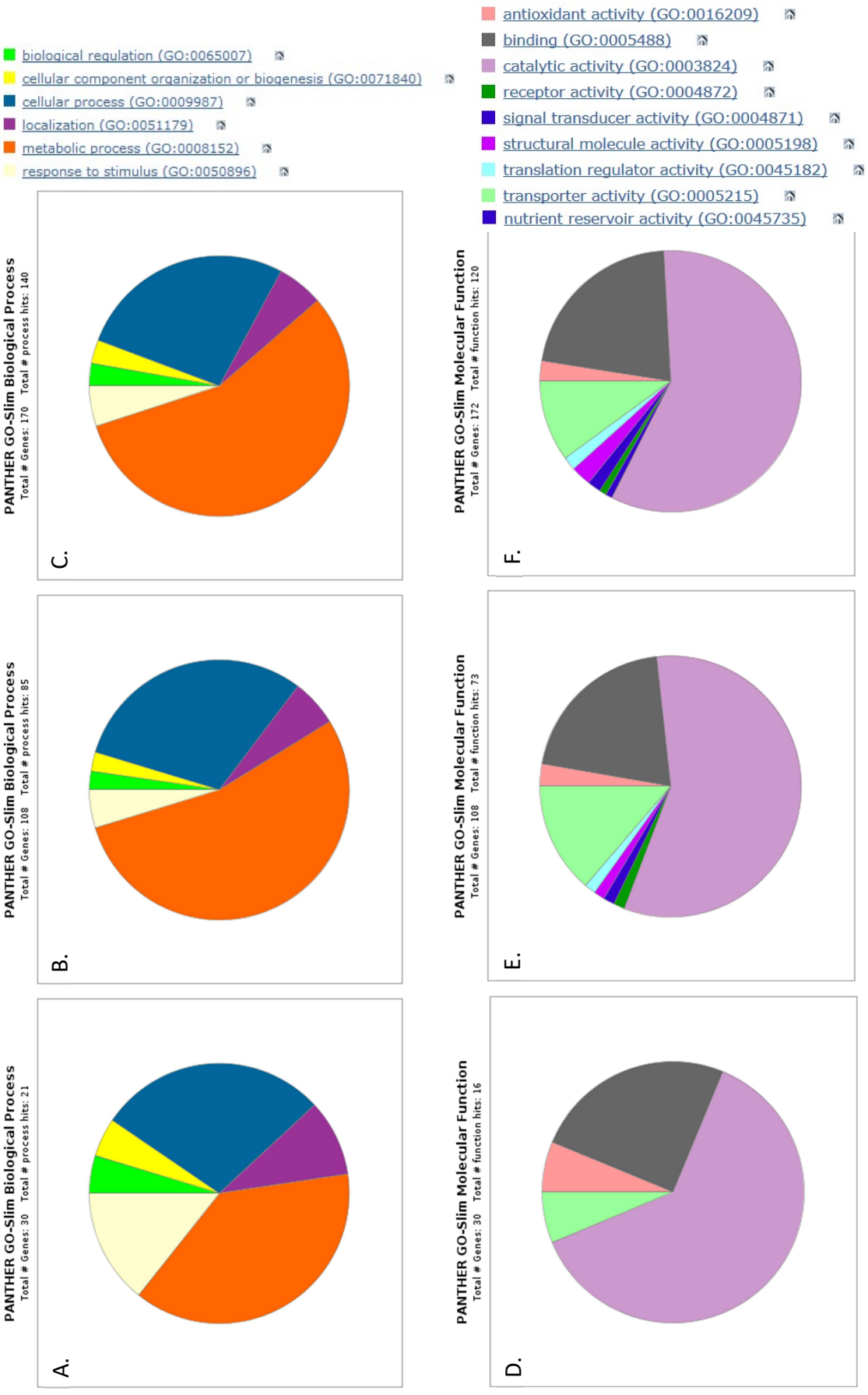

Figure 6.8. Control vs Engineered Strain Protein Change Ontologies

This figure shows the gene ontology breakdown for protein changes identified in the control vs engineered strain comparison, for cells incubated in HCs. Two replicates of each condition were analysed under varying stringency levels – MTC 0.05 (A and D), no MTC 0.01 (B and E), no MTC 0.05 (C and F). A-C show biological process ontologies, while D-F show molecular function ontologies. The distribution of ontologies remains broadly consistent across the stringency levels, though some additional molecular function ontologies become present at the two lower levels.

Figure 6.9. Control + Glucose vs Engineered + Glucose Protein Change Ontologies

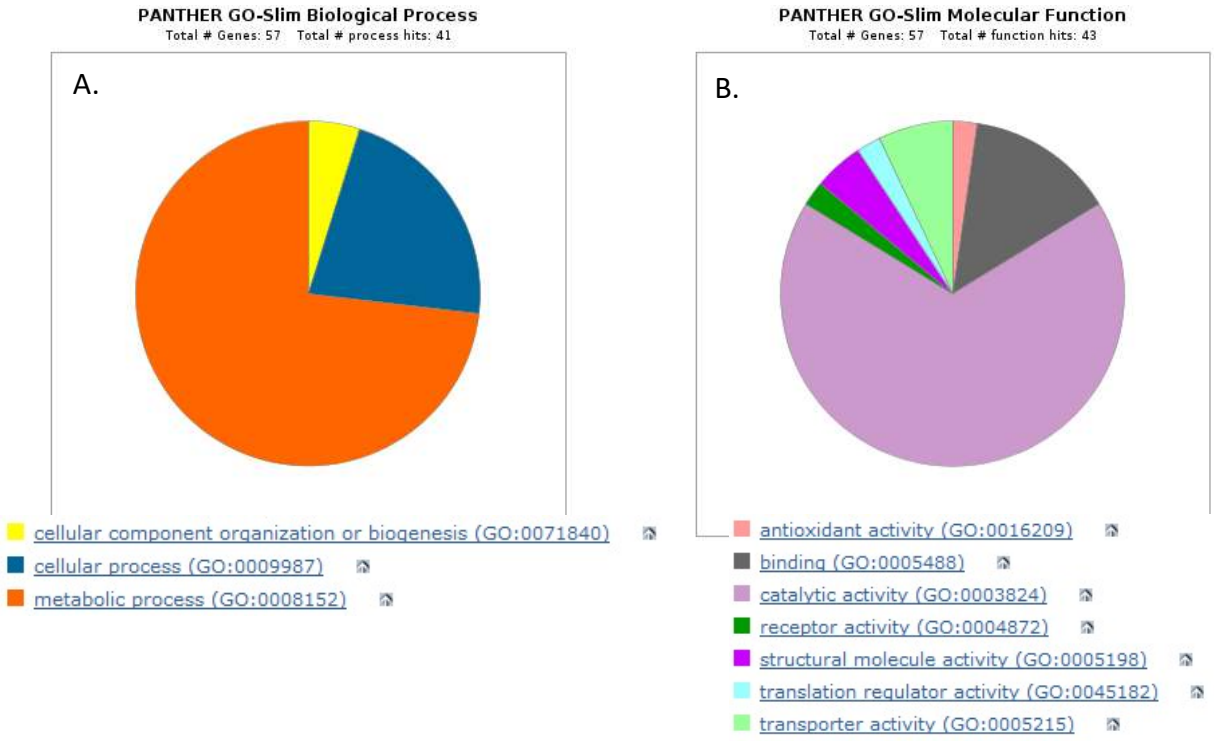

This figure shows the gene ontology breakdown for protein changes identified in the control + glucose vs engineered + glucose strain comparison, for cells incubated in HCs, for the no MTC 0.05 stringency level. Two replicates of each condition were analysed under varying stringency levels, with certain protein changes filtered out by control comparisons. Biological process ontologies (A) and molecular function ontologies (B) both are broadly comparable to those for the original comparison.

6.2.6.2. Heterologous Protein Identification

In addition to the proteins present in the K12 database downloaded from UniProt, the database used for the processing in this study included the protein sequences for the additional genes borne on the added plasmids. Unfortunately, as many of these were membrane proteins, the likelihood of detecting them with a global proteomic technique was low, due to the difficulty in solubilising such proteins during the extraction process. Even if low concentrations were detected, these would likely be too small for the data processing to confidently list in the protein changes for comparisons. Work carried out previously on these strains[28] had demonstrated their expression using haem staining methods, nevertheless in the interests of further confidence in expression, in each comparison we looked to identify any of these heterologous proteins.

While MtrCAB were all identified with more than two unique peptides following MaxQuant processing of the raw data in the engineered strains, only MtrA was found in control vs engineered comparison results. This follows expectations, as out of the heterologous proteins MtrA is a periplasmic protein (and therefore not an integral membrane protein)[186]. As can be seen in the full protein lists in the appendix, MtrA is identified in every comparison of a control vs an engineered strain, glucose or otherwise, as we would expect. When the engineered vs engineered + glucose comparison was made MtrA was present at the two lower stringency levels.

Table 6.1. presents these data for the no MTC 0.01 stringency level. It shows a relative increase of the protein in the glucose containing condition. This may simply be indicative of an increase in metabolic flux leading to higher expression generally but emphasised in the heterologous protein by independent regulation of expression. Regardless, it definitively counters the argument against repression of the *lac*UV5 promoter by glucose, which would lead to lower expression of the T7 promoter controlled EET pathway genes.

Table 6.1. Relative Protein Quantification for MtrA

UniProt ID	Gene Name	Engineered 1	Engineered 2	Engineered + Glucose 1	Engineered + Glucose 2	#Unique	#Quants
Q8EG35	*mtrA*	0.623516	0.644531	0.933484	1	6	24

Quantified (linear, isotopic and multiple corrections applied) protein differences for replicates displayed separately, relative to the second engineered strain + glucose condition replicate. The test setting used was no MTC, p-value limit of 0.01

6.2.7. iTRAQ Comparison of Engineered and Control Strains of *E. coli* Following Adaptation to a Bioelectrochemical System

The proteomes of control and engineered strains of *E. coli* adapted to a BES were quantitatively compared with the aims of better understanding the electroactivity of the engineered *E. coli* strain generally, the connection between the central metabolism and the heterologously expressed EET pathway specifically, and to identify novel factors that might contribute to the electroactivity of that strain.

6.2.7.1. Outer Membrane Proteins and Ion Dependent Regulation

The outer membrane proteins encoded by *ompA* and *ompF* were identified as having particularly large fold changes between the two conditions at hand, as shown in Table 6.2., with the former lower in the control strain relative to the engineered, and the latter higher. Both of these proteins are typically abundant and have porin activity for small molecules across the outer membrane, with consequent roles in ion transport, although OmpA[187,188] has a lower permeability than OmpF[189,190]. Furthermore, there is evidence for voltage gating behaviour in OmpF and similar porins[191]; beyond a specific membrane potential the channels close. Given the potential bioelectrochemical interactions of such a mechanism, ion interaction was investigated further.

A number of other proteins identified in the literature as responsively regulated alongside Mg^{2+} concentration[192] were found in our data, as well as two copper/silver ion exporters. The former group included PhoP, a component of the PhoP/Q two-component system which activates and represses a range of proteins in response to periplasmic Mg^{2+} concentration and redox state[192]; SlyB, an outer membrane lipoprotein

evidenced to interact with PhoP, decreasing its activity, and regulated by it in a feedback inhibition process [193]; DsbA, which assists some periplasmic bounding proteins, including OmpA, in disulphide bond formation, and which suppresses PhoP activity[194]; RstA, another transcriptional regulatory protein that is expressed under low periplasmic Mg^{2+} concentration conditions as regulated by PhoP/Q[192]; and HemL, a biosynthetic protein involved in porphyrin production, and so by extension the haem biosynthesis pathway[192]. Without exception, though to varying degrees, these proteins were found at lower levels in the control strain compared with the engineered strain.

The two copper and silver resistance mediating proteins, CusB and CusF, were identified as less abundant in our control strain relative to our engineered strain, as detailed in Table 6.2. below. Copper toxicity tends to increase under anaerobic conditions, and in *E. coli* resistance to this toxicity is mediated by the tetrapartite transporter consisting cus system, which can export copper ions across the cell envelope[195,196]. CusF acts as a metallochaperone, binding and conveying ions for export, to the membrane fusion protein CusB, through which they are eventually exported from the cell[197]. The small heat shock protein ibpB, a chaperone that is also induced as part of a copper ion stress response, was observed at greatly increased levels in the control relative to the engineered strain. However, we believe this to be separate from the regulation occurring for the other proteins discussed; other heat shock proteins were observed at comparably higher levels in the control strain, likely a product of the expected increased stress resulting from the anaerobic, low nutrient environment. As the HCs were temperature-controlled induction of heat shock response proteins will not have been due to temperature, but may be indicative of metabolic strain disrupting the negative transcriptional regulation of heat-shock genes.

Together these changes help illuminate the differences between engineered electroactive *E. coli* and its control. The pattern of altered expression, particularly for the Mg^{2+} responsive proteins, suggests that redox states are different between strains leading to varying metal toxicity and consequent signal transduction pathway activity. Though alternatively the utilisation of the heterologous EET pathway may be having an unforeseen interaction with ion concentrations, and thus ion homeostasis. The

possibility of bioelectrochemical activity within the BES non-specifically interacting with the metal ion sensitive signal transduction pathways was considered, but the differences between observed strains only lend weight to the argument of a redox state difference, particularly within the periplasm. PhoP, for example, is more active under reducing conditions, which makes sense given that metal ion solubility is improved in such a situation[198]. Either through a redox state, or other bioelectrochemical interaction, we thus infer a link between the heterologous EET pathway expression in *E. coli*, and ion homeostasis regulated proteins.

Increased relative HemL expression in the engineered strain is likely a by-product of Mg^{2+} responsive regulation given its induction by PhoP, but its increased activity might also be assistive in cytochrome maturation; relevant to the heterologous EET pathway. Consequently, adjusting *hemL* regulation might impact electroactivity, though given that it was expressed at greater levels in the engineered strain this would only be relevant under conditions adjusted to down regulate the listed Mg^{2+} responsive proteins discussed. With this in mind, analysis of the response of engineered and control strains of *E. coli* to ion concentration within a BES might assist in further characterising the effect of this regulatory shift on EET. Primarily, however, we felt that these data recommended further investigation of redox processes within the two strains and conditions.

Table 6.2. Relative Protein Quantification for Ion Interactive Proteins

UniProt ID	Gene Name	Significant Settings Used	Control 1	Control 2	Engineered 1	Engineered 2
P02931	*ompF*	A	1.85	2.00	1.04	1.00
P0A910	*ompA*	A	0.50	0.51	0.99	1.00
P0A905	*slyB*	C	0.74	0.70	1.18	1.00
P23893	*hemL*	B	0.88	0.87	0.99	1.00
P77239	*cusB*	B	0.51	0.53	1.02	1.00
P77214	*cusF*	B	0.44	0.43	1.01	1.00
P52108	*rstA*	B	0.69	0.70	1.13	1.00
P23836	*phoP*	C	0.73	0.86	1.00	1.00
P0AEG4	*dsbA*	B	0.78	0.75	1.06	1.00

Quantified (linear, isotopic and multiple corrections applied) protein differences for replicates displayed separately, relative to the second engineered strain

replicate. The best test settings each protein detected with are referred to as A (MTC, p-value limit of 0.05), B (no MTC, p-value limit of 0.01), and C (no MTC, p-value limit of 0.05) for reference.

6.2.7.2. Electron Transport and Redox Activity

While, as discussed in the previous subsection, an interest in proteins that might indicate differences in cellular redox states between the two strains was cultivated, a focus on carbon metabolism was first explored. It was thought that differences in metabolic processes, reflected in protein levels detected for various metabolic enzymes, would provide insights into utilisation of the heterologous EET pathway in *E. coli*. Key protein differences discussed herein are listed in Table 6.3. below.

Proteins involved in the Tricarboxylic acid (TCA) cycle, fermentation, respiration, and the pentose phosphate pathway (PPP) were selected, and the pathways visualised with the EcoCyc cellular overview[199], as Figure 6.10. shows. Pathways affected by protein changes were coloured on a red to purple scale depending on whether they were quantified at a higher or lower level, respectively, than the engineered strain; orange/red indicates a relative increase in the control strain, blue/purple in the engineered strain.

The majority of proteins observed were at a higher relative level in the engineered strain, including TCA cycle enzymes SucB, AcnA, and Mdh; TktB and TalA of the PPP; and glycolysis enzyme FbaB. Given the expected higher metabolic activity of the engineered strain, due to the additional end terminal electron acceptor access afforded by the heterologous EET pathway, this observation was consistent with predictions. This was further supported by differences in certain branched pathways between the two strains, such as a preference for GpmI over GpmA in the glycolysis pathway. Both facilitate the same conversion, but GpmA has a 10-fold higher specific activity[200], so is better suited to a more metabolically active organism.

Greater fermentative acetate production in the control strain can be inferred from the data. Increased Pta, involved in the acetyl-CoA to acetyl phosphate (precursor to acetate) reaction, was observed for the control. An increase of alcohol degradation pathway proteins (glpK, garR, and the TCA relevant aceB) supports an accumulation of

these molecules in the control strain, also. There is also an indication of a reliance on fatty acid degradation to generate acetyl-CoA in the control, with FadI and FadJ detected at higher levels. Conversely, fatty acid biosynthesis was down in the control relative to the engineered strain, with FabA and FabB decreased. Lower fatty acid biosynthesis is usually tied to lower levels of OmpF (not OmpA)[201], however it is interesting to note the opposite was observed herein.

Beyond the central carbon metabolism, it was noticed that oxidative stress proteins OsmC and SodC were present at higher relative values in the engineered strain. OsmC, is a peroxiredoxin that reduced hyperoxides and inorganic hydrogen peroxide, protecting cells in situations of hyperosmotic or oxidative stress [202]. SodC is a superoxide dismutase which functions to destroy toxic oxidising radicals produced normally as a result of general metabolic processes[203,204]. Its differential protein abundances may be supportive of our conclusion of generally increased metabolic activity in our engineered strain. However it may be the result of a higher oxidative stress than accountable for by the increased metabolic activity expected. Combined with an inferred reducing periplasmic state, this may be suggestive of a bottleneck in EET, one that lies not with the heterologous pathway or its interaction with the quinone pool, but with electron transport to that quinone pool.

Two quinone interacting proteins were subsequently observed in the data: WrbA and NuoG. These were up and down regulated, respectively, in the engineered strain relative to the control. WrbA is upregulated in response to oxidative stress, or disruption of specific electron transfer chains, and functions as an NAD(P)H dehydrogenase to reduce quinones, though specificity has not been determined[205,206]. Comparatively, NuoG fulfils a similar function, believed to reduce ubiquinone, specifically, though is not considered to have oxidative stress gene ontology[207,208]. This pattern suggests that heterologous EET pathway quinone pool interaction might be quinone specific. This bore further investigation in the comparison of glucose supplemented cells.

Table 6.3. Relative Protein Quantification for Metabolic and Redox Active Proteins

UniProt ID	Gene Name	Significquant Settings Used	Control 1	Control 2	Engineered 1	Engineered 2
P08997	*aceB*	A	1.47	1.42	1.03	1.00
P25516	*acnA*	B	0.77	0.78	0.94	1.00
P0A6Q3	*fabA*	B	0.79	0.80	1.01	1.00
P0A953	*fabB*	B	0.91	0.88	0.98	1.00
P76503	*fadI*	B	1.29	1.37	1.01	1.00
P77399	*fadJ*	C	1.16	1.19	0.99	1.00
P0A991	*fbaB*	C	0.82	0.83	0.98	1.00
P0ABQ2	*garR*	B	1.23	1.22	0.96	1.00
P0A6F3	*glpK*	B	1.16	1.21	0.99	1.00
P62707	*gpmA*	C	0.92	0.93	0.97	1.00
P37689	*gpmI*	C	1.28	1.25	1.08	1.00
P61889	*mdh*	B	0.90	0.85	0.95	1.00
P33602	*nuoG*	B	1.15	1.15	0.99	1.00
P0C0L2	*osmC*	A	0.77	0.72	1.05	1.00
P23538	*ppsA*	C	1.07	1.07	1.01	1.00
P0A9M8	*pta*	B	1.14	1.16	1.00	1.00
P0AGD1	*sodC*	A	0.58	0.56	1.08	1.00
P0AFG6	*sucB*	B	0.78	0.79	0.92	1.00
P0A867	*talA*	A	0.77	0.78	0.96	1.00
P33570	*tktB*	C	0.83	0.81	0.98	1.00
P0A8G6	*wrbA*	B	0.89	0.89	1.04	1.00

Quantified (linear, isotopic and multiple corrections applied) protein differences for replicates displayed separately, relative to the second engineered strain replicate. The best test settings each protein detected with are referred to as A (MTC, p-value limit of 0.05), B (no MTC, p-value limit of 0.01), and C (no MTC, p-value limit of 0.05) for reference.

Figure 6.10. Mapped Proteomic Changes in Central Metabolic Processes

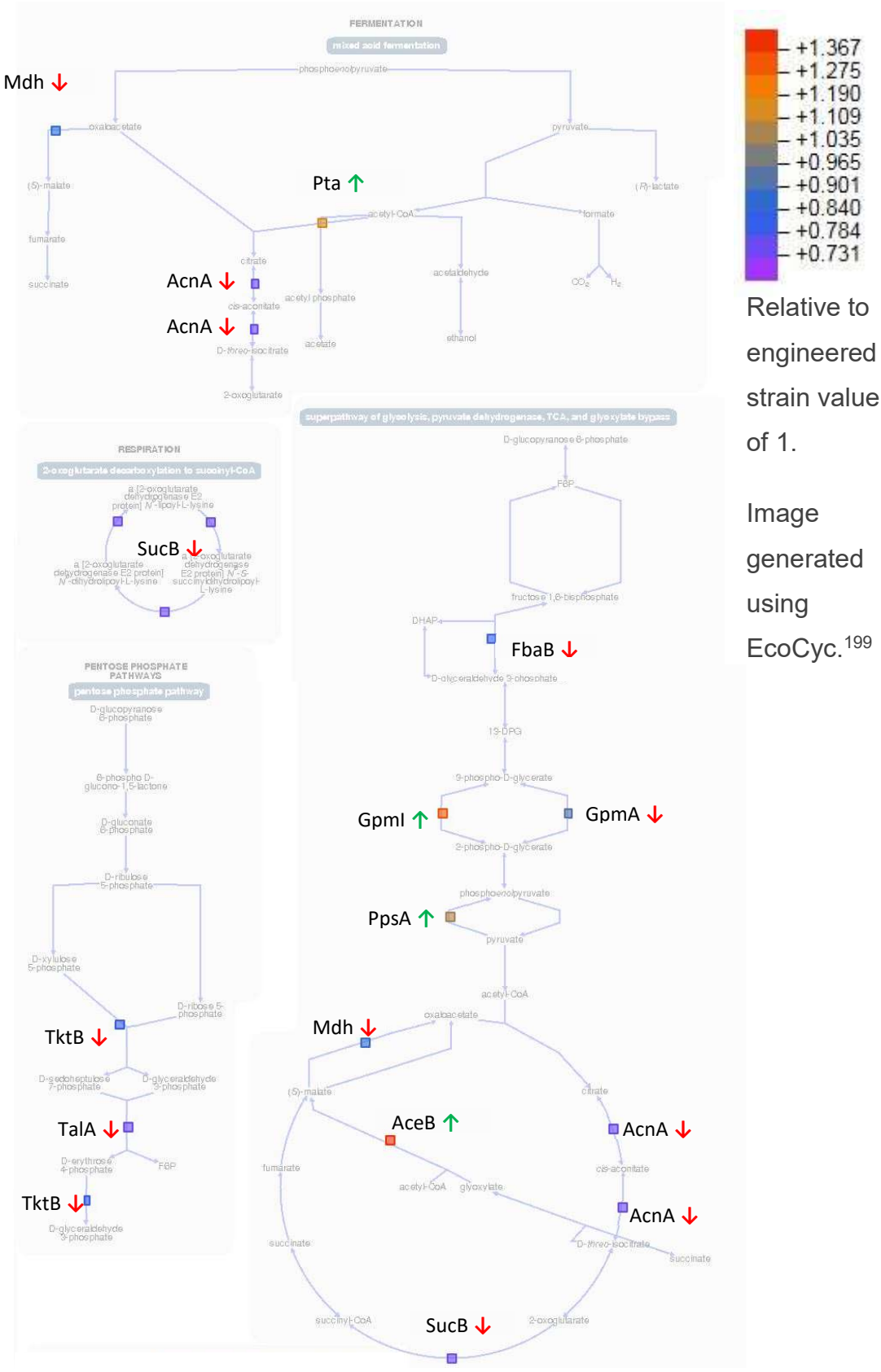

Relative to engineered strain value of 1.

Image generated using EcoCyc.[199]

This figure shows the proteomic changes identified for proteins involved in central carbon metabolism, relative to the engineered strain, with colours and arrows denoting whether an increase or decrease was detected. In this instance a down arrow indicates that the protein was identified to have a lower relative value in the control strain. As with all data in this study two replicates were present for each condition. The data for these proteins is also laid out in the preceding table and in the appendix. Overall a picture of much higher central carbon metabolism activity in the engineered strain is depicted, with greater reliance on acetate production in the control strain.

6.2.7.3. Biosynthetic Processes

Independently of the above investigation, a few, noteworthy biosynthetic proteins were observed to change between the strains, as described in Table 6.4. below. First of these was RibF, which catalyses the conversion of riboflavin to Flavin mononucleotide (FMN)[209], which was observed at a higher level in the control strain. While riboflavin is utilised as a mediative molecule in EET by *S. oneidensis* MR-1[73,127,128], as discussed in Chapter 4 this capability was not shown by our engineered *E. coli* strain. Nevertheless, any future attempts to engineer this capability into *E. coli* should do so with the host riboflavin metabolic processes in mind.

From broadening our previous investigation into metal ion interacting proteins to metalloproteins or those involved in metal homeostasis, three proteins involved in iron-sulphur cluster assembly were revealed that were observed to be up regulated in the engineered strain relative to the control. These were IscU, IscS, and HscA. Iron sulphur clusters are required for the maturation of many proteins involved in respiratory and biosynthetic processes[210]. Many oxidoreductases involved in oxidative stress response require iron sulphur clusters for maturation however, lending support to our earlier conclusions regarding this activity in our engineered strain.

Table 6.4. Noteworthy Biosynthetic Proteins

UniProt ID	Gene Name	Significant Settings Used	Control 1	Control 2	Engineered 1	Engineered 2
P0AG40	ribF	C	1.10	1.12	0.97	1.00
P0ACD4	iscU	A	0.54	0.57	0.97	1.00
P0A6B7	iscS	A	0.52	0.51	1.00	1.00
P0A6Z1	hscA	A	0.63	0.63	0.97	1.00

Quantified (linear, isotopic and multiple corrections applied) protein differences for replicates displayed separately, relative to the second engineered strain replicate. The test settings each protein detected with are referred to as A (MTC, p-value limit of 0.05), B (no MTC, p-value limit of 0.01), and C (no MTC, p-value limit of 0.05) for reference.

6.2.8. iTRAQ Comparison of Engineered and Control Strains of *E. coli* in a Bioelectrochemical System Supplemented with Glucose

As previously described, HCs containing engineered (expressing *mtrCABcymA*) and control strains of *E. coli* were supplemented with glucose following adaptation to the BES conditions, as represented by maximal current being reached. After glucose addition, cells were harvested once the new current maxima were reached. When investigating the proteins with significant relative differences between the control and engineered strains thus collected, those that were also present in the comparison of pre-glucose addition control and engineered strains, as well as those observed for control strains pre-glucose compared with post-glucose, were removed. In this way those protein changes resulting from the difference between the two strains generally within a BES were excluded (since already the focus of the previous subsection), while changes due to non-engineered strain specific regulation in response to the presence of glucose were similarly controlled for. Consequently, a thorough investigation of the 'glucose effect' on the proteomes of the two tested strains was conducted with the aim of informing future engineering of electroactive *E. coli* strains for bioelectrochemical, synthetic biology applications.

6.2.8.1. Changes in Respiratory Processes in Glucose Supplemented Strains

E. coli possesses three types of quinone: ubiquinone, typically involved in aerobic respiration, menaquinone, and demethylmenaquinone[211,212]. The latter two have more of a role in anaerobic respiration, having lower redox potentials[211]. In *S. oneidensis* MR-1 CymA functions to reduce quinols, transporting electrons to terminal pathways, such as the EET Mtr pathway[134]. There is evidence for its specificity for the menaquinone pool[213], though also for a capability to reduce ubiquinol[214].

NuoG and WrbA, proteins which facilitate quinone reduction, were detected at higher and lower abundances in the control strain of the previous comparison respectively. As discussed this, combined with other signs of redox activity, might be descriptive of the Mtr pathway's heterologous utilisation. With the comparison presently being considered, it was hoped that the increased metabolic flux facilitated by the addition of glucose might further illuminate differences between the strains from which electron transfer pathway activity could be inferred. These proteins were detailed in Table 6.3. previously, while other proteins discussed in this section are listed in Table 6.5. below.

Additional dehydrogenase complex proteins were identified in the glucose supplemented strain comparison, with NuoB, NuoC, and NuoF all detected at a decreased level in the engineered strain relative to the control. These proteins are all involved with ubiquinone reduction in aerobic respiration. Conversely, QorA was measured at higher levels in the engineered strain. QorA is not as well characterised[215], however we feel that the result observed here lends support to a role in anaerobic respiration through menaquinone preference. Alternatively, it might just reflect a more thorough shift in protein profile facilitated by the higher metabolic activity of the engineered strain, but with the addition of glucose we would expect sufficient turnover and adaptation to disregard this possibility.

Metabolism of glucose in *E. coli* leads to the formation of the toxic product methylglyoxal, which is further metabolised in the aldehyde degradation pathway[216]. Three proteins were differentially abundant between strains, within this pathway, that are of particular relevance. Gpr, less abundant in the engineered strain, is involved in a

detoxification branch of methylglyoxal degradation through reduction with NADPH. Of particular interest, however, are Dld and LldD. These proteins are D- and L- lactate dehydrogenases, and were more and less abundant in our engineered strain, respectively. The particular interest stems from the potential for greater lactate utilisation being promoted through glucose addition. They each catalyse the formation of pyruvate from the respective lactate isoform, though Dld specifically reduces ubiquinone, while LldD quinone specificity has not been determined[217–220].

While seemingly at odds with other observation regarding quinone specificity in the two strains, an increase in these proteins in the control strain due to greater methylglyoxal production would adequately explain them. This would make sense, given the greater reliance the control strain would have to place on anaerobic glycolysis (a primary methylglyoxal source[216]). The considered aerobic nature of the LldD catalysed lactate metabolism also lends weight to this argument, as does the noted increase in Gpr. Fatty acid degradation, another contributor to methylglyoxal production was also noted to be more abundant in the control as inferred from higher quantitation of FadB. Selective quinone pool usage is further supported by results for FrdA, down in the engineered strain, which oxidises menaquinol in the fermentation reaction that reduces fumarate to succinate.

Collectively, we believe this evidence points to the activity of the heterologous EET pathway in *E. coli*, from quinone pool to EEA, not being the limiting factor in electroactivity of engineered *E. coli* strains under existing experimental procedures. This then merits further investigation, such as into the impact of improved menaquinone pool utilisation, in a further engineered strain of *E. coli,* on electroactivity. Furthermore, evidence for heterologous CymA preferential interaction with menaquinone in *E. coli* is provided by the differences observed herein, consistent with its activity in *S. oneidensis* MR-1. But further evidence is discussed later in this chapter; and such future work is discussed in more detail in the following chapter.

Table 6.5. Glucose Condition Proteomic Changes

UniProt ID	Gene Name	Significant Settings Used	Control 1	Control 2	Engineered 1	Engineered 2
P0AFC7	nuoB	C	1.00	0.98	0.76	0.75
P33599	nuoC	B	1.00	1.02	0.88	0.85
P31979	nuoF	B	1.00	1.06	0.87	0.82
P28304	qorA	C	1.00	0.84	1.12	1.10
Q46851	gpr	C	1.00	1.06	0.91	0.87
P33232	lldD	B	1.00	1.06	0.67	0.62
P06149	dld	C	1.00	0.97	1.07	1.08
P21177	fadB	B	1.00	1.04	0.87	0.80
P00363	frdA	C	1.00	1.01	0.72	0.76

Quantified (linear, isotopic and multiple corrections applied) protein differences for replicates displayed separately, relative to the second engineered strain replicate. The test settings each protein detected with are referred to as A (MTC, p-value limit of 0.05), B (no MTC, p-value limit of 0.01), and C (no MTC, p-value limit of 0.05) for reference.

6.2.8.2. Cytochrome Biogenesis and Condition Overlaps

Interestingly, it was noted in the glucose supplemented comparison that a number of proteins associated with cytochrome biogenesis were identified as being more abundant in the engineered strain relative to the control, as Table 6.6. details. While expressed constitutively on the pEC86 plasmid present in both the control and the engineered strains, the cytochrome maturation proteins CcmG and CcmH were measured at a much higher level in the engineered strain.

It may be the case that the additional metabolic flux provided by the glucose allowed for an increase in the expression of necessary cytochrome biogenesis machinery that was otherwise suppressed in the lactate only condition. However, further analysis reveals CcmE in the list of proteins excluded for appearing in the non-glucose strain comparison, suggesting that the host cytochrome maturation genes may simply be expressed in the engineered strain generally.

Proteins identified in the glucose comparison, continue to support observations previously made. Some of these appear in the data for both comparisons, such as CusB and CusF. CusC, like the previous two, is part of the copper ion efflux system discussed

beforehand. CusR, the signal transduction protein for copper ion homeostasis[221], was also observed. These all follow the pattern of increased abundance in the engineered strain, relative to the control.

Table 6.6. Cytochrome Biogenesis and Copper Ion Homeostasis Proteins

UniProt ID	Gene Name	Significant Settings Used	Control 1	Control 2	Engineered 1	Engineered 2
P0AA86	dsbE/ccmG	C	1.00	1.17	2.25	2.57
P0ABM9	ccmH	C	1.00	1.20	3.40	3.72
P69490	ccmE	C	1.00	1.06	2.38	2.66
P77239	cusB	B	1.00	1.00	1.79	1.63
P77211	cusC	C	1.00	1.02	1.31	1.32
P77214	cusF	B	1.00	0.94	1.58	1.69
P0ACZ8	cusR	C	1.00	0.92	1.20	1.34

Quantified (linear, isotopic and multiple corrections applied) protein differences for replicates displayed separately, relative to the second engineered strain replicate. The test settings each protein detected with are referred to as A (MTC, p-value limit of 0.05), B (no MTC, p-value limit of 0.01), and C (no MTC, p-value limit of 0.05) for reference.

6.2.8.3. Insights into Regulation from Engineered vs Engineered Plus Glucose Comparison Data

While differences in the proteomes of control and engineered strains following addition of glucose has already been discussed, additional insights can be gleaned from looking at changes between the engineered and engineered + glucose samples (EvEG). The protein list from this comparison has been refined by removing changes that overlap with other comparisons. In addition to the removal of changes from the control vs control + glucose comparison, those from the control vs engineered comparison (CvE) were also removed. Thereafter the results were compared with the control + glucose vs engineered + glucose (CGvEG) results, with overlap visually represented in Figure 6.11. and detailed in Table 6.7. below. The overlapping changes are consistent in their direction unless otherwise noted; i.e. if down in engineered for EvEG comparison, then down in control for CGvEG.

6.11. Overlap of Engineered vs Engineered + Glucose and Control + Glucose vs Egineered + Glucose Comparisons

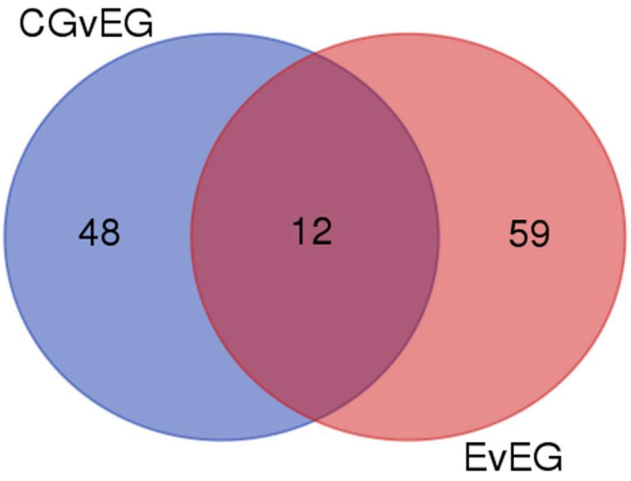

This figure shows the overlap between the two described conditions, when data was analysed using the no MTC $p<0.05$ stringency level. In the highest stringency level only 2 proteins overlapped. This highlights a smaller number of proteins of particular interest, given their correlation with desirable phenotypes (increased current), with non-specific factors such as strain and unrelated glucose response regulation controlled for.

NuoB, as previously discussed, is one of several proteins involved in aerobic respiration that are observed to be present at significantly lower levels in the engineered + glucose condition when compared with control + glucose. As can be seen in Table 6.7. this is also observed when it is compared against the engineered condition. NuoB expression is inhibited under anaerobic conditions both by FNR, a regulator that senses the presence of oxygen within the cell directly, and ArcA-P, the activated form of ArcA that is produced through redox sensing[222]. The latter, due to its sensing being primarily through the redox state of the menaquinone pool, which is sensitive to very low concentrations of oxygen, does not match FNR under microaerophilic conditions. This observation may be an argument that oxygen was allowed to enter the HCs in small concentrations, with the balance altered after the glucose addition, however given the evidence of other proteins which suggest a higher ArcA-P activity in engineered + glucose vs engineered or control + glucose, this seems unlikely.

Many other of these protein changes further reinforce previous conclusions. GdhA is induced by PhoP and is more prevalent in the glucose condition of the EvEG comparison, fitting with expectation. The lower relative quantification in the engineered sample of GrxB, which is induced by the alarmone ppGpp in response to amino acid shortage[223], as well as many amino acid synthesis proteins fits the proposed view of stress and lower metabolic activity. GrxB's inhibition of protein synthesis is naturally to be avoided to maximise electrochemical activity, and these results suggest that a higher metabolic flux will achieve this. Though whether that flux is due to increased EET utilisation or glycolysis is unclear. Even if it were currently the latter, increasing EET pathway utilisation to DMRB comparable levels should have a similar effect.

Table 6.7. Protein Details for Overlap of Engineered vs Engineered + Glucose and Control + Glucose vs Egineered + Glucose Comparisons

				Engineered		Engineered Gluc			
UniProt ID	Gene Name	Change in Engineered	Signifiquant Settings Used	Replicate 1	Replicate 2	Replicate 1	Replicate 2	#Unique	#Quants
P00370	gdhA	↓	B	0.585759	0.609339	0.759354	1	14	18
P0AC59	grxB	↓	B	0.755846	0.775653	0.922492	1	8	20
P06988	hisD	↓	C	0.896505	0.841805	0.967674	1	6	10
P15640	purD	↓	C	0.57742	0.566824	0.747851	1	6	6
P15254	purL	↓	C	0.642214	0.619165	0.827928	1	10	11
P08660	lysC	↓	B	0.372452	0.441716	0.717272	1	9	13
P0AC55	glnK	↓	C	0.351049	0.333201	0.476195	1	3	6
P03023	lacI	↓	C	0.864751	0.900891	1.069001	1	13	31
P33218	yebE	↓	B	0.628437	0.70614	0.910274	1	7	15
P0AFC7	nuoB	↑	C	1.335461	1.188315	1.008199	1	5	9
P0AC41	sdhA	↑	C	1.154716	1.088162	1	1.013032	18	28
P0ADE8	ygfZ	↑	C	1.098265	1.070494	0.992066	1	14	24

Quantified (linear, isotopic and multiple corrections applied) protein differences for replicates displayed separately, relative to the second engineered + glucose strain replicate, except for SdhA where it is relative to the first. The test settings each protein detected with are referred to as A (MTC, p-value limit of 0.05), B (no MTC, p-value limit of 0.01), and C (no MTC, p-value limit of 0.05) for reference.

In the interest of identifying targets for further investigation of electrochemical interaction, YebE presents itself as a suitable candidate. YebE is an uncharacterised integral inner membrane protein with domains in both the periplasm and cytoplasm.

Higher relative quantification is observed to be present in conditions with higher electroactivity in our data. However, *yebE* is under the regulatory control of CpxR, which induces it and other genes involved in the envelope stress response[224]. It senses several associated factors, including membrane lipid composition, and alkaline pH, and as such may reflect the increased stress placed on cells in the respective samples. Lower stress might be expected in conditions with greater metabolic flux, but this might be contributing to membrane instability or influencing one of many other factors. Or this might be an artefact of globally increased expression due to this higher flux, with stress response genes outcompeting others. It is one to keep in mind going forwards, then, but its presence should not be investigated until other more fundamental issues have been resolved.

6.3. Conclusions

In this chapter we have demonstrated the impact of small variations in BES media, strain, and pre-inoculation growth conditions on electroactivity of recombinant *E. coli* strains. They have been shown to have a far stronger influence on current levels in a single chamber BES under a poised potential, than expected from the literature. Consequently a global proteomic analysis of engineered and control strains of *E. coli* was conducted, to assist in characterising the effects of heterologous extracellular electron transport pathway utilisation within *E. coli*. This revealed number of insights. The increase of toxic ion efflux proteins was identified in the engineered strain, with further suggestion of redox activity leading to a reducing periplasmic environment. This, combined with the inferred quinone preference of metabolic processes between the two strains, indicated that heterologous EET pathway utilisation might be limited in *E. coli* by flux through CymA accessible electron transport chains. The general greater metabolic activity expected in the engineered strain was also adequately reflected in the data.

As previously discussed, across the various comparisons there has been an indication that the menaquinone pool has been preferentially reduced by the EET pathway. Upon investigation of the regulatory control of many proteins observed to change in the preceding comparisons it became clear that many were under the control of ArcA, and their altered expression levels were indicative of ArcAB's response to a reduced menaquinone pool. The suggestion that a microaerophilic condition was present within the HCs was argued against and disregarded.

If this conclusion is true, then this could inform a strategy to modify host a strain so that it better regenerates the menaquinone pool over ubiquinone pool. This would in turn ease the ArcAB regulation, allowing host processes to regulate themselves more effectively, no longer reacting to an incorrect situation. And moreover, with increased metabolic utilisation of the menaquinone pool as electron acceptor by central metabolism, this would be eliminated as a bottleneck for EET. Hypothetically this would allow much higher electroactivity to be observed. However, before such an undertaking in metabolic engineering is embarked upon, validation of these conclusions must be carried out. This proposed work is discussed in detail in the future work chapter.

Chapter 7 – Conclusions and Future Work

7.1. Conclusions

In this thesis we have presented variety of considered approaches into furthering the knowledge and development of engineered electroactive *E. coli* strains. The first research chapter explored the progression of a bioelectrochemical cell protocol, with comparisons to existing literature and a discussion of the reasoning behind protocol changes. This half cell (HC) setup was aimed at achieving a higher throughput than that possible with lab scale microbial fuel cells (MFCs), while retaining a high level of electrochemical insight; in this we succeeded, which could be of benefit to future studies seeking higher throughput electrochemical testing equipment that can be commercially procured. Most notably, we observed and investigated the mediator-like behaviour resulting from the chloramphenicol resistance products. This presents an opportunity for alternative, non-toxic mediators to be developed for energy producing or biosensing BES applications.

The second research chapter of this thesis described the construction of genomic libraries of *S. oneidensis* MR-1 in *E. coli* strains for the purpose of identifying novel electroactive factors. To this end a dye reduction assay was developed to facilitate the very high throughput required for screening such a large volume of strains. The stages of the screening process were described and the most interesting of the resultant clones investigated further. From an overlapping region of two separate "hit" fosmid clones, several constructs were produced and tested. Ultimately the gene *SO_0527*, annotated as an antibiotic biosynthesis monooxygenase family protein, was suggested as the causative, novel factor for the increased dye reductive phenotype observed in our clones. Further work is required to conclusively validate these findings, however.

In the third research chapter, a closer look was taken at the impact of methodological variables on electroactivity of engineered and control *E. coli* strains, as well as presenting

a comparison between strains from different studies within the same bioelectrochemical system (BES). It became clear that media choice had a great impact on electroactivity, leading to further investigation through a global proteomics approach. The metabolic activity of electroactive *E. coli* expressing the heterologous Mtr EET pathway was subsequently characterised in the interest of informing future engineering strategies, as it remains clear that a more consistent response to minor environmental variables is required for many synthetic biology applications to be viable. It was concluded that oxidation of the menaquinone pool by the EET pathway was resulting in a regulatory response commensurate with the response to microaerophilic conditions. Once validated a metabolic engineering strategy could be devised that might drastically improve the performance of engineered *E. coli* strains for BES applications.

7.2. Future Work

As with most scientific research, many avenues of progression lay outside the scope of the work presented in this thesis. Some due to time, but others presented themselves only in retrospect; a few of the most interesting are discussed here.

7.2.1. Chloramphenicol Effect Electrode Interaction

The observed mediator activity may have been a direct result of some component of our specific BES, or may have been similarly highlighted by such. Our HCs are single chamber, whereas many BESs use two-chamber, air cathode, or otherwise membrane separated counter electrode (CE). From this, if we assumed that it was something within our setup that was responsible, we could speculate that this was either down to some novel interaction with our working electrode (WE), or an unforeseen interaction with the non-membrane separated CE. In order to investigate these possibilities, we would repeat a core set of the chloramphenicol effect experiments using a range of different equipment.

This suggested work would face challenges; as highlighted in this thesis, BES equipment and protocols can be highly variable, and not commercially available. Thus this would be most practicably achieved through collaboration with other groups focussed on

bioelectrochemical research. Nevertheless, such would present its own difficulties, and the experimental options would still be limited by available equipment.

Modification of the WE could be easily achieved and thus investigated. The difference between the carbon veil used and other carbon cloths used ubiquitously in the literature is minimal, and so we would not expect this to have any effect on the reproducibility of the chloramphenicol effect. The nichrome wire threaded through the veil, and linking it to the potentiostat connectors is not so commonly used however. A range of alternative wire materials (with as identical as possible characteristics) would be tested, and the impact on the chloramphenicol effect noted.

The CE was composed of platinum wire, and is where electrons are donated back to elements within the media. Given the lack of oxygen in the system we would expect this to result in hydrogen when protons ejected by the respiring bacteria met the CE. However, it is possible that acetylated Cm (aCm) or a product of an interaction with the bacterial cell or WE could have been acting as an electron acceptor at the CE. The separation of the CE by a membrane might present a suitable method for testing this hypothesis, providing it was not permeable to aCm. Though if the Cm effect persisted it would not rule out other unforeseen products of the resistance reaction from doing the same if they were membrane permeable.

7.2.2. Chloramphenicol Reactivity and Degradation

The Cm antibiotic is known to naturally degrade over a relatively short time frame, however a study of the rates under the conditions observed herein was not identified. An analysis of this could provide further insights into the nature of the mechanism of the Cm effect, particularly if rates could be matched to bioelectrochemical changes. An analysis using HPLC of the concentrations of Cm and derivatives found in HC media at various time points and different conditions might facilitate this. Less equipment modification would be required relative to the other work previously suggested, as sample collection could be achieved with the equipment currently available, however the HPLC analysis might introduce additional concerns and limitations (e.g. variable degradation of analytes skewing results).

More easily achievable would be investigation of the upper limit of the Cm effect's linearity. Would mediator activity reach maximum efficiency before CAT saturation was reached (represented by Cm concentrations beyond the tolerance of the CmR strains)? While plasmid copy number was briefly investigated, through the creation of a construct with CAT under a tuneable promoter (and verification through mass spectrometry or western blot), the direct effect of varying levels of CAT expression on the Cm effect could be quantitatively explored.

Following on from the discussion over the potential biochemical interaction of chloramphenicol which might lead to its electrochemical activity, it would be logical to investigate this. Given the main barrier to use at higher concentrations, and practical applications for wider use, is the antibiotic activity of the Cm molecule we would aim to test homologues that lacked this activity but retained the active groups we proposed as likely accountable for the electroactivity. The commercial availability of such compounds would likely determine the testing order, with a HC run analysing the effect of different concentrations being run for each. Duplication of the effect with such compounds would strengthen our conclusion about the mechanism of the Cm effect. Furthermore, depending on factors such as stability and cost of functional homologs for the electrochemical activity, these compounds could be assessed for their ability to cost-effectively improve BES technology to meet real world challenges.

7.2.3. *SO_0527* Investigation and Characterisation

The identification of *SO_0527* as the causative factor for improved dye reduction in two of our fosmid clones is potentially greatly interesting within the field of engineered electroactivity, however, it solicits further investigation and validation. Expression of this and possibly the other proteins for the tested constructs would need to be performed. This could be achieved through real time PCR, but this would only check for the mRNA of the genes. Ideally confirmation of expression through mass spectrometry of extracted protein samples would be carried out, with fractionation to improve purity. Other methods, such as western blotting or affinity purification would require further cloning to add in appropriate tags, or the expensive acquisition of tailored antibodies.

The *SO_0527* gene and its product are uncharacterised, with their description generated through inference, unsupported by practical evidence. Consequently, following validation, future work would attempt to characterise its activity, dependent on scope both in *S. oneidensis* MR-1 and *E. coli,* as discussed herein.

The initial priority would be to investigate *SO_0527* constructs within *E. coli* using other bioelectrochemical assays. In addition to the existing pRSF *SO_0527* construct, others containing *mtrCAB, cymA,* and/or *omcA* in the first MCS would ideally be produced for parallel testing. These would then be compared in a BES, such as our HC setup, and with the accepted iron reduction assays (ferric citrate or ferric oxide reduction, soluble and insoluble respectively, measured through the ferrozine method) (REF REF). This would assist in characterising the bioelectrochemical activity of SO_0527, hopefully allowing for continued iterative improvement of an engineered electroactive *E. coli* strain.

Concurrent or subsequent testing of a *SO_0527* deletion mutant, and additional *SO_0527* expression plasmid bearing strain, of *S. oneidensis* MR-1 would also help characterise its role and bioelectrochemical activity in its native biological environment. With respect to BES testing, riboflavin supplementation would be preferably compared additionally with all *S. oneidensis* strains, as due to the presumed cytosolic localisation of SO_0527 soluble, mediative compounds might be required to observe its activity.

7.2.4. Further Fosmid Library Investigation

While we have concluded our approach to the screening of our fosmid library as successful, other approaches were considered and might still be able to derive further novel bioelectrochemical factors from it.

One such approach to library screening that might offer alternative or additional insights would be to conduct selection within a HC. Several HCs would be set up and inoculated with a mixed library culture (though pre-HC growth conditions might introduce bias within the library culture), where the anaerobicity and poised potential would provide a selective pressure that would favour clones with increased electroactivity. The cultures from each HC would be reclaimed and used to inoculate another set of HCs. Successive

rounds would continue, hopefully resulting in increasing observed current. Clones remaining after this process would then be identified and analysed.

It is possible that such a process might favour a mixed community of clones, which would introduce additional difficulties when trying to sequence them. However, it is also possible that rather than favouring the clones with electroactive factors, novel or otherwise, the selection would favour those best able to survive the HC step and flourish in the pre-HC growth step, or those that simply had the lowest burden placed upon them by their fosmid. Nevertheless, these outcomes could still be informative, and their possibility would not rule out this approach as infeasible.

7.2.5. Validation and Investigation of Proteomic Findings

While several individual targets were identified as of potential interest, and the influence the HCs conditions had on the regulation of metal toxicity response genes bears further investigation, the primary hypothesis in need of testing is that of the interaction between the heterologous EET pathway and the host metabolism. Specifically, that the EET pathway preferentially reduces the menaquinone pool, the redox state of which is consequently the limiting factor in its utilisation by the engineered strain. This redox state results in a microaerophilic condition response by the cell's regulatory mechanisms through the action of ArcAB which senses that quinone pool redox state, and FNR which senses the lack of oxygen within the cell directly.

The ArcAB two component system senses redox activity primarily through sensing the redox state of the menaquinone pool. Under anaerobic conditions, the menaquinone pool is in a predominantly reduced state, the sensing of which causes the autophosphorylation of ArcB, resulting in the transphosphorylation of ArcA. ArcA-P represses a host of metabolic proteins, impacting the metabolic activity of the strain. From analysis of our proteomic data we hypothesise that the heterologous extracellular electron transport (EET) pathway within the engineered strain is oxidising the menaquinone pool, inhibiting ArcA-P repression.

In order to test this hypothesis, we intend to visually monitor regulation of ArcAB under BES conditions. First, we would construct two strains of *E. coli,* expressing either iLOV[225]

or superfolder GFP (both of which fluoresce under anaerobic conditions)[226] under an ArcA-regulated promoter[227], using the Mtr nanoconduit, and expression support (negative control) strains. Regulatory control would be subsequently validated by microscopy of cells under aerobic and anaerobic conditions. Following this, E. coli strains containing the Arc-regulated fluorophore protein would be monitored microscopically within a flow cell containing an electrode configuration which could be biased to provide conditions comparable to those in previously tested bioelectrochemical systems (BES). An increase in GFP/iLOV expression under anaerobic conditions when the electrode is biased would support our hypothesis. If unsuccessful, a complementary methodology would be developed using existing techniques for analysing bioelectrochemical activity combined with harvesting of cells and microscopy in order to preclude a false negative result. Other regulators could even be probed in the event of a confident negative result by exchanging promoters or altering conditions, alongside re-evaluation of the proteomic dataset.

8. Appendix

8.1. Plasmid Maps

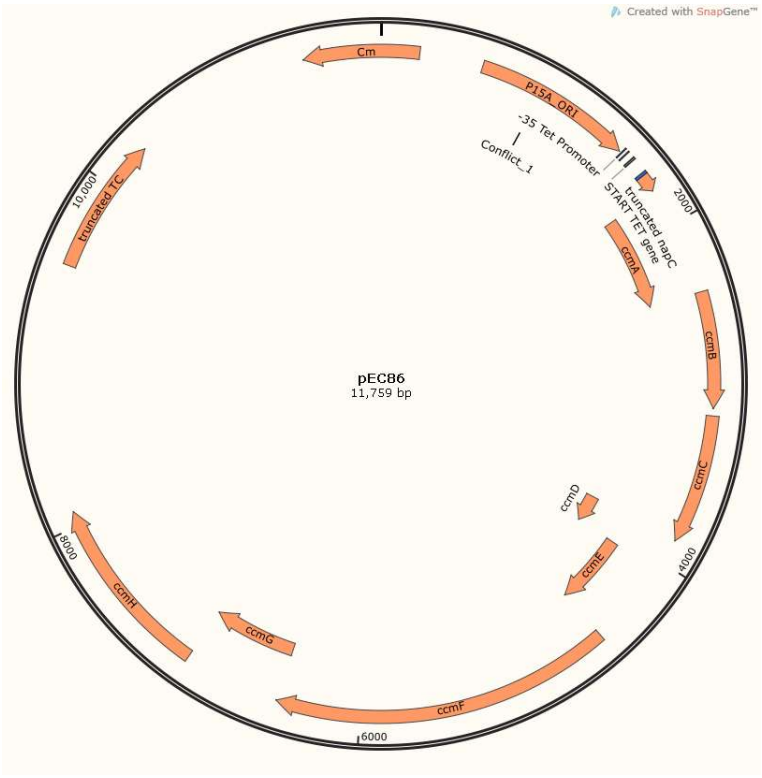

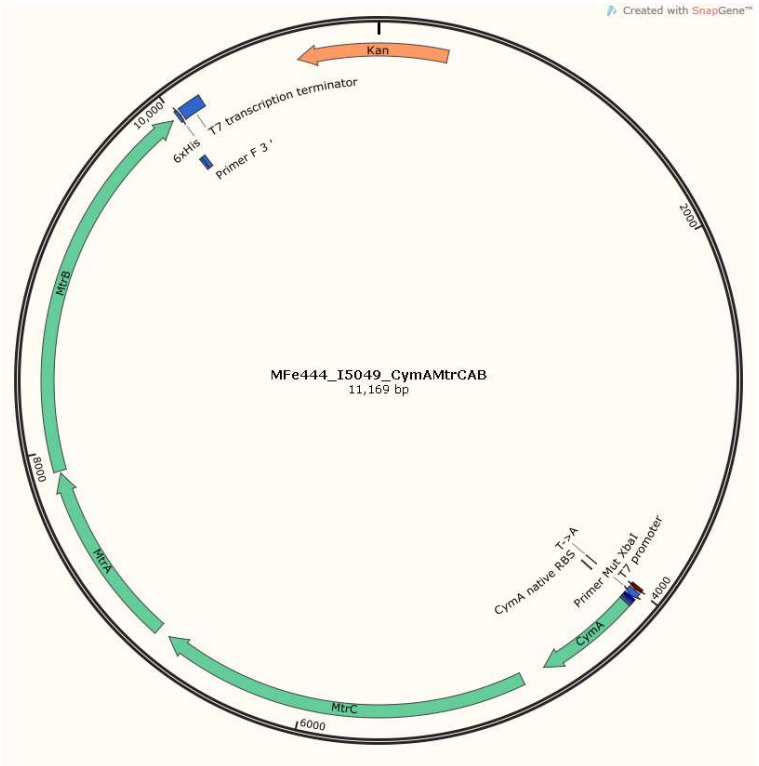

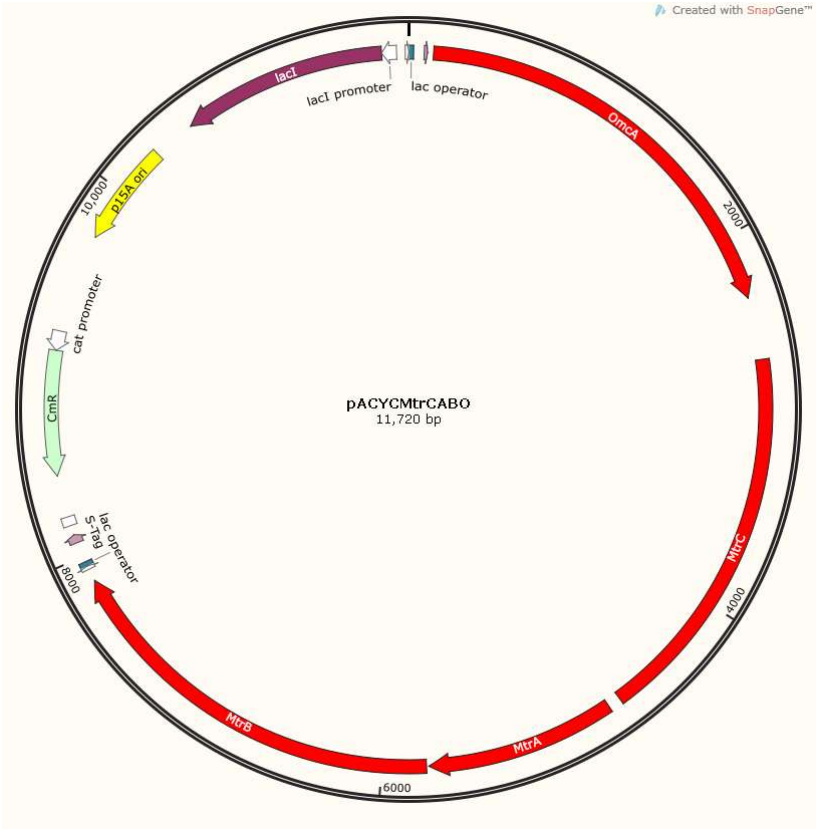
Created with SnapGene™
lacI
lacI promoter
lac operator
OmcA
2000
MtrC
4000
MtrA
MtrB
6000
8000
lac operator
S-Tag
CmR
cat promoter
p15A ori
10,000
pACYCMtrCABO
11,720 bp

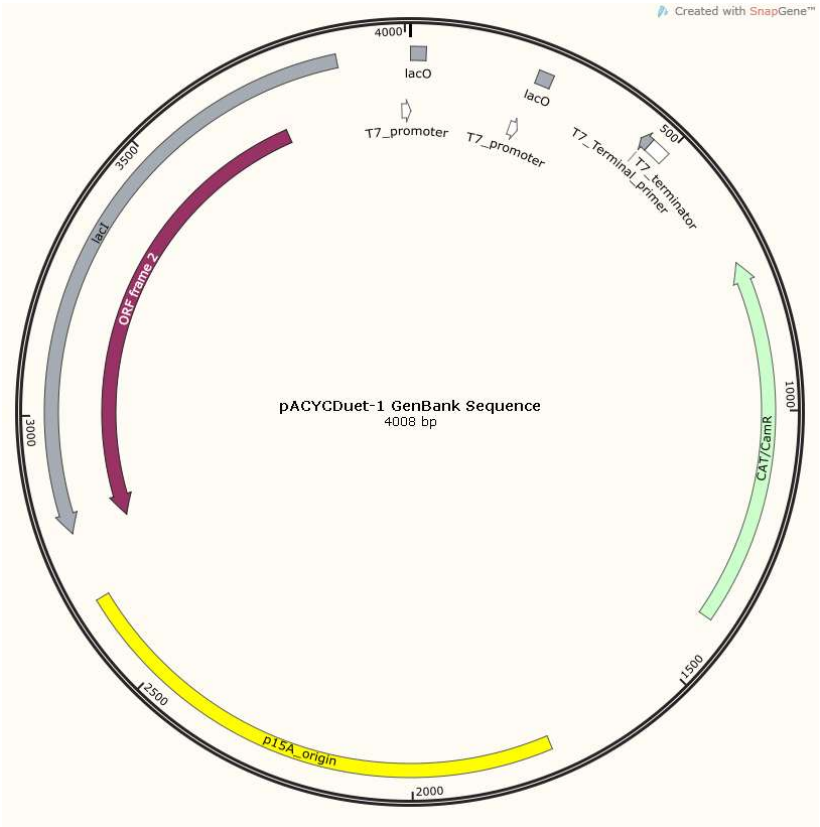
Created with SnapGene™
4000
lacO
lacO
T7_promoter
T7_promoter
T7_Terminal_primer
T7_terminator
500
CAT/CamR
1000
1500
p15A_origin
2000
2500
ORF frame 2
lacI
3000
3500
pACYCDuet-1 GenBank Sequence
4008 bp

8.2. Azo Dye Screen Data

C41 1A												
RB5												
<>	1	2	3	4	5	6	7	8	9	10	11	12
A	0.5908	0.5696	0.4493	0.7167	0.3488	0.2133	0.2977	0.4215	0.3221	0.4242	0.3925	0.1126
B	0.6232	0.4668	0.364	0.4384	0.2519	0.3141	0.327	0.4358	0.4952	0.5461	0.2609	0.1023
C	0.1785	0.3714	0.2802	0.0806	0.3719	0.2502	0.4849	0.3764	0.272	0.3193	0.3377	0.0872
D	0.5411	0.3051	0.3201	0.2644	0.2684	0.3778	0.2902	0.3519	0.3813	0.3353	0.3138	0.109
E	0.2987	0.2887	0.3455	0.4406	0.2018	0.1953	0.2415	0.2606	0.3011	0.2721	0.2286	0.3358
F	0.3468	0.7546	0.6617	0.3997	0.2854	0.2607	0.2558	0.2146	0.3931	0.3787	0.5488	0.2654
G	0.2048	0.4385	0.2983	0.3978	0.2322	0.2713	0.2395	0.2537	0.3398	0.2819	0.1737	0.4144
H	0.2806	0.3697	0.4985	0.3165	0.3948	0.3286	0.3979	0.2052	0.4821	0.3528	0.5422	0.4434

C41 1B												
<>	1	2	3	4	5	6	7	8	9	10	11	12
A	0.3428	0.5704	0.3561	0.4005	0.5827	0.4229	0.4433	0.2964	0.4387	0.3836	0.3294	0.1215
B	0.2508	0.3231	0.3924	0.3359	0.3559	0.3679	0.3497	-0.0399	0.2215	0.3479	0.4836	0.1184
C	0.1541	0.2862	0.368	0.2222	0.4311	0.328	0.4141	0.2499	0.2837	0.3367	0.3444	0.1229
D	0.4046	0.3454	0.3469	0.2348	0.2883	0.3514	0.3192	0.2843	0.3607	0.3843	0.3915	0.1089
E	0.2589	0.3298	0.2667	0.3092	0.2876	0.4169	0.3629	0.078	0.3747	0.3026	0.3451	0.4871
F	0.3213	0.5086	0.3688	0.32	0.3977	0.4224	0.3222	0.2725	0.2985	0.3225	0.3169	0.4231
G	0.7256	0.4093	0.2764	0.2419	0.1851	0.3365	0.2378	0.2226	0.1931	0.2479	0.3997	
H	0.6043	0.4423	0.4564	0.4656	0.3578	0.3938	0.341	0.3489	0.4484	0.4456	0.3501	

BL21 1A												
RB5												
<>	1	2	3	4	5	6	7	8	9	10	11	12
A	0.7562	0.7437	0.6233	0.5247	0.3833	0.3136	0.4039	0.6603	0.5941	0.4837	0.6165	0.1044
B	0.7697	0.6147	0.5844	0.2874	0.3356	0.6328	0.4969	0.4225	0.523	0.4299	0.4398	0.1128
C	0.6071	0.5605	0.6202	0.523	0.3599	0.3755	0.1215	0.5047	0.5768	0.1783	0.502	0.1387
D	0.4193	0.5707	0.6395	0.4962	0.5156	0.4651	0.6489	0.4201	0.5747	0.5199	0.2204	0.1272
E	0.6653	0.6016	0.5921	0.3582	0.2805	0.4169	0.5692	0.5927	0.4071	0.1987	0.3726	0.3161
F	0.6036	0.4607	0.5574	0.5424	0.3277	0.6401	0.1334	0.4042	0.1822	0.3998	0.1161	0.2705
G	0.6977	0.468	0.5728	0.1588	0.3688	0.7134	0.6929	0.2819	0.4928	0.4776	0.319	0.3643
H	0.6415	0.7205	0.6183	0.5645	0.4158	0.7866	0.6281	0.4749	0.5865	0.584	0.6429	0.4759

BL21 1B												
<>	1	2	3	4	5	6	7	8	9	10	11	12
A	0.5882	0.7831	0.8368	0.777	0.5955	0.7514	0.7551	0.6769	0.2263	0.2291	0.5815	0.1229
B	0.6931	0.7488	0.7922	0.8106	0.5968	0.7318	0.7016	0.4826	0.5959	0.7125	0.8004	0.1093
C	0.5636	0.7186	0.7787	0.7044	0.7169	0.4617	0.6403	0.6413	0.7846	0.6888	0.2264	0.1086
D	0.4277	0.7568	0.7994	0.7904	0.5769	0.7584	0.4158	0.675	0.6781	0.6558	0.6286	0.12
E	0.6618	0.7278	0.7761	0.7671	0.6491	0.6587	0.5621	0.6836	0.5486	0.5725	0.6713	0.6479
F	0.7982	0.8494	0.8629	0.6999	0.6076	0.5104	0.6918	0.6328	0.6011	0.6737	0.7614	0.7226
G	0.7027	0.7719	0.6455	0.7581	0.6368	0.7432	0.7836	0.6483	0.7034	0.6092	0.6854	0.7338
H	0.2055	0.1699	0.6803	0.6561	0.8487	0.6871	0.7613	0.6545	0.6695	0.6493	0.7627	0.8369

BL21 1C												
<>	1	2	3	4	5	6	7	8	9	10	11	12
A	0.6533	0.7436	0.7512	0.8045	0.8093	0.7362	0.7697	0.805	0.8014	0.7531	0.296	0.1149
B	0.7862	0.7283	0.7787	0.7026	0.7656	0.7817	0.6565	0.7231	0.6735	0.7213	0.8289	0.2368
C	0.7616	0.7759	0.7728	0.6707	0.7155	0.7049	0.722	0.7183	0.7032	0.7292	0.6846	0.2418
D	0.758	0.7892	0.7581	0.7734	0.7574	0.7607	0.8643	0.7245	0.788	0.7802	0.7344	0.2296
E	0.8172	0.7772	0.7576	0.7603	0.7494	0.7907	0.8052	0.6624	0.7601	0.7648	0.7194	0.4707
F	0.7414	0.7495	0.6609	0.7443	0.7796	0.6634	0.6452	0.7832	0.8082	0.7185	0.8174	0.612
G	0.8395	0.7829	0.7883	0.6967	0.7935	0.6883	0.7314	0.6962	0.7983	0.78	0.756	0.7311
H	0.7311	0.7533	0.746	0.8412	0.7881	0.7099	0.7206	0.8071	0.7822	0.6795	0.8042	0.6839

C41 2A												
RB5												
<>	1	2	3	4	5	6	7	8	9	10	11	12
A	0.2801	0.2643	0.496	0.4522	0.5052	0.4649	0.4632	0.4965	0.4477	0.5195	0.1232	0.0795
B	0.5555	0.4651	0.5261	0.5155	0.4805	0.4602	0.4062	0.5005	0.4896	0.4744	0.5084	0.0892
C	0.5517	0.3445	0.4165	0.4599	0.4022	0.4744	0.4166	0.5941	0.4182	0.3828	0.4772	0.0797
D	0.4886	0.4418	0.4258	0.3656	0.4405	0.4301	0.4424	0.4483	0.5	0.5063	0.3625	0.0809
E	0.4609	0.4342	0.4091	0.421	0.4635	0.4478	0.5082	0.557	0.4516	0.3747	0.5092	0.6651
F	0.5807	0.4716	0.4683	0.408	0.462	0.3224	0.4771	0.4965	0.5154	0.4712	0.4318	0.5935
G	0.2883	0.4703	0.1879	0.3766	0.3684	0.4218	0.4826	0.535	0.5003	0.5536	0.6122	0.6686
H	0.5394	0.4582	0.5206	0.5157	0.3784	0.5739	0.5439	0.546	0.6003	0.5068	0.5714	0.605

C41 2B												
<>	1	2	3	4	5	6	7	8	9	10	11	12
A	0.5719	0.5599	0.6069	0.551	0.5898	0.4789	0.5168	0.6419	0.5587	0.5692	0.6518	0.086
B	0.6575	0.5226	0.5111	0.6235	0.3911	0.6303	0.5026	0.5709	0.5407	0.5912	0.4171	0.0996
C	0.4578	0.4914	0.497	0.5054	0.5991	0.5973	0.5031	0.4565	0.5547	0.6178	0.5699	0.126
D	0.5206	0.5148	0.5879	0.4923	0.5357	0.5387	0.5482	0.5509	0.5429	0.4752	0.5222	0.074
E	0.6057	0.5158	0.5808	0.622	0.6381	0.5056	0.5114	0.599	0.5457	0.4975	0.5843	0.677
F	0.5729	0.5333	0.5291	0.5905	0.5845	0.5996	0.5102	0.567	0.5258	0.4695	0.5679	0.6259
G	0.6187	0.5465	0.5267	0.5857	0.4986	0.4101	0.55	0.566	0.6515	0.3959	0.6375	0.7172
H	0.6259	0.5774	0.6113	0.6402	0.6602	0.6302	0.6436	0.6338	0.6038	0.5946	0.4948	0.7136

C41 2C												
RB5												
<>	1	2	3	4	5	6	7	8	9	10	11	12
A	0.5661	0.5782	0.633	0.5651	0.5116	0.5804	0.5317	0.5209	0.4946	0.5705	0.6519	0.0903
B	0.7026	0.6564	0.647	0.5968	0.6542	0.5205	0.5007	0.533	0.6109	0.6738	0.4519	0.1174
C	0.6857	0.556	0.5156	0.6486	0.5353	0.5982	0.5037	0.4999	0.6193	0.5846	0.5697	0.1091
D	0.5834	0.579	0.5955	0.6632	0.5978	0.652	0.5359	0.4507	0.6251	0.5261	0.6327	0.1159
E	0.5515	0.5213	0.5259	0.7357	0.5424	0.5084	0.4732	0.4843	0.6372	0.6794	0.5918	0.6673
F	0.5441	0.6412	0.6229	0.5436	0.5913	0.5941	0.5753	0.3608	0.6389	0.6571	0.5519	0.645
G	0.5747	0.561	0.3773	0.6486	0.6006	0.6019	0.5443	0.5311	0.6199	0.6051	0.6445	0.7034
H	0.5969	0.5751	0.7009	0.6101	0.5347	0.5808	0.7001	0.5988	0.7088	0.6929	0.5202	0.7101

BL21 2A												
<>	1	2	3	4	5	6	7	8	9	10	11	12
A	0.5837	0.6662	0.638	0.6769	0.3811	0.3794	0.425	0.6321	0.5838	0.457	0.5626	0.0911
B	0.5048	0.6351	0.558	0.6965	0.501	0.6228	0.5707	0.6185	0.5913	0.5045	0.6409	0.1008
C	0.6358	0.6214	0.574	0.5653	0.6708	0.5569	0.6745	0.6288	0.3846	0.5157	0.6514	0.0953
D	0.5711	0.5876	0.5496	0.6725	0.6069	0.6003	0.5512	0.5157	0.553	0.6272	0.6515	0.0982
E	0.6244	0.6039	0.5807	0.6289	0.6322	0.6177	0.6461	0.5638	0.5462	0.6136	0.3677	0.6609
F	0.207	0.5811	0.4911	0.6206	0.5926	0.4817	0.3727	0.6735	0.5071	0.576	0.5449	0.629
G	0.6498	0.6399	0.6236	0.5958	0.6788	0.5608	0.6149	0.6274	0.2759	0.569	0.5923	0.6638
H	0.3939	0.6478	0.2503	0.6491	0.6255	0.626	0.6209	0.6549	0.6833	0.5588	0.6345	0.6943

BL21 2B												
<>	1	2	3	4	5	6	7	8	9	10	11	12
A	0.5214	0.5744	0.5521	0.6441	0.4326	0.5526	0.5354	0.6257	0.6141	0.6114	0.441	0.0924
B	0.6117	0.1482	0.379	0.5624	0.4881	0.5188	0.4979	0.6393	0.3183	0.4529	0.5377	0.1012
C	0.5774	0.5289	0.3978	0.6174	0.6057	0.5059	0.4476	0.5702	0.6468	0.5728	0.5239	0.0987
D	0.4912	0.476	0.5998	0.5607	0.5648	0.5789	0.628	0.6086	0.6062	0.4084	0.5128	0.0955
E	0.47	0.3879	0.6223	0.5004	0.2375	0.4155	0.5418	0.6832	0.5882	0.5831	0.4547	0.7119
F	0.5418	0.51	0.6148	0.1838	0.4511	0.5166	0.5843	0.6709	0.5942	0.6497	0.4966	0.6966
G	0.4731	0.5567	0.4671	0.3368	0.5228	0.5009	0.5379	0.505	0.6186	0.2379	0.5125	0.6879
H	0.6395	0.5706	0.5618	0.5013	0.6644	0.6097	0.6029	0.6221	0.652	0.4367	0.6585	0.7433

8.3. Proteomics Data Tables

8.3.1. MTC p<0.05

EvC

Q8EG35	0.909037	1	2.095165	2.14441
P02925	1.048334	1	1.194304	1.221939
P02931	0.919341	1	0.525135	0.500669
P08331	1.027343	1	1.285339	1.268143
P08997	1.026845	1	0.732879	0.704509
P09546	0.94136	1	0.712752	0.66237
P0A6B7	1.025368	1	1.9946	1.98028
P0A6Z1	0.996895	1	1.562179	1.591719
P0A6Z3	0.993692	1	0.798645	0.832282
P0A867	0.982606	1	1.248907	1.289115
P0A910	0.971689	1	1.946193	1.96004
P0AC38	0.962094	1	0.666698	0.642227
P0ACD4	0.94565	1	1.728464	1.768618
P0AEU0	1.063091	1	1.612392	1.600013
P0AEX9	1.063309	1	1.517209	1.595819
P0AFH8	1.086852	1	1.989594	1.961726
P0AFM6	1.018616	1	0.656998	0.65455
P0AG80	1.12093	1	1.537928	1.635252
P0AGD1	1.039674	1	1.949816	1.790465

P0C058	1.106047	1	0.372247	0.401381
P0C0L2	1.066708	1	1.46672	1.390492
P16700	0.937762	1	1.545952	1.379703
P23847	1.002681	1	1.311454	1.274673
P24215	1.050842	1	0.769439	0.807131
P37095	0.927487	1	1.440997	1.53958
P39325	1.056473	1	1.468737	1.448392
P63284	1.007243	1	0.826805	0.818201
P68206	1.013655	1	1.734359	2.005057
P69441	1.002389	1	1.202482	1.287798
P75691	0.997266	1	1.543496	1.457047
P77754	1.047996	1	2.525321	2.713997
Q46857	1.041052	1	1.604933	1.542253

EGvCG

	117	118	119	121
Q8EG35	1	0.931949	2.426631	2.591319
P04983	1	1.022114	0.826474	0.822723
P09373	1	0.935734	1.20309	1.229006
P09546	1	1.097103	0.794979	0.737294
P0A6B7	1	1.097887	2.142049	2.285163
P0A6Z1	1	1.004848	1.772948	1.709612
P0A6Z3	1	0.991814	0.867106	0.824433
P0A910	1	1.082218	1.703784	1.53637
P0ABB4	1	0.993327	0.798491	0.840734
P0AC38	1	0.994272	0.682341	0.648377
P0ACD4	1	1.104682	2.367168	2.569853
P0AFH8	1	1.059403	1.62514	1.387454
P0AFM6	1	0.952832	0.679738	0.626294
P0C058	1	0.988028	0.444198	0.426164
P0C0L2	1	0.99448	1.328872	1.337222
P16700	1	0.984015	1.365952	1.280224
P24232	1	0.999383	1.49822	1.56231
P37095	1	1.009936	1.763371	1.588439
P39377	1	1.033474	1.669346	1.891937
P68206	1	1.026078	1.806196	1.48112
P77754	1	1.017488	2.37743	1.875388
Q47537	1	0.939349	0.759541	0.656198

EvEG

P00561	1	1.17739	1.913879	1.726395
P00579	1	1.053554	1.314123	1.29564
P00963	1	0.935532	1.878459	1.736074
P00968	1	1.002199	1.323752	1.679406
P05793	1	1.020193	1.771947	2.018086
P06959	1	0.933999	1.313707	1.372727
P07024	1	0.986432	0.789871	0.711161
P08331	1	0.993275	0.760659	0.73023
P08839	1	1.012337	1.365416	1.551718
P09373	1	1.051579	2.02245	2.073324
P09831	1	1.004328	1.587367	2.121669
P0A6P9	1	1.055515	1.398065	1.597497
P0A799	1	1.071985	1.321802	1.398369
P0A8T7	1	0.978119	1.268451	1.265864
P0A9C5	1	1.041406	1.437092	1.829547
P0A9M8	1	0.998036	1.182206	1.226357
P0A9Q7	1	1.009505	1.639015	1.917346
P0AFG8	1	0.959751	1.2975	1.363059
P0AG80	1	1.070453	0.803301	0.689938
P24232	1	1.078199	2.578773	2.698599
P25665	1	1.045837	1.485415	2.026024
P39099	1	1.003378	0.840602	0.815451
P39325	1	0.992798	0.757081	0.616139
P39377	1	0.999482	1.477108	1.679989
P63284	1	0.996268	1.301961	1.147473
Q46857	1	0.967426	0.799884	0.726582

CvCG

P00561	0.652233	0.653389	1	0.998596
P00963	0.484926	0.503265	1	0.875954
P00968	0.87667	0.871121	1	1.009989
P04982	1.735987	1.649087	1	1.03381
P05791	0.600745	0.613162	1	0.81337
P05793	0.471856	0.477488	1	0.829817
P06959	0.734178	0.75389	1	0.997449
P09373	0.602384	0.595835	1	0.935734
P09831	0.713109	0.743662	1	1.001397
P0A6P1	0.896048	0.842659	1	1.031978
P0A6P9	0.721886	0.677777	1	0.886858
P0A799	0.815478	0.800843	1	0.941708
P0A8T7	0.804141	0.81818	1	1.048418

P0A8V2	0.848627	0.865163	1	1.033908
P0A910	0.816289	0.838372	1	1.082218
P0A9Q7	0.591761	0.598284	1	0.930942
P0A9T0	0.518677	0.55317	1	0.915443
P23847	0.795977	0.792243	1	0.964249
P25665	0.614091	0.597274	1	0.913694
P27302	0.884958	0.838167	1	0.975329
P76177	0.662459	0.712397	1	0.947269
Q47537	0.407946	0.439205	1	0.939349

8.3.1. No MTC p<0.01

EvC

Names	**total**	**elements**
user_list1 user_list2 user_list3 user_list4	106	P0ABT2 P04982 P0AAG8 P23843 P0AC62 P77214 P0A9R4 P0AFH8 P04983 SH00003 P0ACB0 P0ABB4 P75797 P0A8G3 P00582 P08331 P0AFJ1 P0A6Q3 P0A817 P30860 P0ACD4 P63020 P02931 P45578 P68206 P24215 P0AE91 P0A6B7 P03841 P77243 P33362 P0AG80 P69783 P21179 P00490 P0AB77 P0AFM6 P0ADV7 Q46857 P0AE63 P76503 P76108 P25665 P16681 P0A7U7 P31802 P13482 P77239 P0AGD1 P09551 P77754 P0ABZ6 P0AC38 P33136 P33363 P25516 P07024 P64588 Q46871 P75691 P63284 P28861 P77541 P0A6Z1 P39325 P0ADE6 P30859 P0A867 P23893 P77581 P0C058 P76128 P37095 P0ACF8 P02925 P45464 P61889 P76177 P0A910 P0AEX9 P68679 P0ABK5 P69441 P39377 P45523 P52108 P16700 P0C0L2 P75694 P0AEU0 P0A9M8 P0A6F3 P09394 P45955 P0A6W5 P08997 P0AFG6 P0AEG4 P23847 P0A6Z3 P09546 P39099 P0A7E5 P0AG82 P0A6M8 P06986
user_list1 *user_list2* *user_list4*	*3*	*P0ABQ2 P0ABH9 P00968*
user_list1 user_list3 user_list4	1	P33602
user_list2 user_list3 user_list4	2	P0A7X3 P76116
user_list1 user_list4	3	P0ACA3 P0C8J8 P0A9A6
user_list1	1	P00448
user_list2	3	P0A8G6 P0A953 P0A805

EGvCG

Names	total	elements
user_list1 user_list2 user_list3 user_list4	95	P04982 P00370 P0AAG8 P77214 P0A9R4 P0AFH8 P04983 P21177 P16095 P0ABB4 P06999 P0A8G3 P0AAI3 P0AFJ1 P0ACD4 P63020 P31979 P02931 P33218 P0A8G6 P08660 P68206 P0A6B7 P69490 P0A8V2 P0A905 P77243 P33362 P0AG80 P21179 P21889 P0AFM6 P0ADV7 P33232 P15254 P09373 Q46857 P0AG30 P0AE63 P76503 P68191 P31802 P31660 P00448 P77239 P0AGD1 P77754 P69797 P0AC38 P25516 P64588 Q46871 P0AFZ1 P75691 P77541 P0A6Z1 P0A867 P64596 P0AE37 P0A9C5 P23893 P0AC59 P77581 P0C058 P76128 P37095 P33599 P0C8J8 P0A910 P0AEX9 P68679 P0ABK5 P69441 P39377 P45523 P35340 P52108 Q47537 P0C0L2 P16700 P75694 P09831 P77258 P0ABB0 P0A6F3 P00968 P60422 P33570 P08997 P17846 P0AEG4 P0A6Z3 P09546 P60438 P24232
user_list1 user_list2 user_list3	1	P0A6W5
user_list1 user_list2 user_list4	1	P00960
user_list1 user_list4	1	P0AB77
user_list2	2	P0A6Q3 P76217
user_list3	1	P0AD49
user_list4	2	P00961 P76585

8.3.1. No MTC p<0.05

EvC

P00448	1.254399	1.178013	1.075067	1
P00490	0.9155	0.931282	1.010753	1
P00582	1.134887	1.087249	1.004084	1
P00959	1.129937	1.151314	1.040999	1
P00968	1.086176	1.075247	0.997806	1
P02925	0.855004	0.818335	0.964069	1
P02931	1.846884	1.997327	1.041841	1
P03841	0.645739	0.644943	1.027746	1
P04982	1.333494	1.261984	0.939712	1
P04983	1.186677	1.314518	1.051792	1
P06610	0.64987	0.628696	0.963197	1
P06720	1.215036	1.132562	0.993576	1

P06986	0.798757	0.775702	0.974152	1
P07012	1.085391	1.081835	0.93877	1
P07024	0.762386	0.732605	1.013754	1
P08331	0.814819	0.788555	1.006771	1
P08997	1.465994	1.419428	1.0333	1
P09394	0.777942	0.764727	0.973885	1
P09424	0.839768	0.884266	1.0636	1
P09546	1.429449	1.50973	1.068854	1
P09551	0.854309	0.834076	0.990694	1
P0A6B7	0.521032	0.505209	1.00094	1
P0A6F3	1.159725	1.206628	0.985749	1
P0A6J5	1.404509	1.531392	1.107465	1
P0A6K6	0.937218	0.918548	0.980257	1
P0A6L9	0.610501	0.580046	1.023348	1
P0A6M8	0.927511	0.943098	0.993092	1
P0A6Q3	0.786859	0.79927	1.011655	1
P0A6W5	0.830569	0.824481	0.931122	1
P0A6X7	0.774478	0.801079	0.941561	1
P0A6Y1	0.85085	0.84039	1.006176	1
P0A6Z1	0.629936	0.628252	0.974867	1
P0A6Z3	1.200867	1.201516	0.953156	1
P0A7E5	1.130603	1.137117	0.995343	1
P0A7M2	1.118131	1.075283	0.982868	1
P0A7S9	0.867575	0.910455	0.986358	1
P0A7U7	0.83381	0.901366	1.071462	1
P0A7W1	0.778067	0.709814	0.845316	1
P0A7X3	0.896381	0.926479	1.061265	1
P0A805	0.874827	0.827716	0.985418	1
P0A817	1.172758	1.163325	0.978628	1
P0A855	0.7664	0.677328	0.938934	1
P0A867	0.766658	0.775726	0.962319	1
P0A8G3	1.311752	1.266935	0.939175	1
P0A8G6	0.889998	0.891732	1.040232	1
P0A8M3	1.070762	1.053025	1.010105	1
P0A8N5	1.084117	1.108039	0.921988	1
P0A8X2	0.789421	0.753537	1.077936	1
P0A905	0.744629	0.704209	1.179068	1
P0A910	0.498627	0.510194	0.986284	1
P0A953	0.906509	0.880555	0.978038	1
P0A991	0.820434	0.830809	0.977714	1
P0A9A6	1.112748	1.101346	1.010155	1
P0A9B6	1.278676	1.246817	0.996712	1
	0.675432	0.694744	1.011598	1
P0A9M8	1.137378	1.158284	1.001968	1
P0A9P4	1.104943	1.064658	0.992536	1
P0A9R4	0.498498	0.50154	1.04069	1

P0AAG8	1.337998	1.41003	1.035349	1
P0AAI3	1.380181	1.284501	1.065425	1
P0AAT6	0.868694	0.847874	1.042833	1
P0AB61	0.908838	0.899484	1.020676	1
P0AB65	0.786873	0.838752	1.026082	1
P0AB77	1.130813	1.081238	0.998742	1
P0ABB4	1.107147	1.104189	1.006008	1
P0ABD3	0.775052	0.813914	1.014109	1
P0ABH9	1.219101	1.17698	1.03188	1
P0ABK5	0.894408	0.864698	1.015911	1
P0ABQ2	1.226058	1.217727	0.959393	1
P0ABQ4	0.943456	0.876122	1.090147	1
P0ABT2	0.699207	0.629969	0.928206	1
P0ABZ6	0.873049	0.83932	1.011357	1
P0AC38	1.506754	1.557081	1.031148	1
P0AC62	0.643577	0.639083	0.892306	1
P0ACA3	1.153179	1.116713	0.961381	1
P0ACB0	1.23521	1.223958	1.030375	1
P0ACD4	0.537786	0.565413	0.97075	1
P0ACF0	0.840843	0.826546	0.922446	1
P0ACF8	0.811314	0.789261	0.909175	1
P0ACL2	1.260974	1.105108	0.970573	1
P0ACX3	0.908414	0.897608	1.079503	1
P0ADE6	0.845181	0.822526	1.017169	1
P0ADS6	0.785714	0.714273	0.997465	1
P0ADU5	0.352767	0.364189	1.042111	1
P0ADV7	0.62654	0.60333	1.062459	1
P0ADZ4	0.850917	0.862398	0.957428	1
P0AE63	0.814344	0.761119	1.02591	1
P0AE91	0.843383	0.784057	1.060444	1
P0AED0	0.905724	0.915852	0.976672	1
P0AEG4	0.779412	0.749923	1.055363	1
P0AEM4	1.294272	1.139883	0.993839	1
P0AEU0	0.668283	0.624995	1.000986	1
P0AEX9	0.670177	0.626637	0.944371	1
P0AF28	0.857282	0.893603	0.962181	1
P0AFG6	0.778083	0.785974	0.921988	1
P0AFH8	0.557244	0.509755	1.007412	1
P0AFI7	1.15676	1.208116	0.957056	1
P0AFJ1	0.759835	0.754524	1.016502	1
P0AFK9	0.795685	0.863025	1.070611	1
P0AFM6	1.565241	1.527767	0.997016	1
P0AFZ1	0.716746	0.562888	0.981126	1
P0AG40	1.102012	1.118968	0.96979	1
P0AG80	0.689457	0.611527	0.934184	1
P0AG82	0.821055	0.756955	1.011551	1

P0AGD1	0.584043	0.558514	1.081705	1
P0C054	1.490758	1.565984	0.912018	1
P0C058	2.771603	2.491401	0.921204	1
P0C0L2	0.771597	0.71917	1.047755	1
P0C8J8	1.131417	1.124861	1.023618	1
P13482	0.570921	0.625258	0.933751	1
P16456	1.090536	1.079805	0.948993	1
P16681	0.733887	0.747589	0.961916	1
P16700	0.683629	0.724794	1.11299	1
P19926	0.819456	0.786246	0.914261	1
P21179	0.724353	0.704369	0.932689	1
P21367	0.594501	0.492354	0.979427	1
P23538	1.068428	1.070009	1.014144	1
P23836	0.731838	0.862829	0.999514	1
P23843	0.891453	0.860584	0.99279	1
P23847	0.791184	0.784515	1.021963	1
P23869	0.907744	0.884453	0.975828	1
P23893	0.876713	0.871015	0.99176	1
P24178	0.863518	0.834673	1.003364	1
P24215	1.309505	1.238957	0.946916	1
P25516	0.769334	0.776576	0.938871	1
P25665	1.312784	1.272039	0.956172	1
P25738	0.740667	0.77161	1.017278	1
P27306	1.132181	1.200689	1.002358	1
P28861	0.763788	0.786229	1.041196	1
	0.831842	0.834043	1.014783	1
P30859	0.748066	0.736364	0.92294	1
P30860	0.764658	0.688023	1.064527	1
P31802	1.157321	1.243288	1.010122	1
P32144	1.274839	1.170909	1.02182	1
P33136	0.881308	0.903019	1.098603	1
P33362	0.667494	0.663287	0.952336	1
P33363	0.87773	0.886889	1.009291	1
P33570	0.831962	0.810203	0.977962	1
P33602	1.146591	1.147015	0.986838	1
	0.807369	0.714816	0.892792	1
P37051	1.111593	1.144924	1.011655	1
P37095	0.60613	0.649626	0.935574	1
P37689	1.282358	1.248425	1.081044	1
P39099	0.826895	0.826232	0.996633	1
P39325	0.733645	0.690421	1.007254	1
P39377	0.751243	0.751394	1.000518	1
P45464	0.731982	0.751034	0.958176	1
P45523	0.770564	0.784249	0.946164	1
P45578	0.892539	0.871275	0.992761	1
P45955	0.749436	0.800236	1.02852	1

P52108	0.688563	0.698529	1.131678	1
P60624	1.062341	1.078756	0.986737	1
P61517	1.233912	1.165527	0.986886	1
P61889	0.89544	0.845583	0.94669	1
P62707	0.921898	0.929652	0.974775	1
P63020	0.786304	0.754714	0.952036	1
P63284	1.238192	1.222193	1.003746	1
P64476	1.47776	1.527183	0.877269	1
P64588	0.57799	0.57058	1.145138	1
P68187	1.258108	1.294903	1.062682	1
P68206	0.508484	0.498739	0.859198	1
P68679	0.833479	0.869283	0.984795	1
P69441	0.782893	0.776519	0.927495	1
P69490	0.652647	0.567991	1.097856	1
P69783	0.815087	0.749302	0.95885	1
P69797	1.185377	1.147868	1.047392	1
P75691	0.688416	0.686319	1.052235	1
P75694	0.548618	0.47001	0.948327	1
P75797	0.806797	0.798295	0.964363	1
P76004	0.778665	0.807684	1.014278	1
P76108	0.579301	0.621368	1.046187	1
P76116	0.879105	0.879776	0.989109	1
P76128	0.698843	0.648978	1.09857	1
P76177	0.733308	0.785624	0.996523	1
P76503	1.287326	1.365087	1.011143	1
P76585	1.20335	1.144286	0.898262	1
P77214	0.44265	0.43158	1.009837	1
P77239	0.513658	0.526378	1.020934	1
P77243	0.639885	0.712855	1.000294	1
P77399	1.155646	1.188303	0.990479	1
P77499	1.228587	1.201045	1.060583	1
P77541	0.753962	0.751041	1.013849	1
P77581	0.785735	0.798094	1.132481	1
P77754	0.389937	0.36843	0.920091	1
Q46857	0.678939	0.648402	1.033671	1
Q46871	0.373279	0.319299	1.016696	1

Names	total	elements
user_list1 user_list2 user_list3 user_list4	173	P04982 P0C054 P23843 P0AC62 P77214 P0A9R4 P0AFK9 P0ABB4 P75797 P0A7X3 P08331 P0A6Q3 P77399 P63020 P27306 P02931 P37689 P0A8G6 P45578 P68187 P0A7S9 P69490 P0A7M2 P03841 P77243 P33362 P21179 P00490 P0AB61 P0AG40 P76004 P0ACF0 Q46857 P0AE63 P76108 P16681 P00448 P77239 P0AGD1 P77754 P69797 P0AED0 P33363 P07024 P64588 P0A953 P0AFI7 P75691 P77541 P39325 P0ADE6 P76585 P30859 P0A867 P23893 P0A805 P0A6X7 P77581 P0A6Y1 P76128 P0ACF8 P23869 P0A6K6 P0A6L9 P23538 P61889 P76177 P0AEX9 P0ACX3 P0ABK5 P69441 P52108 P16700 P0C0L2 P0A6F3 P25738 P0A6W5 P33602 P0AFG6 P06720 P0AEG4 P23847 P23836 P09546 P0A6Z3 P0AG82 P0A6M8 P06986 P0ABT2 P0A8N5 P0AAG8 P0A991 P64476 P0AFH8 P04983 SH00003 P0ACB0 P0A8G3 P19926 P00582 P0AAI3 P0ABQ2 P0ABQ4 P0AFJ1 P0A817 P0AEM4 P30860 P0ACD4 P0ADZ4 P0ACA3 P68206 P0A6B7 P0ADU5 P0AE91 P24215 P0A905 P0AG80 P69783 P0AB77 P0ADV7 P0AFM6 P0AB65 P0AAT6 P76503 SH00002 P0A7U7 P25665 P31802 P13482 P09551 P0ABZ6 P0AC38 P33136 P0ABH9 P25516 Q46871 P24178 P32144 P0AFZ1 P63284 P0A7W1 P28861 P0A6Z1 P06610 P0A855 P0A6J5 P0C058 P37095 P76116 P02925 P45464 P0ABD3 P0C8J8 P0A910 P68679 P39377 P45523 P0A9A6 P75694 P0AEU0 P0A9M8 P00968 P09394 P33570 P16456 P45955 P08997 P21367 P0A8X2 P09424 P39099 P0A7E5 P0ADS6
user_list1 user_list2 user_list3	1	P0AC69
user_list1 user_list2 user_list4	2	P61517 P07012
user_list1 user_list3 user_list4	3	P37051 P00959 P60624
user_list2 user_list3 user_list4	2	P0AF28 P62707
user_list1 user_list4	5	P0A9B6 P0ACL2 P0A8M3 P77499 P0A9P4
user_list1	2	P42593 P0A825
user_list2	7	P16095 P0AEP7 P0AA25 P12282 P21499 P0A850 P0AEU7
user_list3	1	P0ACF4

P00363	1	1.007273	0.722577	0.763277
P00370	1	1.003286	1.195792	1.569898
P00448	1	0.974512	0.795191	0.790243
P00909	1	0.961162	1.105199	1.200677
P00960	1	0.963347	0.87306	0.875532
P00961	1	1.056181	0.949301	0.918141
P00968	1	1.009989	1.071312	1.354351
P02931	1	0.926902	0.622678	0.605201
P03023	1	1.038809	1.180765	1.101333
P03841	1	1.013475	1.371312	1.130096
P04036	1	0.887204	1.17858	1.227654
P04982	1	1.03381	0.774747	0.802628
P04983	1	1.022114	0.826474	0.822723
P06149	1	0.970806	1.071321	1.077997
P06988	1	0.947884	1.07647	1.10919
P06999	1	0.972788	1.105911	1.13053
P08660	1	0.806225	1.579898	2.196234
P08997	1	1.033534	0.789901	0.770309
P09373	1	0.935734	1.20309	1.229006
P09546	1	1.097103	0.794979	0.737294
P09551	1	1.010641	1.085964	1.138222
P09831	1	1.001397	1.098933	1.463652
P0A6B4	1	0.996042	0.901629	0.875938
P0A6B7	1	1.097887	2.142049	2.285163
P0A6F3	1	1.045522	0.908391	0.88831
P0A6J5	1	1.028853	0.775206	0.752656
P0A6L9	1	0.937035	1.589162	1.560875
P0A6P1	1	1.031978	1.085236	1.075159
P0A6Q3	1	0.993916	1.092618	1.082107
P0A6W5	1	0.996234	1.066907	1.097363
P0A6Z1	1	1.004848	1.772948	1.709612
P0A6Z3	1	0.991814	0.867106	0.824433
P0A799	1	0.941708	1.07599	1.134508
P0A7J3	1	1.002117	0.915984	0.882746
P0A7K6	1	1.001365	0.888395	0.905594
P0A7L0	1	0.995792	0.904685	0.893364
P0A7R1	1	0.999381	0.903233	0.912124
P0A817	1	0.934809	0.81407	0.878218
P0A867	1	1.033308	1.307632	1.199741
P0A8G3	1	0.967028	0.777815	0.779325
P0A8G6	1	1.024314	1.180355	1.138746
P0A8J4	1	0.915377	0.682313	0.693835
P0A8N5	1	1.076444	0.950976	0.940746
P0A8V2	1	1.033908	0.930567	0.924638

P0A905	1	1.093088	1.792002	1.858613
P0A910	1	1.082218	1.703784	1.53637
P0A991	1	1.047231	1.169338	1.277952
P0A9A6	1	1.055155	0.888616	0.885979
P0A9C5	1	0.939696	1.080434	1.37064
P0A9M0	1	1.01467	0.95445	0.925431
P0A9R4	1	1.070038	2.073581	2.060193
P0AA86	1	1.170792	2.248142	2.572144
P0AAB6	1	0.92678	0.834944	0.860424
P0AAG8	1	0.99386	0.787366	0.772989
P0AAI3	1	1.099478	0.804606	0.818136
	1	1.077645	0.729368	0.649392
P0AB40	1	1.020773	0.700511	0.596681
P0AB77	1	0.976884	0.92868	0.894229
P0ABA4	1	0.995454	0.841055	0.889918
P0ABB0	1	1.021689	0.910039	0.933043
P0ABB4	1	0.993327	0.798491	0.840734
P0ABK5	1	0.951177	1.122966	1.062694
P0ABM9	1	1.197775	3.402123	3.718618
P0AC38	1	0.994272	0.682341	0.648377
P0AC41	1	1.133562	0.908064	0.917227
P0AC55	1	0.971199	1.258213	2.63453
P0AC59	1	0.91608	1.216132	1.314471
P0AC69	1	1.116977	1.471449	1.43171
P0ACC3	1	0.957661	1.177757	1.213402
P0ACD4	1	1.104682	2.367168	2.569853
P0ACF0	1	0.898796	1.168662	1.078547
P0ACF8	1	0.942348	1.09228	1.059434
P0ACW6	1	0.978084	0.878759	0.816218
P0ACZ8	1	0.917046	1.204613	1.343209
P0AD49	1	0.950761	1.250953	1.143624
P0ADE8	1	1.043519	0.925683	0.930369
P0ADS6	1	1.02698	1.099168	1.161317
P0ADU5	1	0.959318	1.725337	1.392224
P0ADV7	1	0.915004	1.561366	1.32133
P0AE37	1	1.077992	1.475107	1.450803
P0AE63	1	0.981296	1.245615	1.220793
P0AE85	1	0.961833	1.516972	1.28757
P0AEG4	1	0.955868	1.297484	1.418558
P0AEU0	1	0.94746	1.180518	1.217502
P0AEX9	1	1.022039	1.389495	1.147912
P0AFC7	1	0.977819	0.755345	0.74702
P0AFH8	1	1.059403	1.62514	1.387454
P0AFJ1	1	0.923134	1.190655	1.19509
P0AFM6	1	0.952832	0.679738	0.626294
P0AFZ1	1	0.951157	1.961748	1.933084

P0AG30	1	0.986288	0.889174	0.885591
P0AG80	1	1.01909	1.343795	1.150088
P0AG84	1	0.945117	1.355582	1.188105
P0AGD1	1	0.955617	1.471518	1.316282
P0C054	1	0.957607	0.609527	0.576419
P0C058	1	0.988028	0.444198	0.426164
P0C0L2	1	0.99448	1.328872	1.337222
P0C8J8	1	1.059276	0.817239	0.860666
P15254	1	0.936469	1.146691	1.38098
P15640	1	0.931999	1.084214	1.44555
P16095	1	0.984992	1.245589	1.202351
P16659	1	1.017219	0.931021	0.909938
P16700	1	0.984015	1.365952	1.280224
P17846	1	1.017219	1.215082	1.120646
P21177	1	1.035599	0.867523	0.795772
P21179	1	1.136756	1.411357	1.348829
P21889	1	0.987199	0.888416	0.879345
P22333	1	0.953086	0.892532	0.837548
P23836	1	0.935678	1.220803	1.187649
P23893	1	0.991875	1.164811	1.172982
P24232	1	0.999383	1.49822	1.56231
P25516	1	1.018126	1.24637	1.141051
P25526	1	1.034318	1.389608	1.232349
P25738	1	0.964764	1.287011	1.22025
P27302	1	0.975329	0.926139	0.904543
P28304	1	0.84219	1.118271	1.099287
P31660	1	1.083845	1.280291	1.169975
P31802	1	1.06035	0.815836	0.780549
P31828	1	0.93387	0.664269	0.611486
P31979	1	1.059609	0.866374	0.817686
P33218	1	0.968002	1.345067	1.473347
P33232	1	1.059689	0.665355	0.616809
P33362	1	1.040082	1.322677	1.263234
P33570	1	0.954497	1.246847	1.141304
P33599	1	1.023262	0.881242	0.847251
P33602	1	0.921217	0.814657	0.760358
P35340	1	0.975123	0.846436	0.881925
P37095	1	1.009936	1.763371	1.588439
P39377	1	1.033474	1.669346	1.891937
P45523	1	0.91	1.18113	1.09074
P45799	1	1.023762	0.862948	0.896992
P52108	1	0.928446	1.36005	1.5178
P60422	1	1.00398	1.196173	1.120102
P60438	1	0.917729	0.81028	0.808744
P60546	1	0.954424	0.898124	0.895659
P61175	1	0.993583	0.921072	0.927364

P62620	1	0.949259	1.04509	1.123133
P63020	1	1.069956	1.431705	1.37522
P64455	1	0.992255	1.218969	1.170672
P64588	1	1.073151	1.992156	1.897465
P64596	1	1.084499	0.820969	0.873235
P68191	1	0.875979	1.166298	1.218794
P68206	1	1.026078	1.806196	1.48112
P68679	1	0.923691	1.136842	1.15343
P68767	1	1.033527	1.129905	1.136218
P69441	1	0.960842	1.113925	1.097358
P69490	1	1.058022	2.378027	2.657074
P69797	1	0.966346	0.819156	0.840722
P75691	1	1.050237	1.366207	1.258021
P75694	1	1.023186	1.611272	1.310055
P76128	1	1.031173	1.417591	1.304053
P76215	1	1.01571	1.230805	1.339619
P76216	1	1.021689	1.31808	1.308442
P76217	1	1.034543	1.34189	1.324896
P76503	1	1.02848	0.812951	0.712933
P76585	1	1.043317	0.878683	0.866663
P77202	1	0.946239	1.125757	1.121275
P77211	1	1.024341	1.310181	1.315889
P77214	1	0.940118	1.58235	1.688527
P77239	1	1.004951	1.789047	1.633271
P77243	1	1.042862	1.506707	1.288469
P77258	1	1.011275	0.59546	0.561051
P77541	1	1.016242	1.266186	1.182448
P77581	1	1.047754	1.27736	1.284457
P77674	1	1.04215	1.315891	1.209568
P77754	1	1.017488	2.37743	1.875388
P77774	1	1.028359	0.905997	0.930654
Q46851	1	1.056388	0.910915	0.866256
Q46857	1	0.984793	1.303333	1.179721
Q46871	1	1.120204	2.689245	2.205477
Q47537	1	0.939349	0.759541	0.656198

Names	total	elements
user_list1 user_list2 user_list3 user_list4	165	P04982 P0C054 P0ADE8 P77214 P0A9R4 P21177 P16095 P0ABB4 P06999 P76215 P68767 P0A6Q3 P0AB40 P00961 P63020 P0A7L0 P45799 P31979 P02931 P0AC41 P0A8G6 P00960 P69490 P03841 P0A8V2 P77243 P33362 P04036 P21179 P21889 P0ACF0 Q46857 P0A7K6 P0AE63 P76217 P00448 P0AA86 P77239 P0AGD1 P77754 P69797 P28304 P0AC69 P64588 P0AG84 P75691 P77541 P76585 P0A867 P64596 P23893 P16659 P77581 P76128 P0A6L9 P33599 P06988 P0AEX9 P0ABK5 P69441 P35340 P52108 Q47537 P16700 P0C0L2 P0ABM9 P09831 P0A6F3 P25738 P0A6W5 P33602 P0A7R1 P60546 P0ABA4 P0AEG4 P23836 P0AFC7 P09546 P0A6Z3 P77211 P60438 P00370 P0A8N5 P0AAG8 P0A991 P0AFH8 P25526 P04983 SH00003 P0A8G3 P0AAI3 P62620 P0AFJ1 P15640 P0A817 P0ACD4 P00363 P0AAB6 P33218 P08660 P76216 P68206 P0A6B7 P0ADU5 P0AC55 P0A905 P0A7J3 P0AG80 P0ACC3 P0AB77 P0ADV7 P0AFM6 P33232 P09373 P15254 P0AG30 P64455 P76503 P68191 P0AD49 P0AE85 P31660 P31802 P0A8J4 P09551 P0AC38 P77202 P25516 P0A799 Q46871 P0AFZ1 P03023 P22333 P27302 P0A6Z1 P0A9M0 Q46851 P0AE37 P0A9C5 P0AC59 P0ACW6 P0A6J5 P0C058 P37095 P61175 P31828 P0C8J8 P0A910 P68679 P39377 P45523 P00909 P0A9A6 P75694 P77258 P0ABB0 P0AEU0 P00968 P77674 P60422 P33570 P08997 P17846 P0ADS6 P24232
user_list1 user_list2 user_list3	4	P0ACF8 P06149 P0ACZ8 P0A6P1
user_list1 user_list3 user_list4	2	P77774 P0A6B4
user_list2	2	P75797 P69783
user_list3	4	P69506 P32131 P76108 P0AB65
user_list4	7	P77737 P0A6J8 P0A6F5 P00957 P0ABQ2 P38489 P77499

Names	total	elements
user_list1 user_list2 user_list3 user_list4	199	P04982 P0ADE8 P05793 P77214 P0AG63 P69506 P00963 P0A7X3 P08331 P0AB40 P10408 P0A8T7 P0AEZ1 P02924 P02931 P0AB91 P0A7D4 P0AFR4 P37689 P0A8G6 Q8EG35 P0AG78 P77739 P0A6T1 P76097 P69490 P03841 P05020 P0A8V2 P33362 P69811 P0AB80 P05055 P25553 P31142 P18843 Q46857 P40120 P00452 P76108 P00448 P77239 P0AGE0 P0AGD1 P0A6H1 P77754 P21170 P64503 P21156 P0AGD3 P33363 P07024 P23845 P0AFI7 P75691 P77541 P0ADS9 P0ABU2 P39325 P0ADE6 P0AC53 P30859 P76128 P30850 P0A9Q7 P0A6P9 P22106 P0A9W9 P06988 P0AEX9 P0A8M3 P0A879 P00864 P0ABK5 P0AB89 P05791 P35340 P0AES4 Q47537 P16700 P0AFG8 P09831 P0AC33 P0A877 P0ADG7 P00935 P0A9B2 P39187 P0AFC7 P09832 P0AG82 P0A8Y5 P0ABT2 P00370 P00562 P0A9T0 P69828 P64476 P0AFH8 P04983 P0AGL2 P00934 P19926 P17993 P04805 P00582 P06959 P0AAI3 P08312 P15640 P38489 P25888 P0A817 P08839 P23721 P30860 P0ACD4 P0ADZ4 P33218 P08660 P07813 P0A6B7 P0AE91 P0AC55 P0AG80 P69783 P77625 P00579 P37610 P0A705 P0AB77 P0AES6 P0AFM6 P15254 P09373 P0A6F1 A5A614 P22259 P0A912 P25665 P0A7U7 P68191 P0A7U3 P77395 P09551 P27248 P0AD96 P21499 P0A799 P04816 P0ACR9 P63284 P28861 P03023 P27302 P22333 Q2M7R5 P76193 P00547 P0AE37 P0A9C5 P0AC59 P0ACW6 P0A6P1 P0A9M5 P76116 P02925 P45464 P0C8J8 P00956 P39377 P0AA16 P00909 P0A9Q1 P0AB71 P0A9J8 P75694 P0AB52 P0ABB0 P0AEU0 P00393 P00968 P0A9M8 P09394 P16456 P0A7D7 P0AEU7 P0A8X0 P32695 P0A9Q9 P08178 P00561 P09424 P28904 P39099 P0A7E5 P07395 P68066 P24232
user_list1 user_list2 user_list3	1	P0AC41
user_list1 user_list3 user_list4	2	P0ACF4 P02359
user_list1 user_list3	3	P0C0L2 P0AEZ3 P26646
user_list1	1	P77581
user_list2	3	P0A6L2 P28635 P0AFI2
user_list4	1	P69924

CvCG

Names	total	elements
user_list1 user_list2 user_list3 user_list4	145	P04982 P42593 P23843 P05793 P16095 P0ABB4 P69506 P0A796 P00963 P08331 P0A6Q3 P0AB40 P0A8T7 P0C0V0 P02924 P02931 P0AB91 P37689 P0A8G6 P0AG78 P0A761 P0A7M2 P0A8V2 P69811 P0A884 P05055 P21889 P0A6F5 P0A7K6 P0A7G6 P0A9L5 P00448 P0A6H1 P0AED0 P64503 P21156 P0A7Z4 P23845 P0AFG0 P39325 P0AC53 P30850 P0A9Q7 P0A6P9 P22106 P0A9W9 P76177 P0A8M3 P00864 P0A879 P0A6A3 P0ABK5 P05791 P69441 P35340 Q47537 P16700 P0AFG8 P09831 P0AC33 P0A877 P0ADG7 P39187 P0AEZ3 P0AFG6 P0ABA4 P23847 P09832 P0A6Z3 P06986 P0A8Y5 P0A9T0 P69828 P04983 P00934 P19926 P06959 P28635 P00904 P0A817 P08839 P04968 P23721 P0A9L3 P0AG80 P69783 P77625 P00579 P37610 P0AB77 P0AE08 P0AFM6 P09373 A5A614 P22259 P0ACB2 P0A6T9 P0A912 P25665 P68191 P00509 P60716 P0A7U3 P09551 P27248 P0AC38 P0A870 P0A799 P17854 P21499 P04816 P22333 P27302 P0A6A6 P00547 P0AE37 P0A9C5 P0ACW6 P0AFF6 P0A6P1 P0C058 P02925 P45464 P0A836 P0C8J8 P0A910 P0A9P0 P39377 P0AA16 P77735 P00909 P0A6D3 P77258 P0A850 P0ABB0 P00393 P00968 P0A9M8 P09394 P16456 P08997 P00561 P37330 P0ADS6 P24232
user_list1 user_list2 user_list3	1	P32132
user_list1 user_list2 user_list4	2	P0AG44 P24215
user_list1 user_list3 user_list4	1	P06720
user_list1 user_list4	2	P60624 P76015
user_list2	1	P0ABA0
user_list3	7	P02358 P0A8L1 P76422 Q8EG35 P0A6T1 P0A953 P0AEE1
user_list4	2	P77754 P06149

References

1. Buchholz, K. & Collins, J. The roots-a short history of industrial microbiology and biotechnology. *Appl. Microbiol. Biotechnol.* **97,** 3747–3762 (2013).

2. McLaughlin, D. & Kinzelbach, W. Water Resources Research. *Water Resour. Res.* **51,** 4966–4985 (2014).

3. Bajracharya, S. *et al.* An overview on emerging bioelectrochemical systems (BESs): Technology for sustainable electricity, waste remediation, resource recovery, chemical production and beyond. *Renew. Energy* **98,** 153–170 (2016).

4. Guo, K. W. Green nanotechnology of trends in future energy: a review. *Int. J. ENERGY Res.* **36,** 1–17 (2012).

5. Schroeder, U. Discover the possibilities: microbial bioelectrochemical systems and the revival of a 100-year-old discovery. *J. SOLID STATE Electrochem.* **15,** 1481–1486 (2011).

6. Rachinski, S., Carubelli, A., Mangoni, A. P. & Mangrich, A. S. MICROBIAL FUEL CELLS USED IN THE PRODUCTION OF ELECTRICITY FROM ORGANIC WASTE: A PERSPECTIVE OF FUTURE. *Quim. Nova* **33,** 1773–1778 (2010).

7. Richter, K., Schicklberger, M. & Gescher, J. Dissimilatory reduction of extracellular electron acceptors in anaerobic respiration. *Appl. Environ. Microbiol.* **78,** 913–21 (2012).

8. Venkateswaran, K. *et al.* Polyphasic taxonomy of the genus Shewanella and description of Shewanella oneidensis sp. nov. *Int. J. Syst. Bacteriol.* **49,** 705–724 (1999).

9. Lovley, D. R. DISSIMILATORY METAL REDUCTION. *Annu. Rev. Microbiol.* **47,** 263–290 (1993).

10. Rosenbaum, M., Aulenta, F., Villano, M. & Angenent, L. T. Cathodes as electron donors for microbial metabolism: which extracellular electron transfer mechanisms are involved? *Bioresour. Technol.* **102,** 324–33 (2011).

11. Zhang, X., Porcu, L. & Andresen, J. M. Sustainable energy from dairy farm waste using a Microbial Fuel Cell (MFC). in *World Renewable Energy Congress - Sweden* 247–250 (2011).

12. Logan, B. E. Scaling up microbial fuel cells and other bioelectrochemical systems. *Appl. Microbiol. Biotechnol.* **85,** 1665–1671 (2010).

13. WERF. *Energy Production and Efficiency Research – The Roadmap to Net-Zero Energy*. (2011).

14. Roy, S., Schievano, A. & Pant, D. Electro-stimulated Microbial Factory for value added product synthesis. *Bioresour. Technol.* (2016). doi:10.1016/j.biortech.2016.03.052

15. Oliveira, V. B., Simões, M., Melo, L. F. & Pinto, a. M. F. R. Overview on the developments of microbial fuel cells. *Biochem. Eng. J.* **73,** 53–64 (2013).

16. Recio-Garrido, D., Perrier, M. & Tartakovsky, B. Modeling, optimization and control of bioelectrochemical systems. *Chem. Eng. J.* **289,** 180–190 (2016).

17. Kumar, G. G., Sarathi, V. G. S. & Nahm, K. S. Recent advances and challenges in the anode architecture and their modifications for the applications of microbial fuel cells. *Biosens. Bioelectron.* **43,** 461–75 (2013).

18. Rosenbaum, M. A. & Franks, A. E. Microbial catalysis in bioelectrochemical technologies: Status quo, challenges and perspectives. *Appl. Microbiol. Biotechnol.* **98,** 509–518 (2014).

19. Becker, A. Synthetic biology changing the face of biotechnology. *J. Biotechnol.* **169,** iii (2014).

20. Kwok, R. Five hard truths for synthetic biology. *Nature* **463,** 288–290 (2010).

21. Seo, S. W. *et al.* Synthetic biology: tools to design microbes for the production of chemicals and fuels. *Biotechnol. Adv.* **31,** 811–7 (2013).

22. Jinlian, M., Chen, M., Jia, T., Shungui, Z. & Li, Z. Mechanisms and Applications of Electron Shuttle-Mediated Extracellular Electron Transfer. *Prog. Chem.* **27,** 1833–1840 (2015).

23. TerAvest, M. A. & Ajo-franklin, C. M. Transforming exoelectrogens for biotechnology using synthetic biology. *Biotechnol. Bioeng.* **113,** 687–697 (2016).

24. Jaffe, S. Metabolic engineering for increased electrogenic activity and bioenergy production. (2014).

25. Arends, J. B. a & Verstraete, W. 100 Years of Microbial Electricity Production: Three Concepts for the Future. *Microb. Biotechnol.* **5,** 333–46 (2012).

26. Jaffe, S. R. P. Metabolic engineering for increased electrogenic activity and bioenergy production. (2014).

27. Goldbeck, C. *et al.* Tuning Promoter Strengths for Improved Synthesis and Function of Electron Conduits in Escherichia coli. *ACS Synth. …* **2,** 150–9 (2013).

28. Jensen, H., TerAvest, M., Kokish, M. & Ajo-franklin, C. M. CymA and exogenous flavins improve extracellular electron transfer and couple it to cell growth in Mtr-expressing Escherichia coli CymA and exogenous flavins improve extracellular electron transfer and couple it to cell growth in Mtr-expressing Escherichi. *ACS Synth. Biol.* **5,** 679–688 (2016).

29. Schneider, G., Kovács, T., Rákhely, G. & Czeller, M. Biosensoric potential of microbial fuel cells. *Appl. Microbiol. Biotechnol.* **100,** 7001–7009 (2016).

30. Su, L., Jia, W., Hou, C. & Lei, Y. Microbial biosensors: a review. *Biosens. Bioelectron.* **26,** 1788–99 (2011).

31. Golitsch, F., Bücking, C. & Gescher, J. Proof of principle for an engineered microbial biosensor based on Shewanella oneidensis outer membrane protein complexes. *Biosens. Bioelectron.* **47,** 285–91 (2013).

32. Terpe, K. Overview of bacterial expression systems for heterologous protein production: From molecular and biochemical fundamentals to commercial systems. *Appl. Microbiol. Biotechnol.* **72,** 211–222 (2006).

33. Ragauskas, A. J. *et al.* The path forward for biofuels and biomaterials. *Science* **311,** 484–9 (2006).

34. Green, C., Baksi, S. & Dilmaghani, M. Challenges to a climate stabilizing energy future. *Energy Policy* **35,** 616–626 (2007).

35. Du, Z., Li, H. & Gu, T. A state of the art review on microbial fuel cells: A promising technology for wastewater treatment and bioenergy. *Biotechnol. Adv.* **25,** 464–82 (2007).

36. Lovley, D. R. Live wires: direct extracellular electron exchange for bioenergy and the bioremediation of energy-related contamination. *Energy Environ. Sci.* **4,** 4896 (2011).

37. Desloover, J., Arends, J. B. a, Hennebel, T. & Rabaey, K. Operational and technical considerations for microbial electrosynthesis. *Biochem. Soc. Trans.* **40,** 1233–8 (2012).

38. Webster, D. P. *et al.* Biosensors and Bioelectronics An arsenic-speci fi c biosensor with genetically engineered Shewanella oneidensis in a bioelectrochemical system. *Biosens. Bioelectron.* **62,** 320–324 (2014).

39. Bullen, R. A., Arnot, T. C., Lakeman, J. B. & Walsh, F. C. Biofuel cells and their development. *Biosens. Bioelectron.* **21,** 2015–45 (2006).

40. Kim, H. J. *et al.* A mediator-less microbial fuel cell using a metal reducing bacterium, Shewanella putrefaciens. *Enzyme Microb. Technol.* **30,** 145–152

(2002).

41. Logan, B. E. *et al.* Microbial fuel cells: methodology and technology. *Environ. Sci. Technol.* **40,** 5181–5192 (2006).

42. Zhang, X., Cheng, S., Liang, P., Huang, X. & Logan, B. E. Scalable air cathode microbial fuel cells using glass fiber separators, plastic mesh supporters, and graphite fiber brush anodes. *Bioresour. Technol.* **102,** 372–5 (2011).

43. Liu, H. & Logan, B. E. Electricity generation using an air-cathode single chamber microbial fuel cell in the presence and absence of a proton exchange membrane. *Environ. Sci. Technol.* **38,** 4040–6 (2004).

44. Jiang, D. *et al.* A pilot-scale study on utilizing multi-anode/cathode microbial fuel cells (MAC MFCs) to enhance the power production in wastewater treatment. *Int. J. Hydrogen Energy* **36,** 876–884 (2011).

45. Rabaey, K. & Verstraete, W. Microbial fuel cells: novel biotechnology for energy generation. *Trends Biotechnol.* **23,** 291–8 (2005).

46. Pocaznoi, D., Erable, B., Etcheverry, L., Delia, M.-L. & Bergel, A. Towards an engineering-oriented strategy for building microbial anodes for microbial fuel cells. *Phys. Chem. Chem. Phys.* **14,** 13332–43 (2012).

47. Ghasemi, M. *et al.* Nano-structured carbon as electrode material in microbial fuel cells: A comprehensive review. *J. Alloys Compd.* **580,** 245–255 (2013).

48. Ye, D. *et al.* Performance of a microfluidic microbial fuel cell based on graphite electrodes. *Int. J. Hydrogen Energy* **38,** 15710–15715 (2013).

49. Rabaey, K., Angenent, L., Schroder, U. & Keller, J. *Bioelectrochemical Systems: From Extracellular Electron Transfer to Biotechnological Application*. (IWA Publishing, Lodon., 2009).

50. Narayanan, K. B. & Sakthivel, N. Biological synthesis of metal nanoparticles by

microbes. *Adv. Colloid Interface Sci.* **156,** 1–13 (2010).

51. Tan, L. C., Nancharaiah, Y. V, van Hullebusch, E. D. & Lens, P. N. L. Selenium: environmental significance, pollution, and biological treatment technologies. *Biotechnol. Adv.* **34,** 886–907 (2016).

52. Faria, A. *et al.* Resources recovery in the dairy industry: bioelectricity production using a continuous microbial fuel cell. *J. Clean. Prod.* **140,** 971–976 (2017).

53. Hernandez-Fernandez, F. J. *et al.* Recent progress and perspectives in microbial fuel cells for bioenergy generation and wastewater treatment. *FUEL Process. Technol.* **138,** 284–297 (2015).

54. Wei, J., Liang, P. & Huang, X. Recent progress in electrodes for microbial fuel cells. *Bioresour. Technol.* **102,** 9335–44 (2011).

55. Yen, S. J. *et al.* The improvement of catalytic efficiency by optimizing Pt on carbon cloth as a cathode of a microbial fuel cell. *Electrochim. Acta* **108,** 241–247 (2013).

56. Guo, W., Pi, Y., Song, H., Tang, W. & Sun, J. Layer-by-layer assembled gold nanoparticles modified anode and its application in microbial fuel cells. *Colloids Surfaces A Physicochem. Eng. Asp.* **415,** 105–111 (2012).

57. Eduok, S. *et al.* Evaluation of engineered nanoparticle toxic effect on wastewater microorganisms: current status and challenges. *Ecotoxicol. Environ. Saf.* **95,** 1–9 (2013).

58. Park, S. Regulatory ecotoxicity testing of engineered nanoparticles: are the results relevant to the natural environment? *Nanotoxicology* **8,** 583–592 (2014).

59. Mathuriya, A. S. Inoculum selection to enhance performance of a microbial fuel cell for electricity generation during wastewater treatment. *Environ. Technol.* **34,** 1957–1964 (2013).

60. Shi, L., Squier, T. C., Zachara, J. M. & Fredrickson, J. K. Respiration of metal (hydr)oxides by Shewanella and Geobacter: a key role for multihaem c-type cytochromes. *Mol. Microbiol.* **65,** 12–20 (2007).

61. Lovely, D. R. & Phillips, E. J. P. Novel mode of microbial energy metabolism: Organic carbon oxidation coupled to dissimilatory reduction of iron or manganese. *Appl. Environ. Microbiol.* **54,** 1472–1480 (1988).

62. Myers, C. R. & Nealson, K. H. Bacterial manganese reduction and growth with manganese oxide as the sole electron acceptor. *Science (80-.).* **240,** 1319–1321 (1988).

63. Debabov, V. G. Electricity from microorganisms. *Microbiology* **77,** 123–131 (2008).

64. Sikora, A. *et al.* Selection of bacteria capable of dissimilatory reduction of Fe (III) from a long-term continous culture on molasses and their use in a microbial fuel cell. *J. Microbiol. Biotechnol.* **21,** 305–316 (2011).

65. Logan, B. E. Essential data and techniques for conducting microbial fuel cell and other types of bioelectrochemical system experiments. *ChemSusChem* **5,** 988–94 (2012).

66. Kannaiah Goud, R. & Mohan, S. V. Prolonged applied potential to anode facilitate selective enrichment of bio-electrochemically active Proteobacteria for mediating electron transfer: microbial dynamics and bio-catalytic analysis. *Bioresour. Technol.* **137,** 160–70 (2013).

67. Chae, K.-J., Choi, M.-J., Lee, J.-W., Kim, K.-Y. & Kim, I. S. Effect of different substrates on the performance, bacterial diversity, and bacterial viability in microbial fuel cells. *Bioresour. Technol.* **100,** 3518–25 (2009).

68. Jung, S. & Regan, J. M. Comparison of anode bacterial communities and performance in microbial fuel cells with different electron donors. *Appl.*

Microbiol. Biotechnol. **77,** 393–402 (2007).

69. Hou, H., Li, L., Cho, Y., Figueiredo, P. De & Han, A. A MICROFABRICATED MICROBIAL FUEL CELL ARRAY FOR HIGH THROUGHPUT SCREENING (HTS) OF ELECTRICITY. 1191–1194 (2010).

70. Gil, G. *et al.* Operational parameters affecting the performannce of a mediator-less microbial fuel cell. *Biosens. Bioelectron.* **18,** 327–334 (2003).

71. Logan, B. E. *Microbial Fuel Cells*. (John Wiley & Sons, 2008).

72. Richter, H., Lanthier, M., Nevin, K. P. & Lovley, D. R. Lack of electricity production by Pelobacter carbinolicus indicates that the capacity for Fe(III) oxide reduction does not necessarily confer electron transfer ability to fuel cell anodes. *Appl. Environ. Microbiol.* **73,** 5347–53 (2007).

73. Velasquez-Orta, S. B. *et al.* The effect of flavin electron shuttles in microbial fuel cells current production. *Appl. Microbiol. Biotechnol.* **85,** 1373–81 (2010).

74. Nevin, K. P. & Lovley, D. R. Mechanisms for Fe(III) Oxide Reduction in Sedimentary Environments. *Geomicrobiol. J.* **19,** 141–159 (2002).

75. von Canstein, H., Ogawa, J., Shimizu, S. & Lloyd, J. R. Secretion of flavins by Shewanella species and their role in extracellular electron transfer. *Appl. Environ. Microbiol.* **74,** 615–23 (2008).

76. Coursolle, D. P. Characterization of the Mechanisms used to Reduce Anaerobic Electron Acceptors by Shewanella oneidensis strain MR-1. (2010).

77. Okamoto, A. Rate enhancement of bacterial extracellular electron transport involves bound flavin semiquinones. *Proc. …* **110,** 7856–61 (2013).

78. Clarke, T. A. *et al.* Structure of a bacterial cell surface decaheme electron conduit. *J. Mater. Civ. Eng.* **26,** 152–159 (2014).

79. Coursolle, D., Baron, D. B., Bond, D. R. & Gralnick, J. A. The Mtr respiratory

pathway is essential for reducing flavins and electrodes in Shewanella oneidensis. *J. Bacteriol.* **192,** 467–474 (2010).

80. Buecking, C., Popp, F., Kerzenmacher, S. & Gescher, J. Involvement and specificity of Shewanella oneidensis outer membrane cytochromes in the reduction of soluble and solid-phase terminal electron acceptors. *FEMS Microbiol. Lett.* **306,** 144–151 (2010).

81. Meyer, T. *et al.* Identification of 42 possible cytochrome C genes in the Shewanella oneidensis genome and characterization of six soluble cytochromes. *Omi. J. Integr. Biol.* **8,** 57–77 (2004).

82. Breuer, M., Rosso, K. M., Blumberger, J. & Butt, J. N. Multi-haem cytochromes in Shewanella oneidensis MR-1: Structures, functions and opportunities. *J. R. Soc. Interface* **12,** (2015).

83. Church, W., Mandel, N., Mandel, G., Kallai, B. & Trus, B. L. Tuna Cytochrome c at 2.0 Angstrom Resolution. *J. Biol. Chem.* **252,** 776–785 (1976).

84. Smith, L. J., Kahraman, A. & Thornton, J. M. Heme proteins-diversity in structural characteristics, function, and folding. *Proteins Struct. Funct. Bioinforma.* **78,** 2349–2368 (2010).

85. Sharma, S., Cavallaro, G. & Rosato, A. A systematic investigation of multiheme c-type cytochromes in prokaryotes. *J. Biol. Inorg. Chem.* **15,** 559–571 (2010).

86. Heidelberg, J. F. *et al.* Genome sequence of the dissimilatory metal ion-reducing bacterium Shewanella oneidensis. *Nat. Biotechnol.* **20,** 1118–1123 (2002).

87. Shi, L., Squier, T. C., Zachara, J. M. & Fredrickson, J. K. Respiration of metal (hydr)oxides by Shewanella and Geobacter: a key role for multihaem c-type cytochromes. *Mol. Microbiol.* **65,** 12–20 (2007).

88. Okamoto, A., Nakamura, R. & Hashimoto, K. In-vivo identification of direct electron transfer from Shewanella oneidensis MR-1 to electrodes via outer-

membrane OmcA–MtrCAB protein complexes. *Electrochim. Acta* **56,** 5526–5531 (2011).

89. White, G. F. *et al.* Rapid electron exchange between surface-exposed bacterial cytochromes and Fe(III) minerals. *Proc. Natl. Acad. Sci. U. S. A.* **110,** 6346–51 (2013).

90. Johs, A., Shi, L., Droubay, T., Ankner, J. F. & Liang, L. Characterization of the decaheme c-type cytochrome OmcA in solution and on hematite surfaces by small angle x-ray scattering and neutron reflectometry. *Biophys. J.* **98,** 3035–43 (2010).

91. Cai, P.-J. *et al.* Involvement of c-type cytochrome CymA in the electron transfer of anaerobic nitrobenzene reduction by Shewanella oneidensis MR-1. *Biochem. Eng. J.* **68,** 227–230 (2012).

92. Reyes, C. *et al.* Characterization of axial and proximal histidine mutations of the decaheme cytochrome mtra from shewanella sp. Strain ANA-3 and implications for the electron transport system. *J. Bacteriol.* **194,** 5840–5847 (2012).

93. Lovley, D. *et al.* Geobacter: the microbe electric's physiology, ecology, and practical applications. *Adv. Microb. Physiol.* **59,** 1–100 (2011).

94. Reguera, G. *et al.* Extracellular electron transfer via microbial nanowires. *Nature* **435,** 1098–101 (2005).

95. Polizzi, N. F., Skourtis, S. S. & Beratan, D. N. Physical constraints on charge transport through bacterial nanowires. *Faraday Discuss.* **155,** 43 (2012).

96. Reguera, G., Pollina, R. B., Nicoll, J. S. & Lovley, D. R. Possible nonconductive role of Geobacter sulfurreducens pilus nanowires in biofilm formation. *J. Bacteriol.* **189,** 2125–7 (2007).

97. Malvankar, N. S. & Lovley, D. R. Microbial nanowires: a new paradigm for biological electron transfer and bioelectronics. *ChemSusChem* **5,** 1039–46

(2012).

98. Reguera, G. Harnessing the power of microbial nanowires. *Microb. Biotechnol.* **11,** 979–994 (2018).

99. Malvankar, N. S. & Lovley, D. R. Microbial nanowires for bioenergy applications. *Curr. Opin. Biotechnol.* **27C,** 88–95 (2014).

100. Yang, Y., Xu, M., Guo, J. & Sun, G. Bacterial extracellular electron transfer in bioelectrochemical systems. *Process Biochem.* **47,** 1707–1714 (2012).

101. Malvankar, N. S. & Lovley, D. R. Microbial nanowires for bioenergy applications. *Curr. Opin. Biotechnol.* **27,** 88–95 (2014).

102. Pirbadian, S. & El-Naggar, M. Y. Multistep hopping and extracellular charge transfer in microbial redox chains. *Phys. Chem. Chem. Phys.* **14,** 13802–8 (2012).

103. Pirbadian, S. *et al.* Shewanella oneidensis MR-1 nanowires are outer membrane and periplasmic extensions of the extracellular electron transport components. *Proc. Natl. Acad. Sci. U. S. A.* **111,** 12883–12888 (2014).

104. Rosano, G. L. & Ceccarelli, E. A. Recombinant protein expression in Escherichia coli: Advances and challenges. *Front. Microbiol.* **5,** 1–17 (2014).

105. Gardner, T. S. & Hawkins, K. Synthetic Biology: evolution or revolution? A co-founder's perspective. *Curr. Opin. Chem. Biol.* **17,** 871–7 (2013).

106. Decoene, T. *et al.* Standardization in synthetic biology: an engineering discipline coming of age. *Crit. Rev. Biotechnol.* **38,** 647–656 (2018).

107. Knight, T. Idempotent Vector Design for Standard Assembly of Biobricks Standard Biobrick Sequence Interface. *MIT Synthetic Biology Working Group* 1–11 (2003).

108. Shetty, R. P., Endy, D. & Knight, T. F. Engineering BioBrick vectors from BioBrick parts. *J. Biol. Eng.* **2,** 5 (2008).

109. Arkin, A. P. A wise consistency: engineering biology for conformity, reliability, predictability. *Curr. Opin. Chem. Biol.* **17,** 893–901 (2013).

110. Adams, B. L. The Next Generation of Synthetic Biology Chassis: Moving Synthetic Biology from the Laboratory to the Field. *ACS Synth. Biol.* **5,** 1328–1330 (2016).

111. Cheng, A. & Lu, T. Synthetic biology: an emerging engineering discipline. *Annu. Rev. Biomed. Eng.* **14,** 155–178 (2012).

112. Blount, B. a, Weenink, T., Vasylechko, S. & Ellis, T. Rational diversification of a promoter providing fine-tuned expression and orthogonal regulation for synthetic biology. *PLoS One* **7,** e33279 (2012).

113. Cheah, U. E., Weigand, W. a & Stark, B. C. Effects of recombinant plasmid size on cellular processes in Escherichia coli. *Plasmid* **18,** 127–34 (1987).

114. Schaerli, Y. & Isalan, M. Building synthetic gene circuits from combinatorial libraries: screening and selection strategies. *Mol. Biosyst.* **9,** 1559–67 (2013).

115. Cobb, R. E., Si, T. & Zhao, H. Directed evolution: an evolving and enabling synthetic biology tool. *Curr. Opin. Chem. Biol.* **16,** 285–91 (2012).

116. Thieffry, D., Huerta, A. M., Pérez-Rueda, E. & Collado-Vides, J. From specific gene regulation to genomic networks: a global analysis of transcriptional regulation in Escherichia coli. *Bioessays* **20,** 433–40 (1998).

117. Studier, F. W. Protein production by auto-induction in high-density shaking cultures. *Protein Expr. Purif.* **41,** 207–234 (2005).

118. Rolfe, M. D. *et al.* Systems analysis of transcription factor activities in environments with stable and dynamic oxygen concentrations. *Open Biol.* **2,** 120091 (2012).

119. Murray, A. E. *et al.* DNA/DNA hybridization to microarrays reveals gene-specific differences between closely related microbial genomes. *Proc. Natl. Acad. Sci. U.*

S. A. **98,** 9853–8 (2001).

120. McCue, L. A., Thompson, W., Steven Carmack, C. & Lawrence, C. E. Factors influencing the identification of transcription factor binding sites by cross-species comparison. *Genome Res.* **12,** 1523–1532 (2002).

121. Rocha, E. P. C. Codon usage bias from tRNA's point of view: redundancy, specialization, and efficient decoding for translation optimization. *Genome Res.* **14,** 2279–86 (2004).

122. Jensen, H. M. *et al.* Engineering of a synthetic electron conduit in living cells. *Proc. Natl. Acad. Sci. U. S. A.* **107,** 19213–8 (2010).

123. Szöllosi, A., Rezessy-szabó, J. M., Hoschke, Á. & Nguyen, Q. D. Novel method for screening microbes for application in microbial fuel cell. *Bioresour. Technol.* **179,** 123–127 (2015).

124. Zhou, S., Wen, J., Chen, J. & Lu, Q. Rapid measurement of microbial extracellular respiration ability using a high-throughput colorimetric assay. *Environ. Sci. Technol. Lett.* **2,** 26–30 (2015).

125. Pereira-Medrano, A. G. *et al.* Quantitative proteomic analysis of the exoelectrogenic bacterium Arcobacter butzleri ED-1 reveals increased abundance of a flagellin protein under anaerobic growth on an insoluble electrode. *J. Proteomics* **78,** 197–210 (2013).

126. TerAvest, M. a., Zajdel, T. J. & Ajo-Franklin, C. M. The Mtr Pathway of Shewanella oneidensis MR-1 Couples Substrate Utilization to Current Production in Escherichia coli. *ChemElectroChem* **1,** 1874–1879 (2014).

127. Coursolle, D., Baron, D. B., Bond, D. R. & Gralnick, J. a. The Mtr respiratory pathway is essential for reducing flavins and electrodes in Shewanella oneidensis. *J. Bacteriol.* **192,** 467–474 (2010).

128. Coursolle, D. & Gralnick, J. a. Modularity of the Mtr respiratory pathway of

Shewanella oneidensis strain MR-1. *Mol. Microbiol.* **77,** 995–1008 (2010).

129. Rebstock, M. C., Crooks Jr., H. M., Controulis, J. & Bartz, Q. R. Chloramphenicol (Chloromycetin). Chemical Studies. *J. Am. Chem. Soc.* **71,** 2458–2462 (1948).

130. Schlünzen, F. *et al.* Structural basis for the interaction of antibiotics with the peptidyl transferase centre in eubacteria. *Nature* **413,** 814–821 (2001).

131. Nikaido, H. Prevention of drug access to bacterial targets: permeability barriers and active efflux. *Science (80-.).* **264,** 382–388 (1994).

132. Murray, I. A. *et al.* Analysis of hydrogen bonding in enzyme-substrate complexes of chloramphenicol acetyltransferase by infrared spectroscopy and site-directed mutagenesis. *Biochemistry* **33,** 9826–9830 (1994).

133. Coursolle, D. & Gralnick, J. A. Reconstruction of extracellular respiratory pathways for iron(III) reduction in Shewanella oneidensis strain MR-1. *Front. Microbiol.* **3,** 1–11 (2012).

134. Gescher, J. S., Cordova, C. D. & Spormann, A. M. Dissimilatory iron reduction in Escherichia coli: Identification of CymA of Shewanella oneidensis and NapC of E. coli as ferric reductases. *Mol. Microbiol.* **68,** 706–719 (2008).

135. Feissner, R. E. *et al.* Recombinant cytochromes c biogenesis systems I and II and analysis of haem delivery pathways in Escherichia coli. *Mol. Microbiol.* **60,** 563–577 (2006).

136. Richard-Fogal, C. L., San Francisco, B., Frawley, E. R. & Kranz, R. G. Thiol redox requirements and substrate specificities of recombinant cytochrome c assembly systems II and III. *Biochim. Biophys. Acta - Bioenerg.* **1817,** 911–919 (2012).

137. Arslan, E., Schulz, H., Zufferey, R., Ku, P. & Tho, L. Overproduction of the Bradyrhizobium japonicum c -Type Cytochrome Subunits of the cbb 3 Oxidase in Escherichia coli. *Biochem. Biophys. Res. Commun.* **747,** 744–747 (1998).

138. Pitts, K. E. *et al.* Characterization of the Shewanella oneidensis MR-1 decaheme cytochrome MtrA: expression in Escherichia coli confers the ability to reduce soluble Fe(III) chelates. *J. Biol. Chem.* **278,** 27758–65 (2003).

139. Moffatt, B. A. & Studier, F. W. T7 lysozyme inhibits transcription by T7 RNA polymerase. *Cell* **49,** 221–227 (1987).

140. Wagner, S. *et al.* Tuning Escherichia coli for membrane protein overexpression. *Proc. Natl. Acad. Sci. U. S. A.* **105,** 14371–14376 (2008).

141. Ellis, J., Bagshaw, C. R. & Shaw, W. V. Kinetic Mechanism of Chloramphenicol Acetyltransferase: The Role of Ternary Complex Interconversion in Rate Determination. *Biochemistry* **34,** 16852–16859 (1995).

142. Fowler, G. J. S. *et al.* An iTRAQ characterisation of the role of TolC during electron transfer from *Shewanella oneidensis* MR-1. *Proteomics* 1–12 (2016). doi:10.1002/pmic.201500538

143. Kovach, M. E., Phillips, R. W., Elzer, P. H., Roop, R. M. 2nd & Peterson, K. M. pBBR1MCS: a broad-host-range cloning vector. *Biotechniques* **16,** 800–802 (1994).

144. Antoine, R. & Locht, C. Isolation and molecular characterization of a novel broad-host-range plasmid from Bordetella bronchiseptica with sequence similarities to plasmids from Gram-positive organisms. *Mol. Microbiol.* **6,** 1785–1799 (1992).

145. Tolia, N. H. & Joshua-Tor, L. Strategies for protein coexpression in Escherichia coli. *Nat. Methods* **3,** 55–64 (2006).

146. Berg, J. M., Tymoczko, J. L. & Stryer, L. *Biochemistry*. (W.H. Freeman, 2012).

147. Corbett, M. D. & Chipko, B. R. Synthesis and antibiotic properties of chloramphenicol reduction products. *Antimicrob. Agents Chemother.* **13,** 193–198 (1978).

148. Ichida, H. *et al.* Construction and characterization of a copy number-inducible fosmid library of Xanthomonas oryzae pathovar oryzae MAFF311018. *Gene* **546,** 68–72 (2014).

149. Ruegg, T. L. *et al.* An auto-inducible mechanism for ionic liquid resistance in microbial biofuel production. *Nat. Commun.* **5,** 1–7 (2014).

150. An, Y., Toyoda, A., Zhao, C., Fujiyama, A. & Agata, K. A Colony Multiplex Quantitative PCR-Based 3S3DBC Method and Variations of It for Screening DNA Libraries. *PLoS One* **10,** 1–11 (2015).

151. Cao, D.-M. *et al.* Role of electricity production in the anaerobic decolorization of dye mixture by exoelectrogenic bacterium Shewanella oneidensis MR-1. *Bioresour. Technol.* **136,** 176–81 (2013).

152. Pearce, C. & Christie, R. Reactive azo dye reduction by Shewanella strain J18 143. *Biotechnol. …* **95,** 692–703 (2006).

153. Chen, K.-C., Wu, J.-Y., Liou, D.-J. & Hwang, S.-C. J. Decolorization of the textile dyes by newly isolated bacterial strains. *J. Biotechnol.* **101,** 57–68 (2003).

154. Hong, Y.-G. & Gu, J.-D. Physiology and biochemistry of reduction of azo compounds by Shewanella strains relevant to electron transport chain. *Appl. Microbiol. Biotechnol.* **88,** 637–43 (2010).

155. Nigam, P., Banat, I. M., Singh, D. & Marchant, R. Microbial process for the decolorization of textile effluent containing azo, diazo and reactive dyes. *Process Biochem.* **31,** 435–442 (1996).

156. ZIMMERMANN, T., KULLA, H. G. & LEISINGER, T. PROPERTIES OF PURIFIED ORANGE-II AZOREDUCTASE, THE ENZYME INITIATING AZO DYE DEGRADATION BY PSEUDOMONAS KF46. *Eur. J. Biochem.* **129,** 197–203 (1982).

157. Solanki, K., Subramanian, S. & Basu, S. Microbial fuel cells for azo dye treatment with electricity generation: a review. *Bioresour. Technol.* **131,** 564–71 (2013).

158. Hong, Y.-G., Guo, J., Xu, Z.-C., Xu, M.-Y. & Sun, G.-P. Humic Substances Act as Electron Acceptor and Redox Mediator for Microbial Dissimilatory Azoreduction by. *J. Gen. Appl. Microbiol.* **17,** 428–437 (2007).

159. Bagherian, G., Chamjangali, M. A., Goudarzi, N. & Namazi, N. Selective spectrophotometric determination of periodate based on its reaction with methylene green and its application to indirect determination of ethylene glycol and glycerol. *Spectrochim. Acta. A. Mol. Biomol. Spectrosc.* **76,** 29–32 (2010).

160. Usha, M., Sasirekha, B. & Bela, R. Batch, repeated batch and continuous degradation of Reactive Black 5 and Reactive Red 120 dye by immobilized bacteria. *J. Sci. …* **71,** 504–510 (2012).

161. Beliaev, A. S. *et al.* Global Transcriptome Analysis of Shewanella oneidensis MR-1 Exposed to Different Terminal Electron Acceptors. *J. Bacteriol.* **187,** 7138–7145 (2005).

162. Brown, R. N., Romine, M. F., Schepmoes, A. A., Smith, R. D. & Lipton, M. S. Mapping the Subcellular Proteome of Shewanella oneidensis MR-1 using Sarkosyl-Based Fractionation and LC - MS / MS Protein Identification research articles. *J. Proteome Res.* **9,** 4454–4463 (2010).

163. Fang, R. *et al.* Differential Label-free Quantitative Proteomic Analysis of Shewanella oneidensis Cultured under Aerobic and Suboxic Conditions by Accurate Mass and Time Tag Approach * □. *Mol. Cell. Proteomics* **5,** 714–725 (2006).

164. Binnenkade, L., Lassak, J. & Thormann, K. M. Analysis of the BarA/UvrY Two-Component System in Shewanella oneidensis MR-1. *PLoS One* **6,** (2011).

165. Moore, J. C. METABOLIC ENGINEERING OF ESCHERICHIA COLI ATCC 8739 FOR PRODUCTION OF BIOELECTRICITY. (2009).

166. Proft, T. & Baker, E. N. Pili in Gram-negative and Gram-positive bacteria -

structure, assembly and their role in disease. *Cell. Mol. Life Sci.* **66,** 613–35 (2009).

167. Kuhlman, T., Zhang, Z., Saier Jr., M. H. & Hwa, T. Combinatorial transcriptional control of the lactose operon of Escherichia coli. *Proc. Natl. Acad. Sci. U. S. A.* **104,** 6043–6048 (2007).

168. Holms, H. Flux analysis and control of the central metabolic pathways in Escherichia coli. *FEMS Microbiol. Rev.* **19,** 85–116 (1996).

169. Lee, J.-W. & Helmann, J. D. Functional specialization within the Fur family of metalloregulators. *BIOMETALS* **20,** 485–499 (2007).

170. Hurme, R. & Rhen, M. Temperature sensing in bacterial gene regulation - what it all boils down to. *Mol. Microbiol.* **30,** 1–6 (1998).

171. AMABILECUEVAS, C. F. & DEMPLE, B. MOLECULAR CHARACTERIZATION OF THE SOXRS GENES OF ESCHERICHIA-COLI - 2 GENES CONTROL A SUPEROXIDE STRESS REGULON. *Nucleic Acids Res.* **19,** 4479–4484 (1991).

172. Bentley, W. E., Mirjalili, N., Andersen, D. C., Davis, R. H. & Kompala, D. S. Plasmid-encoded protein: the principal factor in the 'metabolic burden' associated with recombinant bacteria. Biotechnology Bioengineering, 1990. *Biotechnol. Bioeng.* **102,** 1284–97; discussion 1283 (2009).

173. Wang, H., Correa, E., Dunn, W. B. & Lloyd, J. R. Metabolomic analyses show that electron donor and acceptor ratios control anaerobic electron transfer pathways in Shewanella oneidensis. 642–656 (2013). doi:10.1007/s11306-012-0488-3

174. Pitts, K. E. *et al.* Characterization of the Shewanella oneidensis MR-1 decaheme cytochrome MtrA: Expression in Escherichia coli confers the ability to reduce soluble FE(III) chelates. *J. Biol. Chem.* **278,** 27758–27765 (2003).

175. Baumgarten, T. *et al.* Isolation and characterization of the E. coli membrane protein production strain Mutant56(DE3). *Sci. Rep.* **7,** 1–14 (2017).

176. Ross, P. L. *et al.* Multiplexed Protein Quantitation in Saccharomyces cerevisiae Using Amine-reactive Isobaric Tagging Reagents. *Mol. Cell. Proteomics* **3,** 1154–1169 (2004).

177. Ow, S. Y. *et al.* iTRAQ Underestimation in Simple and Complex Mixtures : " The Good , the Bad and the Ugly ". *J. Proteome Res.* **8,** 5347–5355 (2009).

178. Evans, C. *et al.* An insight into iTRAQ : where do we stand now ? *Anal. Bioanal. Chem.* **404,** 1011–1027 (2012).

179. Noirel, J. *et al.* Methods in Quantitative Proteomics: Setting iTRAQ on the Right Track. *Curr. Proteomics* **8,** 17–30 (2011).

180. Tyanova, S. *et al.* Visualization of LC-MS / MS proteomics data in MaxQuant. *Proteomics* **15,** 1453–1456 (2015).

181. Cox, J. & Mann, M. MaxQuant enables high peptide identification rates, individualized p.p.b.-range mass accuracies and proteome-wide protein quantification. *Nat. Biotechnol.* **26,** 1367–1372 (2008).

182. Kwon, S. K., Kim, S. K., Lee, D. H. & Kim, J. F. Comparative genomics and experimental evolution of Escherichia coli BL21(DE3) strains reveal the landscape of toxicity escape from membrane protein overproduction. *Sci. Rep.* **5,** 16076 (2015).

183. Consortium, T. U. UniProt : the universal protein knowledgebase. *Nucleic Acids Res.* **45,** 158–169 (2017).

184. D'Ascenzo, M., Choe, L. & Lee, K. iTRAQPak: an R based analysis and visualization package for 8-plex isobaric protein expression data. *Briefings Funct. Genomics Proteomics* **7,** 127–135 (2008).

185. Mi, H. *et al.* PANTHER version 11: expanded annotation data from Gene Ontology and Reactome pathways, and data analysis tool enhancements. *Nucleic Acids Res.* **45,** D183–D189 (2017).

186. Firer-Sherwood, M. A., Ando, N., Drennan, C. L. & Elliott, S. J. Solution-Based Structural Analysis of the Decaheme Cytochrome, MtrA, by Small-Angle X-ray Scattering and Analytical Ultracentrifugation. *J. Phys. Chem. B* **115,** 11208–11214 (2011).

187. Sugawaras, E. & Nikaido, H. Pore-forming Activity of OmpA Protein of Escherichia coli. *J. Biol. Chem.* **267,** 2507–2511 (1992).

188. Koebnik, R. Structural and Functional Roles of the Surface-Exposed Loops of the Beta-Barrel Membrane Protein OmpA from Escherichia coli. *J. Bacteriol.* **181,** 3688–3694 (1999).

189. Kumar, A., Hajjar, E., Ruggerone, P. & Ceccarelli, M. Molecular Simulations Reveal the Mechanism and the Determinants for Ampicillin Translocation through OmpF. *J. Phys. Chem.* **114,** 9608–9616 (2010).

190. Dhakshnamoorthy, B., Raychaudhury, S., Blachowicz, L. & Roux, B. Cation selective pathway of OmpF porin revealed by anomalous X-ray diffraction. *J. Mol. Biol.* **396,** 293–300 (2013).

191. Koebnik, R., Locher, K. P. & Van, P. MicroReview Structure and function of bacterial outer membrane proteins : barrels in a nutshell. **37,** (2000).

192. Minagawa, S. *et al.* Identification and Molecular Characterization of the Mg2+ Stimulon of Escherichia coli. *J. Bacteriol.* **185,** 3696–3702 (2003).

193. Perez, J. C. *et al.* Evolution of a Bacterial Regulon Controlling Virulence and Mg 2 + Homeostasis. *PLoS Genet.* **5,** (2009).

194. Lippa, A. M. & Goulian, M. Perturbation of the Oxidizing Environment of the Periplasm Stimulates the PhoQ / PhoP System in Escherichia coli. *J. Bacteriol.* **194,** 1457–1463 (2012).

195. Outten, F. W., Huffman, D. L., Hale, J. A. & Halloran, T. V. O. The Independent cue and cus Systems Confer Copper Tolerance during Aerobic and Anaerobic

Growth in Escherichia coli. *J. Biol. Chem.* **276,** 30670–30677 (2001).

196. Franke, S., Grass, G., Rensing, C. & Nies, D. H. Molecular Analysis of the Copper-Transporting Efflux System CusCFBA of Escherichia coli. *J. Bacteriol.* **185,** 3804–3812 (2003).

197. Mealman, T. D. *et al.* Interactions between CusF and CusB identified by NMR spectroscopy and chemical cross-linking coupled to mass spectrometry. *Biochemistry* **50,** 2559–2566 (2012).

198. Chuan, M. C., Shu, G. Y. & Liu, J. C. Solubility Of Heavy Metals In A Contaminated Soil: Effects Of Redox Potential And pH. *Water. Air. Soil Pollut.* **90,** 543–556 (1996).

199. Keseler, I. M. *et al.* EcoCyc: fusing model organism databases with systems biology. *Nucleic Acids Res.* **41,** 605–612 (2013).

200. Fraser, H. I., Kvaratskhelia, M. & White, M. F. The two analogous phosphoglycerate mutases of Escherichia coli. *FEBS Lett.* **455,** 344–348 (1999).

201. Rodríguez-moyá, M. & Gonzalez, R. Proteomic analysis of the response of Escherichia coli to short-chain fatty acids. *J. Proteomics* **122,** 86–99 (2015).

202. Lesniak, J. & Barton, W. A. Structural and functional features of the Escherichia coli hydroperoxide resistance protein OsmC. *Protein Sci.* **12,** 2838–2843 (2003).

203. Imlay, K. R. & Imlay, J. A. Cloning and Analysis of sodC , Encoding the Copper-Zinc Superoxide Dismutase of Escherichia coli. *J. Bacteriol.* **178,** 2564–2571 (1996).

204. Benov, L., Chang, L., Day, B. & Fridovich, I. Copper, zinc superoxide dismutase in Escherichia coli: periplasmic localization. *Arch. Biochem. Biophys.* **319,** 503–511 (1995).

205. Lacour, S. & Landini, P. Sigma S -Dependent Gene Expression at the Onset of

Stationary Phase in Escherichia coli : Function of Sigma S -Dependent Genes and Identification of Their Promoter Sequences †. *J. Bacteriol.* **186,** 7186–7195 (2004).

206. Grandori, R. *et al.* Biochemical Characterization of WrbA , Founding Member of a New Family of Multimeric Flavodoxin-like Proteins. *J. Biol. Chem.* **273,** 20960–20966 (1998).

207. Nakamaru-Ogiso, E., Yano, T., Yagi, T. & Ohnishi, T. Characterization of the Iron-Sulfur Cluster N7 (N1c) in the Subunit NuoG of the Proton-translocating NADH-quinone Oxidoreductase from Escherichia coli *. *J. Biol. Chem.* **280,** 301–307 (2005).

208. Prub, B. M., Nelms, J. M., Park, C. & Wolfe, A. J. Mutations in NADH:Ubiquinone Oxidoreductase of Escherichia coli Affect Growth on Mixed Amino Acids. *J. Bacteriol.* **176,** 2143–2150 (1994).

209. Lin, Z. *et al.* Metabolic engineering of Escherichia coli for the production of riboflavin. *Microb. Cell Fact.* **13,** 1–12 (2014).

210. Béatrice, P. & Barras, F. Building Fe – S proteins : bacterial strategies. *Nat. Rev. Microbiol.* **8,** 436–446 (2010).

211. Unden, G. & Bongaerts, J. Alternative respiratory pathways of Escherichia coli : energetics and transcriptional regulation in response to electron acceptors. (1997).

212. Tielens, A. & Van Hellemond, J. The electron transport chain in anaerobically functioning eukaryotes. *Biochem. Biophys. Acta* **1365,** 71–78 (1998).

213. Mcmillan, D. G. G., Marritt, S. J., Butt, J. N. & Jeuken, L. J. C. Menaquinone-7 Is Specific Cofactor in Tetraheme Quinol Dehydrogenase CymA. *J. Biol. Chem.* **287,** 14215–14225 (2012).

214. Fu, H., Jin, M., Ju, L., Mao, Y. & Gao, H. Evidence for function overlapping of

CymA and the cytochrome bc 1 complex in the Shewanella oneidensis nitrate and nitrite respiration. *Environ. Microbiol.* **16,** 3181–3195 (2014).

215. Maruyama, A. *et al.* Oxidative-stress-inducible qorA encodes an NADPH-dependent quinone oxidoreductase catalysing a one-electron reduction in Staphylococcus aureus. *Microbiology* **149,** 389–398 (2003).

216. Ferguson, G. P., Tötemeyer, S., MacLean, M. J. & Booth, I. R. Methylglyoxal production in bacteria : suicide or survival ? *Arch. Microbiol.* **170,** 209–219 (1998).

217. Dym, O., Pratt, E. A., Ho, C. & Eisenberg, D. The crystal structure of D -lactate dehydrogenase , a peripheral membrane respiratory enzyme. *PNAS* **97,** 9413–9418 (2000).

218. Futai, M. & Kimura, H. Inducible Membrane-bound L-Lactate Dehydrogenase from Escherichia coli. *J. Biol. Chem.* **252,** 5820–5827 (1977).

219. Dong, J. M., Taylor, J. S., Latour, D. J., Iuchi, S. & Lin, E. C. C. Three Overlapping Ict Genes Involved in L-Lactate Utilization by Escherichia coli. *J. Bacteriol.* **175,** 6671–6678 (1993).

220. Lopez-campistrous, A. *et al.* Localization , Annotation , and Comparison of the Escherichia coli K-12 Proteome under Two States of Growth. *Mol. Cell. Proteomics* **4,** 1205–1209 (2005).

221. Munson, G. P., Lam, D. L. & Outten, F. W. Identification of a Copper-Responsive Two-Component System on the Chromosome of Escherichia coli K-12. *J. Bacteriol.* **182,** 5864–5871 (2000).

222. GUNSALUS, R. P. & PARK, S. J. AEROBIC-ANAEROBIC GENE-REGULATION IN ESCHERICHIA-COLI - CONTROL BY THE ARCAB AND FNR REGULONS. *Res. Microbiol.* **145,** 437–450 (1994).

223. Potamitou, A., Neubauer, P., Holmgren, A. & Vlamis-Gardikas, A. Expression of

Escherichia coli glutaredoxin 2 is mainly regulated by ppGpp and sigma(S). *J. Biol. Chem.* **277,** 17775–17780 (2002).

224. Otto, K. & Silhavy, T. J. Surface sensing and adhesion of Escherichia coli controlled by the Cpx-signaling pathway. *Proc. Natl. Acad. Sci. U. S. A.* **99,** 2287–2292 (2002).

225. Chapman, S. *et al.* The photoreversible fluorescent protein iLOV outperforms GFP as a reporter of plant virus infection. *Proc. Natl. Acad. Sci. U. S. A.* **105,** 20038–20043 (2008).

226. Pedelacq, J. D., Cabantous, S., Tran, T., Terwilliger, T. C. & Waldo, G. S. Engineering and characterization of a superfolder green fluorescent protein. *Nat. Biotechnol.* **24,** 79–88 (2006).

227. Bekker, M. *et al.* The ArcBA two-component system of Escherichia coli is regulated by the redox state of both the ubiquinone and the menaquinone pool. *J. Bacteriol.* **192,** 746–754 (2010).